

CONTROL OF A MACRO-MINI ROBOTIC MANIPULATOR

LU XIUJUAN

NATIONAL UNIVERSITY OF SINGAPORE

2008

CONTROL OF A MACRO-MINI ROBOTIC MANIPULATOR

LU XIUJUAN

*(B.Eng., University of Electronic Science and Technology of
China)*

A THESIS SUBMITTED

FOR THE DEGREE OF MASTER OF ENGINEERING

DEPARTMENT OF MECHANICAL ENGINEERING

NATIONAL UNIVERSITY OF SINGAPORE

2008

Acknowledgements

First and foremost, I owe my deepest thanks to my supervisors, Dr. Marcelo Ang H. Jr. and Dr. Henk Corporaal, for their valuable supervision, constructive guidance, incisive insight, and most importantly, their understanding and encouragement throughout my project. Thanks also to Dr. Oussama Khatib, for his inspiration and many details taught through a graduate level course at NUS.

I would like to thank National University of Singapore for the financial support in the form of research scholarship, and research facilities, to make this work possible to be done. I am also grateful for the assistance and support provided by the staff in the Control and Mechatronics Laboratory and Center for Design Technology.

My gratitude is also extended to the colleagues and friends in Control lab, Mr. Zhou Longjiang, Mr. Wang Chen, Mr. Wan Jie, Ms. Yang Lin, Mr. Dandy Barata Soewandito, Mr. James Fu Guo Ming, Mr Koh Niak Wu, Mr. Li Yuanping, Mr. Tirthankar Bandyopadhyay and many others, for their helpful discussion, suggestions and friendship. I wish to specially express my sincere gratitude to Mr. Lalit Kumar Verma and Dau Van Huan, my friends, for their constant help in this work.

Last but not the least; I am truly grateful for the unconditional love and support provided by my parents, husband Peng Jun, my baby Peng Jiakuan and many relatives. Special thanks to my mom who helps me taking care of the child when I write this thesis, as well as Auntie Wang Jun.

Table of Content

ACKNOWLEDGEMENTS	I
TABLE OF CONTENT	II
SUMMARY	IV
LIST OF TABLES	VII
LIST OF FIGURES	VIII
LIST OF SYMBOLS	XI
CHAPTER 1	1
INTRODUCTION	1
1.1 BACKGROUND AND MOTIVATION	1
1.2 LITERATURE REVIEW	5
1.3 OBJECTIVES AND SCOPE OF THE STUDY	10
1.4 ORGANIZATION OF THESIS	14
CHAPTER 2	15
STRUCTURE AND PARAMETERS FOR MACRO AND MINI MANIPULATORS	15
2.1 ROBOT STRUCTURE.....	15
2.2 SOFTWARE MODEL AND PARAMETERS OF MACRO-MINI MANIPULATOR....	17
2.3 ROBOT WORKSPACE ANALYSIS.....	19
CHAPTER 3	21
KINEMATICS, DYNAMICS AND CONTROL OF MACRO MANIPULATOR	21
3.1 KINEMATIC MODEL OF THE MACRO ROBOT	21

3.2 DYNAMIC MODEL OF THE MACRO ROBOT.....	27
3.3 OPERATIONAL SPACE MACRO MANIPULATOR CONTROL	35
3.3.1 Goal position.....	35
3.3.2 Trajectory tracking.....	39
CHAPTER 4.....	44
KINEMATICS, DYNAMICS AND CONTROL OF MINI	
MANIPULATOR.....	44
4.1 KINEMATIC MODEL OF THE ROBOT.....	44
4.2 DYNAMIC MODEL OF THE MINI ROBOT	47
4.3 OPERATIONAL SPACE ROBOT CONTROL.....	51
4.3.1 Goal position.....	51
4.3.2 Trajectory tracking.....	52
CHAPTER 5.....	54
OVERALL CONTROL FOR COMBINED MACRO-MINI	
MANIPULATOR SYSTEM	54
5.1 MACRO-MINI MANIPULATOR STRUCTURE AND MODELING.....	54
5.2 CONTROL STRUCTURE FOR MACRO-MINI MANIPULATOR.....	56
5.3 MACRO-MINI MANIPULATOR CONTROL SIMULATIONS.....	60
5.3.1 Goal position control with one way coupling	60
5.3.2 Goal position control with two way coupling	63
5.3.3 Trajectory tracking control with one way coupling	65
5.3.4 Trajectory tracking control with two way coupling	67
5.3.5 Summary	69
CHAPTER 6.....	70
CONCLUSIONS AND FUTURE WORK.....	70
6.1 CONCLUSIONS.....	70
6.2 FUTURE WORK	71
BIBLIOGRAPHY.....	73
APPENDIX: EQUATIONS OF MOTION FOR COMBINED	
MACRO-MINI MANIPULATOR SYSTEM	77

Summary

In recent years, a great demand of robotic manipulators with large workspace, having fast and precise motion throughout its workspace has arisen. Traditional robotic manipulators with long reach arms can offer a large workspace and fast response. However, correction of small end-point errors requires movement of several manipulator actuators. Thus, each actuator has to be capable of handling two different tasks, namely high speed for large range motion with accurate positioning for fine motion. The bandwidth of these manipulator actuators slow down the response of their arm, and thus lead to a compromise between the positioning accuracy of their end-effecters, and the high speed operation of the robot.

In a new design of manipulators, an additional rigid small robot (called the Mini manipulator) is attached at the end of the long reach manipulator (called the Macro manipulator), and its fine motion is applied to compensate for the positioning or tracking error of the Macro manipulator. The combined system (often referred to as a Macro-Mini, or Macro-Micro manipulator system), if integrated with appropriate controller design, offers a possible solution to a wide range of applications that require fast, and precise manipulation over a large workspace.

In this study, we designed a six degrees-of-freedom (6DOF) Macro-Mini manipulator system. A software model of the designed system is built in Matlab in order to analyze controller performance. The Macro and Mini manipulators kinematics, dynamics and

control are first studied separately, and then incorporated into one system. Individual performance of trajectory tracking and positioning was simulated. A new control strategy for combined Macro-Mini manipulator system was proposed. It is based on the individual dynamics of Macro and Mini manipulator system, aiming to achieve the best possible system performance. The dynamics of the overall system is not required. The overall system effectiveness was evaluated by software simulations.

Simulation results show that the combined system can reach the goal position or track the designed trajectory in a large workspace with fast response (similar to that of the Macro manipulator), small tracking and steady state errors (similar to that of the Mini manipulator). Thus, the combined system has taken full advantage of the Macro and Mini manipulators.

It is further concluded that the Macro manipulator performance can be improved by mounting a Mini manipulator at the end. High performance control of the combined system does not need calculation of full dynamics of the overall system. It can be based on individual dynamics of Macro and Mini manipulator. The successful breaking down of robot dynamics in controller design enables dynamic control of higher degrees-of-freedom manipulators.

This study also enables a modular design approach for industrial robots. The Mini manipulator can be designed locally to meet different requirements. This feature would

indicate cost saving in some industrial applications where a common base (Macro manipulator) can be used to perform multiple tasks, by mounting a different Mini manipulator module on it each time.

List of Tables

Table 2.1 Parameters of Macro and Mini manipulators.....	18
Table 3.1 D-H parameters for the Macro manipulator.....	24
Table 4.1 D-H parameters for the Mini manipulator	45
Table 5.1 D-H parameters for Macro-Mini manipulator	55

List of Figures

Figure 1.1 Inspection of underground tanks [15].....	5
Figure 1.2 Inspection of bridges [20].....	5
Figure 1.3 Macro-Micro manipulator system with optical sensor [2]	6
Figure 2.1 (a) Overview of Macro-Mini manipulator system (b) Human arm and hand bone structure.....	16
Figure 2.2 Model of a one-axis Macro-Micro manipulator [2]	18
Figure 2.3 Workspace of Macro manipulator	19
Figure 2.4 Workspace of Mini manipulator	20
Figure 3.1 Assignment of coordinate frames to the Macro robot at the robot's home position.....	22
Figure 3.2 Denavit-Hartenberg (D-H) frame assignment [8]	23
Figure 3.3 Position of center of mass	29
Figure 3.4 Goal position control block diagram of the Macro robot, in time domain..	37
Figure 3.5 Torque of each joint and tip position error in x, y and z directions for Macro goal position control	38
Figure 3.6 A quintic curve in x direction	39
Figure 3.7 Control block diagram of the Macro robot, in time domain.....	41
Figure 3.8 Desired trajectory, velocity and acceleration for Macro manipulator	41
Figure 3.9 Torque of each joint and tip position error in x, y and z directions for Macro	

trajectory tracking control, with torque limit.....	42
Figure 3.10 Torque of each joint and tip position error in x, y and z directions for Macro trajectory tracking control, without torque limit.....	42
Figure 4.1 Assignment of coordinate frames to the Mini robot at the robot's home position.....	44
Figure 4.2 Torque of each joint and tip position error in x, y and z directions for Mini manipulator goal position control	51
Figure 4.3 Desired trajectory, velocity and acceleration for Mini manipulator.....	53
Figure 4.4 Torque of each joint and tip position error in x, y and z directions for Mini manipulator trajectory tracking control	53
Figure 5.1 Assignment of coordinate frames to the Macro-Mini robotic system.....	55
Figure 5.2 Tip position control using an overall control strategy regardless of individual controllers for Macro and Mini manipulators.....	56
Figure 5.3 Determination of Macro and Mini manipulator trajectories, in x direction	58
Figure 5.4 Control structure for Macro-Mini manipulator system when the two subsystems are controlled separately	58
Figure 5.5 Tip position control using an overall control strategy on top of individual controllers for Macro and Mini manipulators.....	59
Figure 5.6 Macro-Mini manipulator overall control steps.....	61
Figure 5.7 Overall control strategies on top of individual controllers for Macro and Mini manipulators (one way coupling)	61
Figure 5.8 Torque of each joint and tip position error in x, y and z directions for	

Macro-Mini manipulator goal position control with one way coupling.....	62
Figure 5.9 Overall control strategies on top of individual controllers for Macro and Mini manipulators (two way coupling)	64
Figure 5.10 Torque of each joint and tip position error in x, y and z directions for Macro-Mini manipulator goal position control with two way coupling.....	64
Figure 5.11 Desired tip trajectory, velocity and acceleration for Macro-Mini manipulator	65
Figure 5.12 Torque of each joint and tip position error in x, y and z directions for Macro-Mini manipulator trajectory tracking control with one way coupling	66
Figure 5.13 Torque of each joint and tip position error in x, y and z directions for Macro-Mini manipulator trajectory tracking control with two way coupling	68

List of Symbols

b_{ijk}	Christoffel symbols
F	Generalized force vector expressed in operational space
F^*	Control input
$G(q)$	Gravity term
I	Moment of inertia
$J(q)$	Jacobian matrix
0J	Basic Jacobean
K_p, K_v	Control gains
$M(q)$	Inertia mass matrix
P	Position vector
$p(x)$	Gravitational force expressed in operational space
R	Rotational matrix
T	Homogeneous transformation matrix, size is 4×4
$V(q, \dot{q})$	Centrifugal and Coriolis terms
ε	Position error
$\mu(x, \dot{x})$	Centrifugal and Coriolis forces expressed in operational space
$\Lambda(x)$	Kinetic energy matrix expressed in operational space
$\theta_i, d_i, a_i, \alpha_i$	D-H parameters
ω_n	Natural frequency
ξ	Dumping ratio

Chapter 1

Introduction

1.1 Background and motivation

In recent years, a great demand of robotic manipulators with large workspace, having fast and precise motion throughout its workspace has arisen. For example, long arms are needed to offer a wide motion in space applications. In such robots, a small high performance manipulator is attached at its end-effector region to obtain fast and precise local mobility.

In assembly lines, robotic manipulators are usually lightweight with long reach arms, but their performances are limited due to its flexibility (vibrations and the static deflections). In these robots, the existing joint actuators are usually controlled to carry out the corrective action for enhancement of their motion performances [1,6,12,13,21,24]. However, correction of small end-point errors requires movement of several manipulator actuators. Thus, each actuator has to be capable of handling two different tasks, namely high speed and good response for large range motion with accurate positioning for fine motion [1,24]. The bandwidth of these manipulator actuators slow down the response of their arm, and thus lead to a compromise between the positioning accuracy of their end-effecters, and the high speed operation of the robot [21].

In a new design of manipulators, an additional rigid small robot is attached at the end of the flexible manipulator, and its fine motion is applied to compensate for the positioning or tracking error of the flexible manipulator. Such a structure is often referred to as a Macro-Mini (or Macro-Micro) manipulator system. The long reach arm of this system is called a Macro manipulator and it is characterized by 'poor' performance and 'slow' response. 'Poor' accuracy is caused primarily by the unmeasured deflections of the robot structure or drive, and low actuator/servo resolution. 'Slow' response time is attributed to low actuator power and control-related limitations.

The small robot connected at the end of the flexible manipulator, is called a Mini (or Micro) manipulator. It is characterized by a small work volume with fast and precise manipulation capability over its work volume.

Combining these two approaches, where a Mini manipulator rides on the end of a Macro manipulator integrated with appropriate controller design, offers a possible solution to a wide range of applications that require fast, and precise manipulation over a large workspace. [2]

There are several advantages offered by the manipulator of a Macro-Mini approach. First of all, this enables a modular approach in manipulator designs. The Mini manipulator can be designed locally to meet different requirements, such as control

bandwidth, accuracy, response time, etc. This feature would indicate cost saving in some industrial applications where a common base (Macro manipulator) can be used to perform multiple tasks, by mounting a different Mini manipulator module on it each time.

Second, not to consider for a moment any control problems that might arise, a fast Mini manipulator should be able to enhance the performance of the Macro manipulator, by compensating for the settling time thus reducing cycle time, and compensating for tracking errors encountered in following a designed trajectory thus improve accuracy.

Third, when it comes to flexible manipulators, the added Mini manipulator should be able to account for vibration and static deflections in the links.

In some application domains such as hazardous waste cleanup, the narrow access of storage tank constrains the cross sectional area of the manipulator system. In such situation, a long reach manipulator with either minimum mass or minimum cross sectional area will be required.

Similar flexibility in manipulator links also exists in space applications with the requirement of manipulator's ability to boost its mass into orbit. In this case, a minimization of the robotic system mass while maintaining a large work volume is necessary. But the light weight manipulators with long links often vibrate with low

frequencies, typically within or near the desired bandwidth of the control system. The requirements of above mentioned tasks complicated the controller design of robotic systems, which is mainly attributed to their flexibility.

With the Mini manipulator mounted at the end of the Macro manipulator, it offers a possible solution to account for these low frequency vibration modes, thus maintain stability and ensure desired performance.

Fourth, a Macro-Mini approach enables dynamic control of higher degrees-of-freedom manipulators. Dynamic analysis is a rather complicated issue. See Appendix for a sample equations-of-motion of a six degrees-of-freedom manipulator. It is impractical to use such complicated results in real-time controls. Also, using currently computation technologies, eg. Matlab 7 program runs on a computer with 2GB processor speed, 2 GB of Random Access Memory (RAM), the computation is limited to six degrees-of-freedom manipulator. One degree higher, the complexity increases exponentially. The computer hangs in such a computation, and never shows the results. Theoretically speaking, if controller design is based on dynamics of Macro and Mini manipulators separately, the number of degrees-of-freedom that we can control using dynamics can be largely increased.

In many field environments such as nuclear facilities or civil infrastructure sites, there is a need for remotely operated servicing tasks. Examples of such operations are the

inspection of underground storage tanks (Figure 1.1) [15] and the repair of bridges (Figure 1.2) [20]. Due to difficult accessibility and hazards, manipulators need to have long arms, which carry small dexterous manipulators close to the task locations. The full dynamics of such long reach manipulator systems (LRMS) are normally complicated due to the number of degrees-of-freedom. Modeling the systems as Macro-Mini manipulator systems offers a possible solution to the control system design with dynamics.

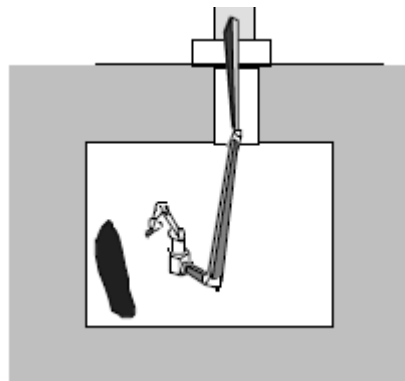


Figure 1.1 Inspection of underground tanks [15]

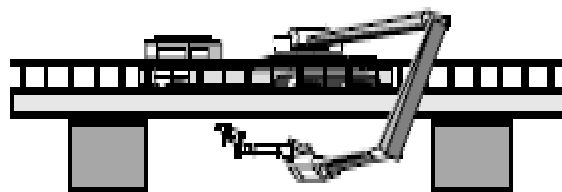


Figure 1.2 Inspection of bridges [20]

1.2 Literature review

The concept of using a fast, short reach manipulator mounted on a slower, long reach manipulator, also called a Macro-Micro or Macro-Mini manipulator, was first introduced by Sharon and Hogan [2] as a general means of improving a robot's

controlled dynamic behavior. The Macro manipulator carries the Micro manipulator to the nearby area of a task, where the inherent features of both the Macro and Micro robots are used together with endpoint sensing to achieve the desired goal (see Figure 1.3). The test-bed comprises a five degrees-of-freedom Micro manipulator (with only one axis in operation) and a one-axis flexible Macro manipulator. All the experiments carried out in this research involved motion along one axis only. The end-point position was measured using an optical sensor. It is seen that the Micro manipulator reaches its target very quickly and stabilizes itself on the target while the Macro manipulator is still moving. The Macro-Micro manipulator architecture was shown to be stable and well suited for high performance end-point control.

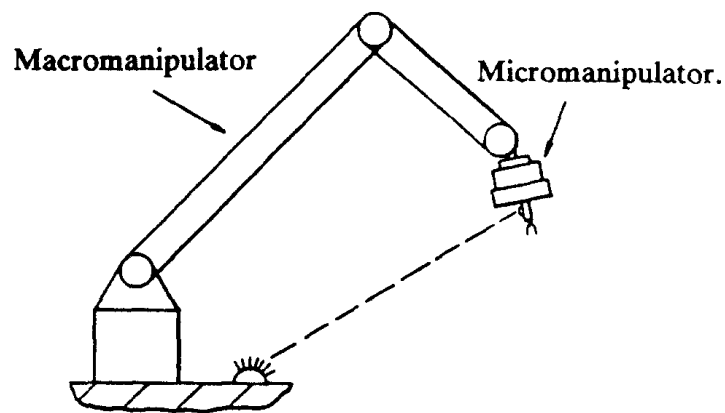


Figure 1.3 Macro-Micro manipulator system with optical sensor [2]

The critical issue that had to be addressed was the dynamic coupling between the Micro manipulator and Macro manipulator structure. It is tested by experiments and concluded, that if the effective end-point inertia of the Macro manipulator is much greater than the inertia of the Micro manipulator and load, the dynamic coupling can

be neglected, and the system remains stable for all gains.

There were a great deal of physical properties of a Macro-Mini structure been analyzed. But the test bed used in this study is only a one axis manipulator system. The potential dynamic analysis and control issues may lie with higher degrees-of-freedom manipulators were not studied.

The control of a two-link flexible manipulator with a Mini manipulator fixed at its end was studied by Ballhaus and Rock [30]. They implemented a controller where the Macro and the Mini manipulators were controlled independently with a PD law to achieve the desired end-point motion of the system. The results demonstrate that such a separated approach is limited and may lead to instability because of the dynamic coupling between the Macro and Mini manipulators.

H.D. Stevens et al. [9] examined the controller design for a multiple-link flexible Macro manipulator carrying a rigid Mini manipulator. They have denied independent controller design, which assumes no coupling between the subsystems and partitions the controller design into two pieces: a Macro manipulator controller and a Mini manipulator controller. Because the Mini manipulator rides on the Macro manipulator, there will be coupling from the Mini manipulator control torques to the Macro manipulator. This one-way dynamic coupling leads to the interactions that reduce performance. They proposed a coupled control architecture, where the Mini

manipulator reference input is the difference between the desired tip position and the Macro manipulator end-point position. The application of this control architecture to an experimental flexible Macro- Rigid Mini manipulator system has shown that the Mini manipulator dynamic reference input creates a feedback loop between the two subsystems resulting in two-way coupling. It is further concluded that control system design must account for the effects of the two-way coupling between Macro and Mini manipulators to achieve guaranteed stability and desirable system performance. Failure to include the two-way coupling in the control system design reduces performance and can cause instability.

Sharf [11] addressed the use of the Mini manipulators to damp the vibrations of the Macro manipulator when the task is outside the workspace of the Mini manipulators. A novel active damping algorithm was described. The algorithm was developed by using a different formulation for the dynamics of the system and it led to a solution of a novel manipulator dynamics problem. Sharf's simulations also illuminated the shortcomings of partitioning the control. Once the task enters the workspace of the Mini manipulator, the Mini manipulator not only discontinues damping the vibration modes, but allows the energy previously removed from the Macro subsystem returns to it. The performance of the system can be quite poor. Sharf's research also recognized the effects of the Mini manipulator control torques on the Macro subsystem, but did not address system performance.

Yoshikawa et al. [26] have proposed the trajectory tracking control of flexible Macro and rigid Micro manipulator systems - a rigid Micro manipulator mounted in the end-effector region of a large flexible link manipulator. The fast and high accuracy motion of this Micro manipulator is applied to compensate for the tip error of the Macro manipulator. The Macro-Mini manipulator system is analyzed as a complete system. They first develop a scheme for planning the joint trajectories of both the Macro and Micro manipulators, by utilizing the inherent kinematic redundancy of the system. The redundancy resolution problem is solved by maximizing the compensability measure, which essentially reflects the ability of the Micro robot to compensate for the deformation of the Macro manipulator. Yoshikawa et al. used a PD controller to realize the desired trajectory, by taking into account the corrections to the joint angles in the micro-robot to compensate for the deformations in the Macro manipulator. We note that the motion planning component of their procedure is based strictly on the kinematics of the system. Yoshikawa et al. [27] modified their previous PD controller to account for the dynamics of Macro-Micro manipulator. They also discussed the approach of hybrid position/ force control based on this flexible Macro and rigid Micro manipulator systems [28, 29]. In this control algorithm, the Macro manipulator part is controlled roughly to realize the desired trajectory, and suppress vibration. The Micro manipulator part is controlled to compensate for the position and force errors due to the deformation of the Macro part. But exact knowledge of the dynamics of the overall system is required for this control scheme. Generally it is very difficult to establish an accurate dynamic model of the system. As mentioned earlier, it

is even impractical, with current computation technologies, to solve for full dynamics of a manipulator system which has seven degrees-of-freedom or more. So this approach is limited to lower degrees-of-freedom manipulator systems, as compared to the controller designer proposed in this study.

Cheng et al. [31] have developed a new algorithm for the trajectory tracking control of a Macro–Micro manipulator (M^3) system based on neural networks. The control algorithm allows constraining the tracking errors within an arbitrarily small region around the origin. The designed neural network performs learning and control tasks online simultaneously and off-line training. Identification of the dynamic model is not required. The performance of the control scheme has been tested and compared with that of a proportional-derivative (PD) controller by simulations involving a three-link rigid Micro manipulator attached to a one-link flexible arm. However, this control scheme was not implemented in real-time.

1.3 Objectives and scope of the study

Based on research finding by Yoshikawa et al. [29], there is little difference between quasi-static control and dynamic control when the manipulator moves slowly (See below for definitions of these two controllers). This is because the effect of inertia at the tip of the Macro-Micro manipulator system is small [22]. When the manipulator moves fast, however, the dynamic control is more effective. Position and force errors of the dynamic control are much smaller than those of the quasi-static control.

Quasi-static trajectory tracking controller [26]: The complex dynamics of the Macro manipulator part is not taken into account in the control, and resultant tracking error is compensated by the Mini manipulator part using only geometry relationship.

Dynamic trajectory tracking controller [27]: The kinematic relationship and equations of motion, relation between the manipulation vector and the input torque has been derived for the overall Macro-Micro manipulator system. The dynamic controller is obtained from these relationships.

In this project, the aim is to explore the possibilities of position/trajectory tracking control of Macro-Mini manipulator system, using the kinematics and dynamics of separate Macro and Mini manipulators, instead of that of the overall system. This controller design would provide at least two benefits if proved to be effective:

1. The Macro-Mini manipulator system will follow the given trajectory more closely or reach the goal position faster, as that compared to controlling the manipulators without dynamic analysis.
2. A separated dynamic controller can be applied to higher degrees-of-freedom Macro-Mini manipulator systems, as compared to an overall dynamic controller. This is because of the limitations of current computation technology, as mentioned in previous sections.

To break down the tasks in detail, the following works are to be done:

1. Building computational/software models of the Macro and the Mini manipulators separately, analyzing their kinematics, dynamics;
2. Simulating trajectory tracking / position control of Macro and Mini manipulators to obtain individual performance. This also serves as an indirect indication of the correctness of Macro and Mini dynamics;
3. Derivation of the overall control strategy for combined Macro-Mini manipulator system for trajectory tracking / positioning tasks, knowing the dynamics of a Macro system, and a Mini manipulator system;
4. Comparing effectiveness of independent and coupled controller design [9];
5. Evaluation of effectiveness of the overall controller by software simulations; and
6. Exploration of a few theoretical questions that remain unanswered, such as how good it can be to use a Macro-Mini manipulator system together to accomplish a task, as compared to a Macro manipulator system functions alone (when the Mini hold itself still); can an inaccurate Macro system achieve the accuracy and response of a Mini manipulator system if it carries a Mini manipulator system;

The operational space formulation [16] [17] will be used for modeling robot dynamics.

The operational space formulation is a framework for the analysis and control of manipulator systems with respect to the dynamic behavior of their end-effectors instead of joint positions.

The joint space dynamic models (equations of joint motions) have been the basis for

various approaches to dynamic control of manipulators. However, task specification for motion and contact forces, dynamics, and force sensing feedback are closely linked to the end-effector. The dynamic behavior of the end-effector is one of the most significant characteristics in evaluating the performance of robot manipulator systems.

The main contributions of this thesis are summarized as follows,

1. A Macro-Mini manipulator structure is designed and tested with software simulation. The simulation results show that the Macro manipulator performance can be improved by mounting a Mini manipulator at the end. A Macro-Mini manipulator structure is suitable for applications that require fast and precise motion over a large workspace.
2. An overall controller for the Macro-Mini manipulator is designed based on independent controllers of Macro and Mini manipulators. High performance control of the combined system does not need calculation of full dynamics of the overall system. The successful breaking down of robot dynamics in controller design enables dynamic control of higher degrees-of-freedom manipulators.
3. This study also enables a modular design approach for industrial robots. The Mini manipulator can be designed locally to meet different requirements. This feature would indicate cost saving in some industrial applications where a common base (Macro manipulator) can be used to perform multiple tasks, by mounting a different Mini manipulator module on it each time.

1.4 Organization of thesis

The remaining chapters of this thesis are organized as follows. Chapter 2 introduces the structure and parameters for both Macro and Mini manipulator. In Chapter 3 the kinematics and dynamics of Macro robot are derived. The end-effector equations of motion are obtained in both joint space and operational space. Goal position and trajectory tracking control in operational space is simulated in Matlab. Chapter 4 follows similar organization as Chapter 3. It presents the kinematics, dynamics and control of the Mini robot. Chapter 5 describes the structure and modeling of Macro-Mini manipulator, the combined system. Different overall control strategies are reviewed and a new overall control is proposed. The control strategy is simulated and results are discussed. Chapter 6 gives conclusions and suggestions of the future work.

Chapter 2

Structure and Parameters for Macro and Mini Manipulators

2.1 Robot structure

Figure 2.1 (a) is a conceptual representation of the proposed Macro-Mini manipulator system for this study. The Mini manipulator rides on top of the Macro manipulator to form a Macro-Mini manipulator system. The figure is for illustration purpose only; the sizes of Macro and Mini manipulators shown may not be proportional to its designed size.

This design is inspired by the bone structure of human arm and hand, as shown in Figure 2.1 (b). The Macro manipulator part, which has three revolute joints, joint 1 to 3, rotating about z , x , x , respectively, resembles the human arm with two degrees-of-freedom at the shoulder, and one degree-of-freedom at the elbow. L_1 , L_2 and L_3 denotes the three links of the Macro manipulator. θ_1 , θ_2 and θ_3 are the joint positions.

Similarly, The Mini manipulator part, which also has three revolute joints, joint 4 to 6, rotating about z , x , x , respectively, resembles the human hand, with two degrees-of-freedom at the wrist, and one degree-of-freedom at the bottom of all fingers.

Since the human hand motion is very complicated and it is not the focus of this study, the design only included one axis, joint 6, to resemble all the finger motions. One can imagine all the fingers are attached together. Thumb motion is neglected. The links of the Mini manipulator are defined as L_4 , L_5 and L_6 . Joint positions are defined as θ_4 , θ_5 and θ_6 , as shown in Figure 2.1 (a).

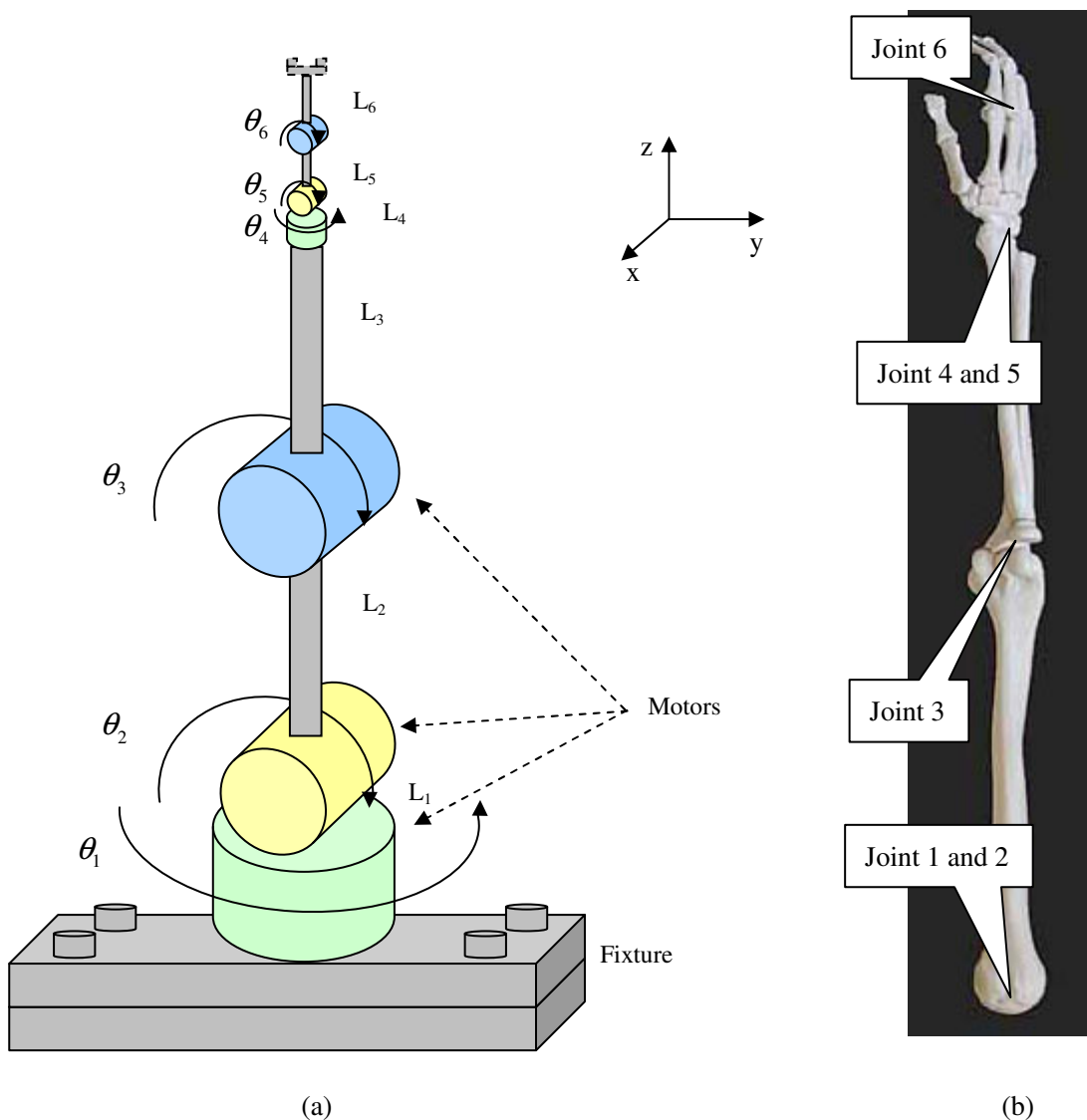


Figure 2.1 (a) Overview of Macro-Mini manipulator system (b) Human arm and hand bone structure

2.2 Software model and parameters of Macro-Mini manipulator

In order to conduct software simulations of Macro-Mini manipulator system control, parameters have to be assigned to represent the manipulator structure proposed. We first decide on the link lengths and masses for the Macro manipulator. Since Link 1 is very short, for easy calculation and presentation, we approximate its link length to zero. That results zero mass for Link 1. We assume Link 2 and 3 both have unit length equals one meter and unit point mass at the end of each link equals one kilogram.

In the Mini manipulator software model design, we have to consider the dynamic coupling between the Macro and Mini systems. In order that the dynamic coupling effect can be neglected during control, yet the system remains stable for all gains, we have to design the effective end-point inertia of the Macro manipulator is much greater than the inertia of the Mini manipulator and load. [2]

With reference to the research of A. Sharon, et al. [2], the one-axis Macro manipulator has a mass equals to 2.97 kg, the one-axis Micro manipulator has a mass equals to 0.88 kg. See Figure 2.2 for the modeling of their Macro-Micro manipulator system.

The masses and lengths of the Mini manipulator are carefully chosen to much smaller than those of the Macro manipulator so that the dynamic coupling effect can be safely neglected in the simulations. The Mini manipulator was designed to have a set of

similar parameters as the Macro manipulator. See Table 2.1 for a full list of the assumed link lengths and masses.

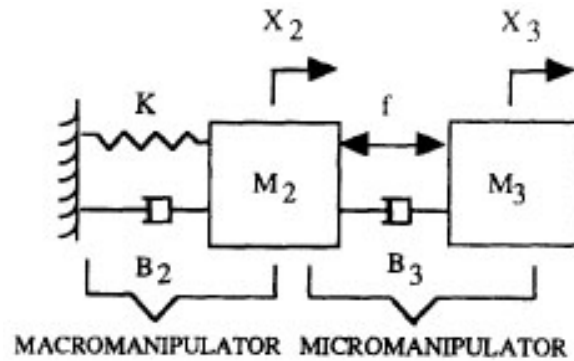


Figure 2.2 Model of a one-axis Macro-Micro manipulator [2]

The Macro manipulator controller sample time is chosen to be 10 ms, which is a typical value for robot manipulators. The Mini manipulator has a sample time of 1 ms, which one tenth of that for the Macro manipulator. With this parameter set, we are expecting to see a much faster response of the Mini manipulator than that of the Macro manipulator.

Table 2.1 Parameters of Macro and Mini manipulators

Manipulator Model	Link Length Matrix (m)	Link Mass Matrix (kg)	Joint Limit (degree)	Joint Error Limit (rad)	Sample Time (ms)	Max. Continuous Torque (Nm)
Macro	[0 1 1]	[0 1 1]	(0°,360°)	$\pm 10^{-3}$	10	50
Mini	[0 0.1 0.1]	[0 0.1 0.1]	(0°,360°)	$\pm 10^{-5}$	1	5

It is assumed there is no joint limit for all joints. Maximum continuous torque is arbitrarily chosen. It is used for examples only. The real numbers can be found from

robot specifications. Noise is added to joint positions to enhance the realism in simulations. The joint error limits are arbitrarily chosen. Intuitively, the Macro manipulator can exert larger torque and has larger joint position errors than the Mini manipulator.

2.3 Robot workspace analysis

Macro manipulator

Since there is no limit set on joint positions, the workspace of Macro manipulator is shown in Figure 2.3. It is a sphere with radius $R=2\text{m}$.

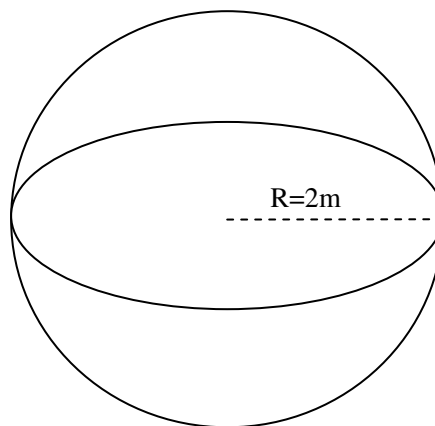


Figure 2.3 Workspace of Macro manipulator

Mini manipulator

The workspace of Mini manipulator is shown in Figure 2.4. Similarly, it is a sphere with radius $r=0.2\text{m}$.

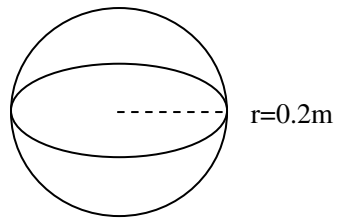


Figure 2.4 Workspace of Mini manipulator

Chapter 3

Kinematics, Dynamics and Control of Macro manipulator

The Macro manipulator has poorer accuracy, larger workspace, and slower response, as compared to the Mini manipulator. The kinematics and dynamics model are firstly studied and a software model of the Macro manipulator is built. The manipulator software model behavior is based on its kinematics and dynamics. An operational space framework [16] [17] is used to control the manipulator for a goal positioning task and a quintic trajectory tracking task. The simulation work is performed using Matlab and the performance of the Macro robot is analyzed.

3.1 Kinematic model of the Macro robot

The development of kinematic model of the Macro robot starts with frame assignment. We follow the Denavit-Hartenberg (D-H) convention shown by Fu et al [8] to assign frames to the Macro robot.

Following procedure to form frame $O_i - x_i y_i z_i$ (attached to link i) is used:

1. Origin of the i th coordinate frame O_i is located at the intersection of joint axis $i+1$ and the common normal between joint axis i and $i+1$;
2. x_i axis is directed along the extension line of the common normal;
3. z_i is along the joint axis $i+1$; and

4. y_i axis is chosen such that the resultant frame $O_i - x_i y_i z_i$ forms a right-hand coordinate system.

In the Macro robot, Frame 0 is attached to the ground and serves as the reference frame. The three joint coordinates are defined such that the positive rotation is counter-clockwise along the axis, and their zero positions are with respect to the previous link, frame attachments at the robot's initial position (also known as home position) are shown in Figure 3.1.

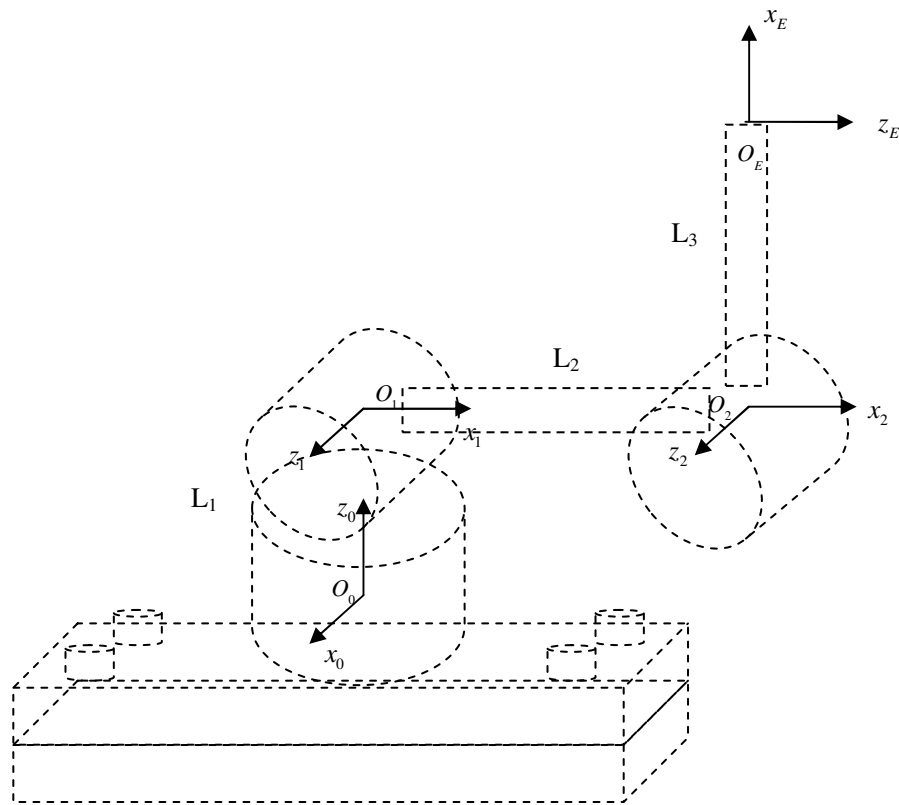


Figure 3.1 Assignment of coordinate frames to the Macro robot at the robot's home position

Transformation matrix from Frame E to Frame 0 is derived as follows,

$${}^0T_E = {}^0T_1 {}^1T_2 {}^2T_E \quad (3.1)$$

According to D-H representation, the homogeneous transformation matrix from Frame i to Frame $i-1$ is in the following form,

$${}^{i-1}T_i = \begin{bmatrix} \cos \theta_i & -\sin \theta_i \cos \alpha_i & \sin \theta_i \sin \alpha_i & a_i \cos \theta_i \\ \sin \theta_i & \cos \theta_i \cos \alpha_i & -\cos \theta_i \sin \alpha_i & a_i \sin \theta_i \\ 0 & \sin \alpha_i & \cos \alpha_i & d_i \\ 0 & 0 & 0 & 1 \end{bmatrix} \quad (3.2)$$

The four parameters $a_i, d_i, \alpha_i, \theta_i$ in equation (3.2) are called D-H parameters. They are defined as follows. Figure 3.2 illustrates how to get D-H parameters.

- a_i Length of common normal
- d_i Distance between the origin O_{i-1} & point H_i
- α_i Angle between the joint axis i and z_i axis (in the right hand sense)
- θ_i Angle between x_{i-1} and the common normal $H_i O_i$ measured about z_{i-1} axis (in the right hand sense)

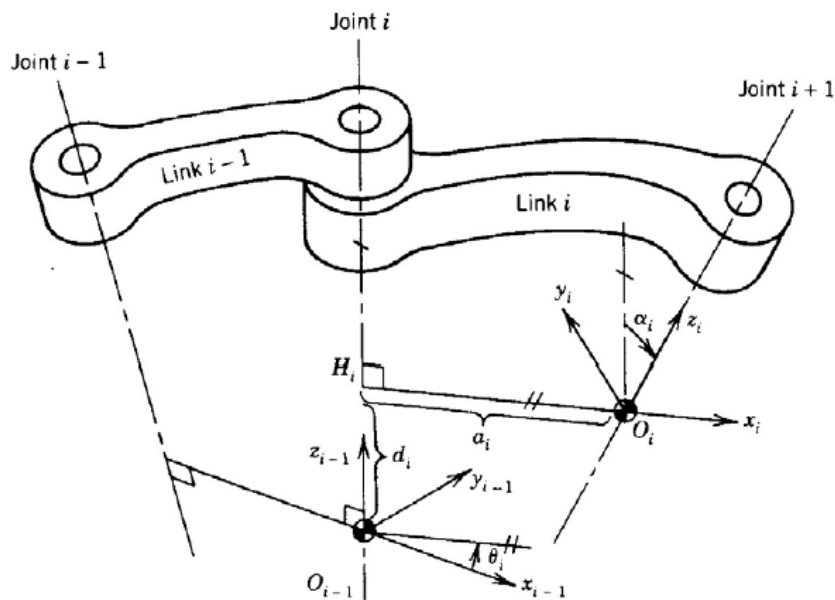


Figure 3.2 Denavit-Hartenberg (D-H) frame assignment [8]

From Figure 3.1, we get the values of D-H parameters for the Macro manipulator as follows:

Table 3.1 D-H parameters for the Macro manipulator

Link	θ_i (rad)	d_i (m)	a_i (m)	α_i (rad)
1	$\frac{\pi}{2} + q_1$	$L_1 = 0$	0	$\frac{\pi}{2}$
2	q_2	0	$L_2 = 1$	0
3	$\frac{\pi}{2} + q_3$	0	$L_3 = 1$	$\frac{\pi}{2}$

where q_1 , q_2 and q_3 are the generalized positions for joint 1, 2 and 3, respectively.

Applying equation (3.2) and substituting the values of the kinematic parameters from

Table 3.1, we have,

$${}^0T_1 = \begin{bmatrix} -s1 & 0 & c1 & 0 \\ c1 & 0 & s1 & 0 \\ 0 & 1 & 0 & 0 \\ 0 & 0 & 0 & 1 \end{bmatrix} \quad {}^1T_2 = \begin{bmatrix} c2 & -s2 & 0 & c2 \\ s2 & c2 & 0 & s2 \\ 0 & 0 & 1 & 0 \\ 0 & 0 & 0 & 1 \end{bmatrix}$$

$${}^2T_E = \begin{bmatrix} -s3 & 0 & c3 & -s3 \\ c3 & 0 & s3 & c3 \\ 0 & 1 & 0 & 0 \\ 0 & 0 & 0 & 1 \end{bmatrix} \quad {}^0T_2 = \begin{bmatrix} -s1c2 & s1s2 & c1 & -s1c2 \\ c1c2 & -c1s2 & s1 & c1c2 \\ s2 & c2 & 0 & s2 \\ 0 & 0 & 0 & 1 \end{bmatrix}$$

Applying Equation 3.1, we have the complete transformation from Frame 0 to Frame E

as follows,

$${}^0T_E = \begin{bmatrix} -\frac{1}{2}c123 + \frac{1}{2}c(1-2-3) & c1 & -\frac{1}{2}s123 - \frac{1}{2}s(1-2-3) & -\frac{1}{2}c123 + \frac{1}{2}c(1-2-3) - \frac{1}{2}s12 - \frac{1}{2}s(1-2) \\ \frac{1}{2}s(1-2-3) - \frac{1}{2}s123 & s1 & \frac{1}{2}c(1-2-3) + \frac{1}{2}c123 & \frac{1}{2}s(1-2-3) - \frac{1}{2}s123 + \frac{1}{2}c(1-2) + \frac{1}{2}c12 \\ c23 & 0 & s23 & c23 + s2 \\ 0 & 0 & 0 & 1 \end{bmatrix}$$

The following shows the equivalent expressions used in the above result and throughout this thesis.

$$c1 = \cos(q1), c2 = \cos(q2), c3 = \cos(q3), s1 = \sin(q1), s2 = \sin(q2), s3 = \sin(q3)$$

$$c12 = \cos(q1+q2), s12 = \sin(q1+q2), c(1-2) = \cos(q1-q2), s(1-2) = \sin(q1-q2)$$

$$c123 = \cos(q1+q2+q3), s123 = \sin(q1+q2+q3)$$

$$c(1-2-3) = \cos(q1-q2-q3), s(1-2-3) = \sin(q1-q2-q3)$$

Velocity of the end-effector

Velocity of the end-effector comprises of linear and angular components,

$$\begin{pmatrix} v \\ \omega \end{pmatrix}_{6 \times 1} = J(q)_{6 \times n} \dot{q}_{n \times 1} \quad (3.3)$$

where v and ω are the linear and angular velocity vectors respectively. n is the number of degrees-of-freedom. $J(q)$ is the Jacobian matrix whose elements are

$$J_{ij}(q) = \frac{\partial}{\partial q_i} G_j(q)$$

The Jacobian matrix $J(q)$ is computed as follows,

$$J(q) = \begin{pmatrix} \frac{\partial x_p}{\partial q_1} & \frac{\partial x_p}{\partial q_2} & \dots & \frac{\partial x_p}{\partial q_n} \\ \bar{\varepsilon}_1 \cdot Z_1 & \bar{\varepsilon}_2 \cdot Z_2 & \dots & \bar{\varepsilon}_n \cdot Z_n \end{pmatrix} \quad (3.4)$$

The binary parameter $\bar{\varepsilon}_i$ is defined as follows,

$$\bar{\varepsilon}_i = \begin{cases} 1 & \text{for a revolute joint } \theta_i \\ 0 & \text{for a prismatic joint } \rho_i \end{cases}$$

$$Z_i = {}^0R_i {}^iZ_i = {}^0R_i Z, \quad Z = \begin{bmatrix} 0 \\ 0 \\ 1 \end{bmatrix}$$

The Jacobian matrix expressed in Base Frame is called **Basic Jacobian** 0J .

$${}^0J = \begin{pmatrix} \frac{\partial^0 x_p}{\partial q_1} & \frac{\partial^0 x_p}{\partial q_2} & \dots & \frac{\partial^0 x_p}{\partial q_n} \\ \bar{\varepsilon}_1 ({}^0R_1 Z) & \bar{\varepsilon}_2 ({}^0R_2 Z) & \dots & \bar{\varepsilon}_n ({}^0R_n Z) \end{pmatrix} \quad (3.5)$$

where

$$\frac{\partial^0 x_p}{\partial q_i} = (1 - \bar{\varepsilon}_i) Z_{i-1} + \bar{\varepsilon}_i (Z_{i-1} \times P_{in}) \quad (3.6)$$

P_{in} is a vector from origin of Frame i to origin of Frame n .

Applying equation (3.5) to the Macro robot, we have

$${}^0J_M = \begin{pmatrix} Z_0 \times P_{0E} & Z_1 \times P_{1E} & Z_2 \times P_{2E} \\ Z_0 & Z_1 & Z_2 \end{pmatrix}$$

$$Z_0 = \begin{bmatrix} 0 \\ 0 \\ 1 \end{bmatrix}$$

$$Z_1 = \begin{bmatrix} c1 \\ s1 \\ 0 \end{bmatrix}$$

$$Z_2 = \begin{bmatrix} c1 \\ s1 \\ 0 \end{bmatrix}$$

Then we get the **Basic Jacobian** of Macro manipulator in its Base Frame, i.e. Frame 0.

It is denoted by 0J_M .

$${}^0J_M = \begin{bmatrix} s_3c_1c_2+c_3c_1s_2-c_1c_2 & \frac{1}{2}s_{123}+\frac{1}{2}s_{(1-2-3)}-\frac{1}{2}c_{12}+\frac{1}{2}c_{(1-2)} & \frac{1}{2}s_{123}+\frac{1}{2}s_{(1-2-3)} \\ c_3s_1s_2+s_3s_1c_2-s_1c_2 & -\frac{1}{2}c_{123}-\frac{1}{2}c_{(1-2-3)}-\frac{1}{2}s_{12}+\frac{1}{2}s_{(1-2)} & -\frac{1}{2}c_{123}-\frac{1}{2}c_{(1-2-3)} \\ 0 & -s_{23}+c_2 & -s_{23} \\ 0 & c_1 & c_1 \\ 0 & s_1 & s_1 \\ 1 & 0 & 0 \end{bmatrix}$$

Linear velocity for the Macro manipulator at its end-effector in its Base Frame, i.e.

Frame 0 is denoted by 0v_M ,

$${}^0J_M = \begin{bmatrix} {}^0J_{Mv} \\ {}^0J_{M\omega} \end{bmatrix} \quad (3.7)$$

$${}^0v_M = {}^0J_{Mv}\dot{q}_M \quad (3.8)$$

$${}^0v_M = \begin{bmatrix} c_1c_2s_3+c_1s_2c_3-c_1c_2 & \frac{1}{2}s_{123}+\frac{1}{2}s_{(1-2-3)}-\frac{1}{2}c_{12}+\frac{1}{2}c_{(1-2)} & \frac{1}{2}s_{123}+\frac{1}{2}s_{(1-2-3)} \\ s_1s_2c_3+s_1c_2s_3-s_1c_2 & -\frac{1}{2}c_{123}-\frac{1}{2}c_{(1-2-3)}-\frac{1}{2}s_{12}+\frac{1}{2}s_{(1-2)} & -\frac{1}{2}c_{123}-\frac{1}{2}c_{(1-2-3)} \\ 0 & -s_{23}+c_2 & -s_{23} \end{bmatrix} \begin{bmatrix} \dot{q}_1 \\ \dot{q}_2 \\ \dot{q}_3 \end{bmatrix}$$

3.2 Dynamic model of the Macro robot

To derive a dynamic controller for Macro manipulator system, a relationship between an input torque vector and the joint position vector is calculated in this subsection.

Dynamic model of the robot is derived using **Lagrange** Equation. The equations of motion in joint space of an n-degrees-of-freedom manipulator are

$$\frac{d}{dt} \left(\frac{\partial K}{\partial \dot{q}} \right) - \frac{\partial K}{\partial q} = \tau - G \quad (3.9)$$

where K is the total kinetic energy of the manipulator. G is the gravity vector. τ is the generalized force vector.

Equation 3.9 can also be rewritten as follows,

$$M(q)\ddot{q} + V(q, \dot{q}) = \tau - G(q) \quad (3.10)$$

$M(q)$ is called the **Inertia Matrix**. It is calculated as follows,

$$M = \sum_{i=1}^3 \left(m_i J_{v_i}^T J_{v_i} + J_{\omega_i}^T {}^0 R_{C_i} I_{C_i} {}^0 R_{C_i}^T J_{\omega_i} \right) \quad (3.11)$$

where m_i is the mass of link i . C_i is the center of mass of link i . I_{C_i} is the inertia matrix of link i expressed in Frame C_i . ${}^U R_{C_i}$ is the rotation matrix that rotates the expressions in Frame C_i to Base Frame 0.

$V(q, \dot{q})$ is called the **Coriolis and Centrifugal terms**. It is calculated as follows,

$$V(q, \dot{q}) = \dot{M}\dot{q} - \frac{1}{2} \begin{bmatrix} \dot{q}^T \frac{\partial M}{\partial q_1} \dot{q} \\ \vdots \\ \dot{q}^T \frac{\partial M}{\partial q_n} \dot{q} \end{bmatrix} \quad (3.12)$$

The **Jacobian matrix** J_{v_i} can be directly obtained by differentiating the position vector p_{C_i} , which locates the center-of-mass of link i with respect to the manipulator base, as shown in Figure 3.3

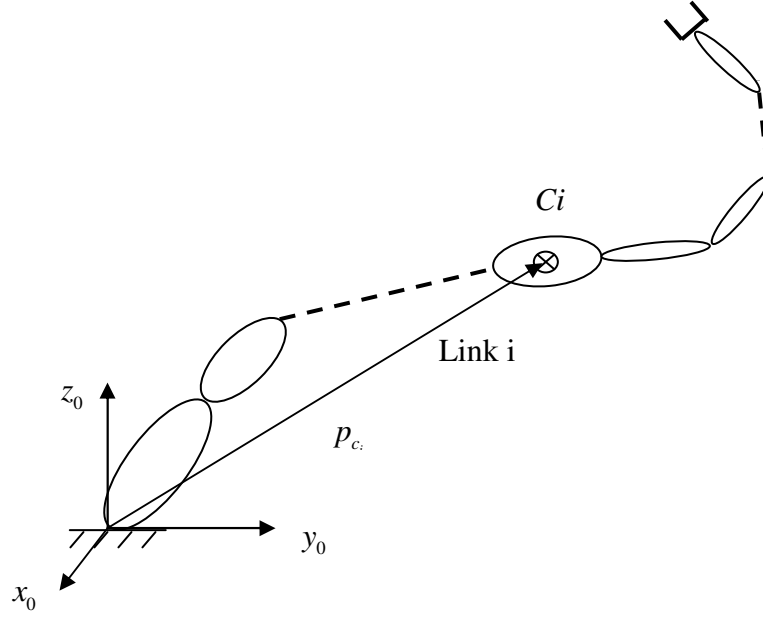


Figure 3.3 Position of center of mass

$$J_{v_i}(q) = \begin{bmatrix} \frac{\partial p_{C_i}}{\partial q_1} & \frac{\partial p_{C_i}}{\partial q_2} & \dots & \frac{\partial p_{C_i}}{\partial q_i} & 0 & 0 & \dots & 0 \end{bmatrix} \quad (3.13)$$

The matrix J_{v_i} can also be obtained from the general form,

$$J_{v_i}(q) = \begin{bmatrix} (1 - \bar{\epsilon}_1)Z_0 + \bar{\epsilon}_1 Z_0 \times p_{1c_i} & \dots & (1 - \bar{\epsilon}_i)Z_{i-1} + \bar{\epsilon}_i Z_{i-1} \times p_{jc_i} & 0 & \dots & 0 \end{bmatrix} \quad (3.14)$$

where p_{jc_i} is the vector connecting joint j to C_i , as shown in Figure 3.3.

$$P_{01} = \begin{bmatrix} 0 \\ 0 \\ 0 \end{bmatrix} \quad P_{02} = \begin{bmatrix} -s1c2 \\ c1c2 \\ s2 \end{bmatrix} \quad P_{03} = \begin{bmatrix} -\frac{1}{2}c123 + \frac{1}{2}c(1-2-3) - \frac{1}{2}s12 - \frac{1}{2}s(1-2) \\ -\frac{1}{2}s123 + \frac{1}{2}s(1-2-3) + \frac{1}{2}c12 + \frac{1}{2}c(1-2) \\ c23 + s2 \end{bmatrix}$$

Because the Macro manipulator has 3 point mass at the end of each joint, $m_1 = 0$ kg,

$m_2 = 1$ kg, $m_3 = 1$ kg, p_{jc_i} can easily be obtained from the following equation

$$p_{jc_i} = P_{(j-1)i}$$

P_{ij} is the vector from origin of Frame i to origin of Frame j . which can be obtained from the last column of the transformation matrices ${}^i T_j$.

$$J_{v_1} = \begin{bmatrix} \frac{\partial p_{c_1}}{\partial q_1} & 0 & 0 \end{bmatrix} = [Z_0 \times P_{01} \quad 0 \quad 0]$$

$$J_{v_2} = \begin{bmatrix} \frac{\partial p_{c_2}}{\partial q_1} & \frac{\partial p_{c_2}}{\partial q_2} & 0 \end{bmatrix} = [Z_0 \times P_{02} \quad Z_1 \times P_{12} \quad 0]$$

$$J_{v_3} = \begin{bmatrix} \frac{\partial p_{c_3}}{\partial q_1} & \frac{\partial p_{c_3}}{\partial q_2} & \frac{\partial p_{c_3}}{\partial q_3} \end{bmatrix} = [Z_0 \times P_{03} \quad Z_1 \times P_{13} \quad Z_2 \times P_{23}]$$

$$J_{v_1} = \begin{bmatrix} 0 & 0 & 0 \\ 0 & 0 & 0 \\ 0 & 0 & 0 \end{bmatrix}$$

$$J_{v_2} = \begin{bmatrix} -c_1 c_2 & s_1 s_2 & 0 \\ -s_1 c_2 & -c_1 s_2 & 0 \\ 0 & c_2 & 0 \end{bmatrix}$$

$$J_{v_3} = \begin{bmatrix} c_1 c_2 s_3 + c_1 s_2 c_3 - c_1 c_2 & \frac{1}{2} s_1 23 + \frac{1}{2} s(1-2-3) - \frac{1}{2} c_1 2 + \frac{1}{2} c(1-2) & \frac{1}{2} s_1 23 + \frac{1}{2} s(1-2-3) \\ s_1 s_2 c_3 + s_1 c_2 s_3 - s_1 c_2 & -\frac{1}{2} c_1 23 - \frac{1}{2} c(1-2-3) - \frac{1}{2} s_1 2 + \frac{1}{2} s(1-2) & -\frac{1}{2} c_1 23 - \frac{1}{2} c(1-2-3) \\ 0 & -s_2 3 + c_2 & -s_2 3 \end{bmatrix}$$

The **Jacobian matrix** J_{ω_i} is given by

$$J_{\omega_i} = [\bar{\varepsilon}_1 Z_0 \quad \bar{\varepsilon}_2 Z_1 \quad \cdots \quad \bar{\varepsilon}_i Z_{i-1} \quad 0 \quad 0 \quad \cdots \quad 0] \quad (3.15)$$

$$J_{\omega_1} = [Z_0 \quad 0 \quad 0] = \begin{bmatrix} 0 & 0 & 0 \\ 0 & 0 & 0 \\ 1 & 0 & 0 \end{bmatrix}$$

$$J_{\omega_2} = [Z_0 \quad Z_1 \quad 0] = \begin{bmatrix} 0 & c1 & 0 \\ 0 & s1 & 0 \\ 1 & 0 & 0 \end{bmatrix}$$

$$J_{\omega_3} = [Z_0 \quad Z_1 \quad Z_2] = \begin{bmatrix} 0 & c1 & c1 \\ 0 & s1 & s1 \\ 1 & 0 & 0 \end{bmatrix}$$

Inertia tensor of link i ($i = 1, 2, 3$) is given by

$$I_{Ci} = {}^0R_{Ci} \begin{pmatrix} I_{xxi} & 0 & 0 \\ 0 & I_{yyi} & 0 \\ 0 & 0 & I_{zzi} \end{pmatrix} {}^0R_{Ci}^T \quad (3.16)$$

where I_{xxi} , I_{yyi} , I_{zzi} are the moment of inertia about the principle axis of the hollow cylinder. ${}^0R_{Ci}$ is the rotational matrix that transforms the expressions in Frame Ci to Frame 0. And Ci is the center of mass of i^{th} link.

Since the mass of each link is centered at one single point mass, the moment of inertia of each link is zero.

$$I_{Ci} = {}^0R_{Ci} \begin{pmatrix} I_{xxi} & 0 & 0 \\ 0 & I_{yyi} & 0 \\ 0 & 0 & I_{zzi} \end{pmatrix} {}^0R_{Ci}^T = \begin{pmatrix} 0 & 0 & 0 \\ 0 & 0 & 0 \\ 0 & 0 & 0 \end{pmatrix}$$

Then we have the Inertia Mass Matrix for the Macro manipulator,

$$M = \sum_{i=1}^3 (m_i J_{v_i}^T J_{v_i} + J_{\omega_i}^T {}^0R_{Ci} I_{Ci} {}^0R_{Ci}^T J_{\omega_i}) = \sum_{i=1}^3 m_i J_{v_i}^T J_{v_i} \quad (3.17)$$

$$M(q) = \begin{bmatrix} \frac{3}{2} - \frac{1}{2} \cos(2q_3 + 2q_2) - s_3 - \sin(q_3 + 2q_2) + \cos(2q_2) & 0 & 0 \\ 0 & 3 - 2s_3 & 1 - s_3 \\ 0 & 1 - s_3 & 1 \end{bmatrix}$$

Centrifugal and Coriolis terms

Using the **Christoffel symbols**, the vector $b(q, \dot{q})$ can be obtained from the partial derivatives of $M(q)$ and the generalized velocities, \dot{q} . The **Christoffel symbols** are

$$b_{ijk} = \frac{1}{2}(m_{ijk} + m_{ikj} - m_{jki})$$

where m_{ijk} is the partial derivative with respect to q_k of the $\{ij\}$ element of the matrix $M(q)$.

$$m_{ijk} = \frac{\partial m_{ij}}{\partial q_k} \quad (3.18)$$

Using the **Christoffel symbols**, the centrifugal and Coriolis force vector can be written as

$$V(q, \dot{q}) = C(q)[\dot{q}^2] + B(q)[\dot{q}\dot{q}] \quad (3.19)$$

where $B(q)$ is the $n \times \frac{n(n-1)}{2}$ matrix associated with the Coriolis term given by

$$B(q) = 2 \times \begin{bmatrix} b_{1,12} & \cdots & b_{1,1n} & b_{1,23} & \cdots & b_{1,2n} & \cdots & b_{1,(n-1)n} \\ b_{2,12} & \cdots & b_{2,1n} & b_{2,23} & \cdots & b_{2,2n} & \cdots & b_{2,(n-1)n} \\ \vdots & \vdots & \vdots & \vdots & \vdots & \vdots & \vdots & \vdots \\ b_{n,12} & \cdots & b_{n,1n} & b_{n,23} & \cdots & b_{n,2n} & \cdots & b_{n,(n-1)n} \end{bmatrix} \quad (3.20)$$

and $C(q)$ is the $n \times n$ matrix associated with the centrifugal term given by

$$C(q) = \begin{bmatrix} b_{1,11} & b_{1,22} & \cdots & b_{1,nn} \\ b_{2,11} & b_{2,22} & \cdots & b_{2,nn} \\ \vdots & \vdots & \vdots & \vdots \\ b_{n,11} & b_{n,22} & \cdots & b_{n,nn} \end{bmatrix} \quad (3.21)$$

$[\dot{q}^2]$ and $[\dot{q}\dot{q}]$ are the symbolic notations for the $\frac{n(n-1)}{2} \times 1$ and $n \times 1$ column matrices

$$[\dot{q}^2] = [\dot{q}_1^2 \quad \dot{q}_2^2 \quad \cdots \quad \dot{q}_n^2]^T \quad (3.22)$$

and

$$[\dot{q}\dot{q}] = [\dot{q}_1\dot{q}_2 \quad \dot{q}_1\dot{q}_3 \quad \cdots \quad \dot{q}_1\dot{q}_n \quad \dot{q}_2\dot{q}_3 \quad \dot{q}_2\dot{q}_4 \quad \cdots \quad \dot{q}_2\dot{q}_n \quad \cdots \quad \dot{q}_{n-1}\dot{q}_n]^T \quad (3.23)$$

Apply Equations (3.20) and (3.21), the following can be obtained for the Macro robot,

$$B(q) = \begin{bmatrix} -2 \cdot \cos(q_3+2 \cdot q_2) - 2 \cdot \sin(2 \cdot q_2) + \sin(2 \cdot q_3+2 \cdot q_2), & -c_3 - \cos(q_3+2 \cdot q_2) + \sin(2 \cdot q_3+2 \cdot q_2) & 0 \\ 0 & 0 & -2c_3 \\ 0 & 0 & 0 \end{bmatrix}$$

$$C(q) = \begin{bmatrix} 0 & 0 & 0 \\ \cos(q_3+2 \cdot q_2) + \sin(2 \cdot q_2) - \frac{1}{2} \sin(2 \cdot q_3+2 \cdot q_2) & 0 & -c_3 \\ \frac{1}{2} c_3 + \frac{1}{2} \cos(q_3+2 \cdot q_2) - \frac{1}{2} \sin(2 \cdot q_3+2 \cdot q_2) & c_3 & 0 \end{bmatrix}$$

Gravity terms

Gravity term is given by

$$G(q) = -\left(J_{v1}^T m_1 g + J_{v2}^T m_2 g + \cdots + J_{vn}^T m_n g \right) \quad (3.24)$$

$$G(q) = \begin{bmatrix} 0 \\ 19.62 \cdot c_2 - 9.81 \cdot s_2 \\ -9.81 \cdot s_2 \end{bmatrix}$$

$g = [0 \ 0 \ -9.81]^T$ is specified in Frame 0.

Equations of Motion

The equations of motion is in the form

$$M(q)\ddot{q} + V(q, \dot{q}) + G(q) = \tau \quad (3.25)$$

Apply Equation (3.25) to the Macro robot, we get

$$\begin{aligned}
& \begin{bmatrix} \frac{3}{2} - \frac{1}{2} \cos(2q_3+2q_2) - s_3 - \sin(q_3+2q_2) + \cos(2q_2) & 0 & 0 \\ 0 & 3-2s_3 & 1-s_3 \\ 0 & 1-s_3 & 1 \end{bmatrix} \begin{bmatrix} \ddot{q}_1 \\ \ddot{q}_2 \\ \ddot{q}_3 \end{bmatrix} + \\
& \begin{bmatrix} 0 & 0 & 0 \\ \cos(q_3+2q_2) + \sin(2q_2) - \frac{1}{2} \sin(2q_3+2q_2) & 0 & -c_3 \\ \frac{1}{2} c_3 + \frac{1}{2} \cos(q_3+2q_2) - \frac{1}{2} \sin(2q_3+2q_2) & c_3 & 0 \end{bmatrix} \begin{bmatrix} \dot{q}_1^2 \\ \dot{q}_2^2 \\ \dot{q}_3^2 \end{bmatrix} + \\
& \begin{bmatrix} -2\cos(q_3+2q_2) - 2\sin(2q_2) + \sin(2q_3+2q_2) & -c_3 - \cos(q_3+2q_2) + \sin(2q_3+2q_2) & 0 \\ 0 & 0 & -2c_3 \\ 0 & 0 & 0 \end{bmatrix} \begin{bmatrix} \dot{q}_1 \dot{q}_2 \\ \dot{q}_1 \dot{q}_3 \\ \dot{q}_2 \dot{q}_3 \end{bmatrix} + \\
& \begin{bmatrix} 0 \\ 19.62 \cdot c_2 - 9.81 \cdot s_2 s_3 \\ -9.81 \cdot s_2 s_3 \end{bmatrix} = \begin{bmatrix} \tau_1 \\ \tau_2 \\ \tau_3 \end{bmatrix}
\end{aligned}$$

Operational Space Dynamics

The end-effector equations of motion in operational space can be written [16] [17] in the form

$$\Lambda(x)\ddot{x} + \mu(x, \dot{x}) + p(x) = F \quad (3.26)$$

where $\Lambda(x)$ is the kinetic energy matrix of the system with respect to the operational point, x . $\mu(x, \dot{x})$ represents the centrifugal and Coriolis forces acting at the same operational point, and $p(x)$ depicts the gravitational forces also expressed at that point.

F is the generalized force vector expressed in the operational space.

The relationship between the components of the joint space dynamic model and those of the operational space dynamic model are

$$\Lambda(x) = J^{-T}(q)M(q)J^{-1}(q) \quad (3.27)$$

$$\mu(x, \dot{x}) = J^{-T}(q)V(q) - \Lambda(q)h(q, \dot{q}) \quad (3.28)$$

$$p(x) = J^{-T}(q)G(q) \quad (3.29)$$

where

$$h(q) = \dot{J}(q)\dot{q} \quad (3.30)$$

$$\dot{J}(q) = \frac{dJ(q)}{dt} \quad (3.31)$$

3.3 Operational space Macro manipulator control

3.3.1 Goal position

The task is to control the 3DOF Macro robot end-effector to reach a goal position within its workspace in 3D space. The task is non-redundant with respect to its degree of freedom.

Operational space control

We apply the following control structure,

$$F = \hat{\Lambda}(x)F^* + \hat{\mu}(x, \dot{x}) + \hat{p}(x) \quad (3.32)$$

where $\hat{\Lambda}(x)$, $\hat{\mu}(x, \dot{x})$ and $\hat{p}(x)$ represent the estimates of $\Lambda(x)$, $\mu(x, \dot{x})$ and $p(x)$.

F^* is the control input.

A linear dynamic behavior can be obtained by selecting

$$F^* = -k_v\dot{x} - k_p(x - x_g) \quad (3.33)$$

where x_g is the goal position of the end-effector. k_p and k_v are the PD gains.

Knowing that \dot{x}_g and \ddot{x}_g are zeros, the above dynamic decoupling and motion control result in the following end-effector closed loop behavior,

$$\ddot{\varepsilon} + K_v \dot{\varepsilon} + K_p \varepsilon = 0 \quad (3.34)$$

where

$$\varepsilon = x - x_g \quad (3.35)$$

The following working shows how the closed loop behavior is obtained

Assume we have an exact dynamic model of the robot,

$$\hat{\Lambda}(x) = \Lambda(x), \hat{\mu}(x, \dot{x}) = \mu(x, \dot{x}) \quad \text{and} \quad \hat{p}(x) = p(x)$$

from

$$\Lambda(x) \ddot{x} + \mu(x, \dot{x}) + p(x) = \hat{\Lambda}(x) F^* + \hat{\mu}(x, \dot{x}) + \hat{p}(x)$$

we get

$$\ddot{x} = F^* = -k_v \dot{x} - k_p (x - x_g)$$

The closed loop system is a second order system. In Laplace domain, it is

$$(s^2 + 2\xi\omega_n s + \omega_n^2)\varepsilon = 0 \quad (3.36)$$

where ω_n is the natural frequency of the second order system. ξ is the dumping ratio.

Choose the following value for the gains

$$k_p = \omega_n^2 \quad (3.37)$$

$$k_v = 2\xi\omega_n \quad (3.38)$$

Figure 3.4 illustrates the control structure.

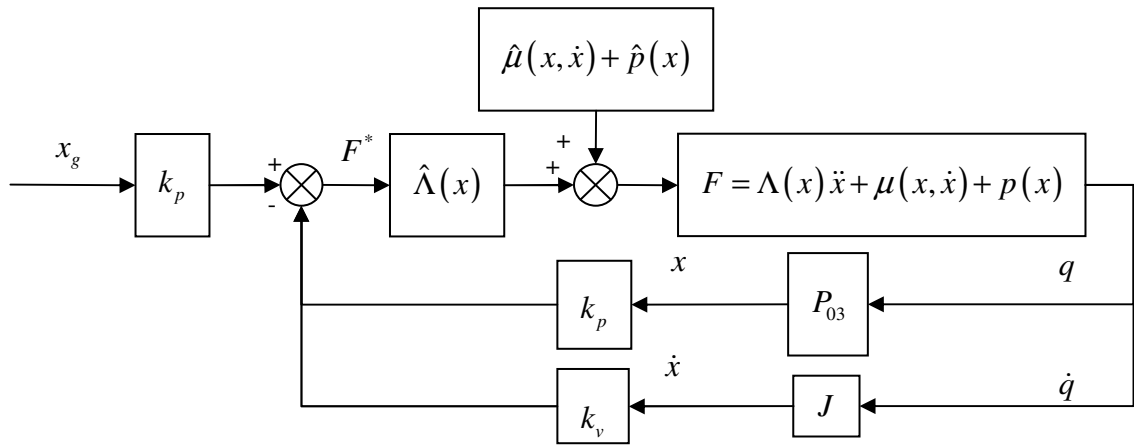


Figure 3.4 Goal Position control block diagram of the Macro robot, in time domain

Assume we have sensors to measure q and \dot{q} , from which we can compute tip position P_{03} by knowing forward kinematics. P_{03} is composed of the first three rows of the last column in Matrix T_{03} . We can also compute \dot{x} from \dot{q} using Basic Jacobian (Equation (3.3)).

Simulation

The simulation platform is created using MATLAB. We arbitrarily choose $[0.1679 \ -0.7571 \ 0.4255]$ as the goal position. Maximum continuous torque is set to 50(Nm). This number is often determined by the physical limits of real-life robots, which can be found in robot specifications. Depending on the motor type, gear ratio, and other motor attributes, this number may vary. The 50 (Nm) maximum continuous torque is used as an example only. In the simulation, if the computed torque acquired by Equation (3.25),

the end-effector equations of motion in joint space, exceeds the maximum continuous torque, it is set at the maximum 50(Nm). Random noise of up to 10^{-3} rad is added to joint positions, to make the simulation more realistic and closer to real robots. Sampling time is chosen as 10(ms). The following set of parameters is used for computation of PD gains: $\omega_n = 30, \xi = 1$.

The simulation results using this set of parameters are shown in Figure 3.5.

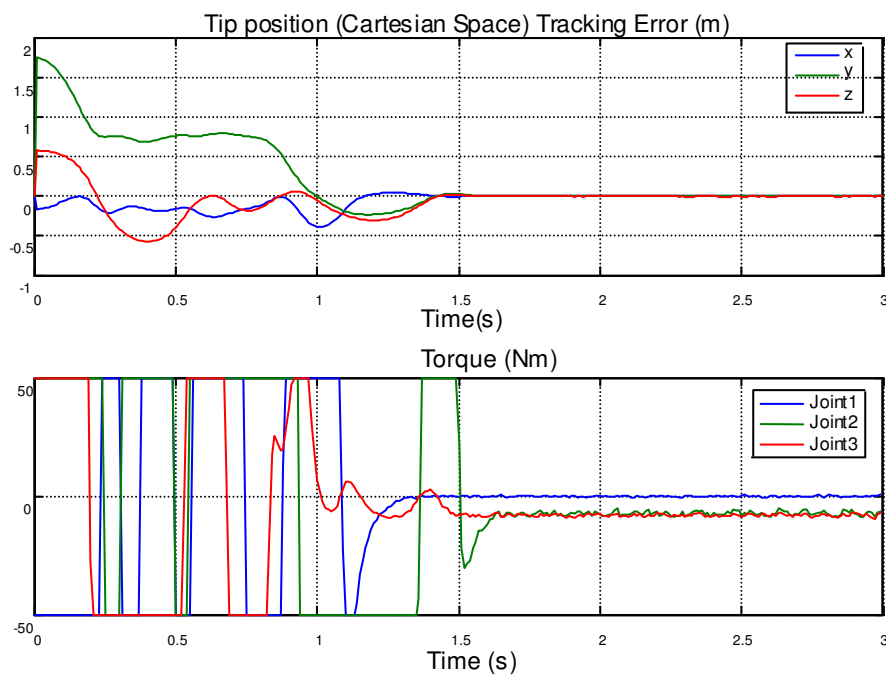


Figure 3.5 Torque of each joint and tip position error in x, y and z directions for Macro goal position control

Conclusion

The response is similar to a second-order system reference input response. After about 1.4 seconds, the tip reaches the goal position and stays there. The steady state error is about $0\sim 9\times 10^{-3}$ m.

3.3.2 Trajectory tracking

The task is to control the 3DOF Macro robot end-effector to follow 3D trajectory. The starting and ending points are given, a fifth order quintic curve is then generated between the starting and ending point.

Trajectory generation

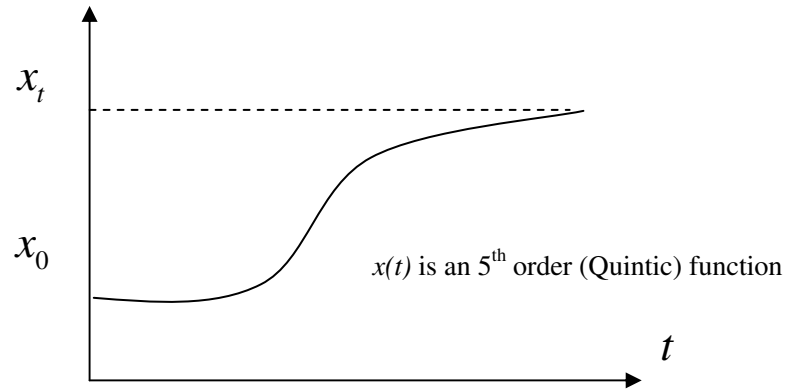


Figure 3.6 A quintic curve in x direction

Define the trajectory as a quintic curve in x , y , and z directions. In x direction, the equation is

$$x(t) = c_0 + c_1t + c_2t^2 + c_3t^3 + c_4t^4 + c_5t^5 \quad (3.39)$$

At time $t=0$, and $t=t_f$ we have the following initial and ending conditions, respectively,

$$t = 0 \quad \begin{cases} x = x_0 \\ \dot{x} = 0 \\ \ddot{x} = 0 \end{cases} \quad t = t_f \quad \begin{cases} x = x_t \\ \dot{x} = 0 \\ \ddot{x} = 0 \end{cases}$$

Put these conditions into Equation (3.39), we can then solve for c_i using the follows,

$$\left\{ \begin{array}{l} c_0 = x_1 \\ c_1 = 0 \\ c_2 = 0 \\ c_0 + c_1 t_f + c_2 t_f^2 + c_3 t_f^3 + c_4 t_f^4 + c_5 t_f^5 = x_2 \\ c_1 + 2c_2 t_f + 3c_3 t_f^2 + 4c_4 t_f^3 + 5c_5 t_f^4 = 0 \\ 2c_2 + 6c_3 t_f + 12c_4 t_f^2 + 20c_5 t_f^3 = 0 \end{array} \right.$$

The same procedures are applied on y and z directions to solve for the coefficients respectively.

Operational space control

For tasks where the desired motion of the end-effector is specified, a linear dynamic behavior can be obtained by selecting

$$F^* = \ddot{x}_d - k_v(\dot{x} - \dot{x}_d) - k_p(x - x_d) \quad (3.40)$$

where x_d , \dot{x}_d and \ddot{x}_d are the desired position, velocity and acceleration, respectively, of the end-effector. k_p and k_v are the position and velocity gains.

Similar to goal position control, the above dynamic decoupling and motion control result in the following end-effector closed loop behavior

$$\ddot{\epsilon} + K_v \dot{\epsilon} + K_p \epsilon = 0 \quad (3.41)$$

where

$$\epsilon = x - x_d \quad (3.42)$$

Figure 3.7 illustrates the control structure.

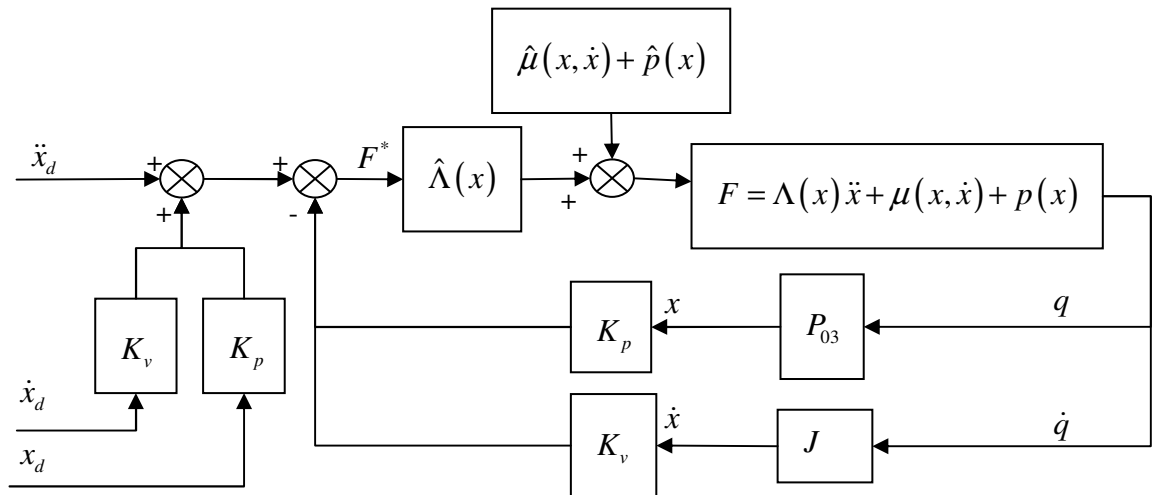


Figure 3.7 Control block diagram of the Macro robot, in time domain

Simulation

For Macro robot, the end-effector starts at its home position $[0 \ 1 \ 1]$, ends at an arbitrary position within its workspace. We use the same set of numbers chosen for goal position control, $[0.1679 \ -0.7571 \ 0.4255]$, as ending position. All other parameters remain the same as those in goal position control. Figure 3.8 shows the desired trajectory, velocity and acceleration generated from the starting and ending points.

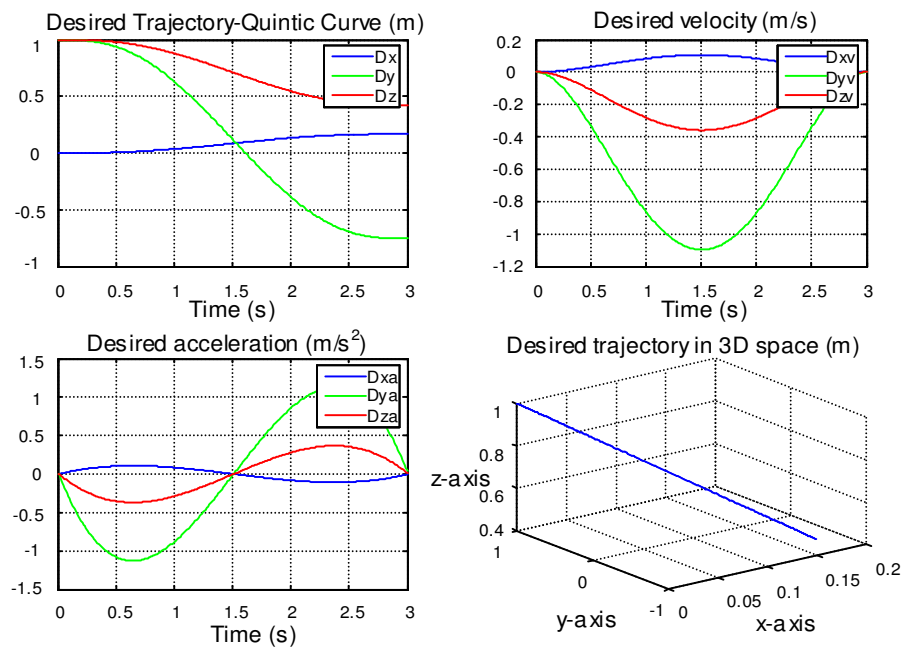


Figure 3.8 Desired trajectory, velocity and acceleration for Macro manipulator

The simulation results using this set of parameters are shown in Figure 3.9.

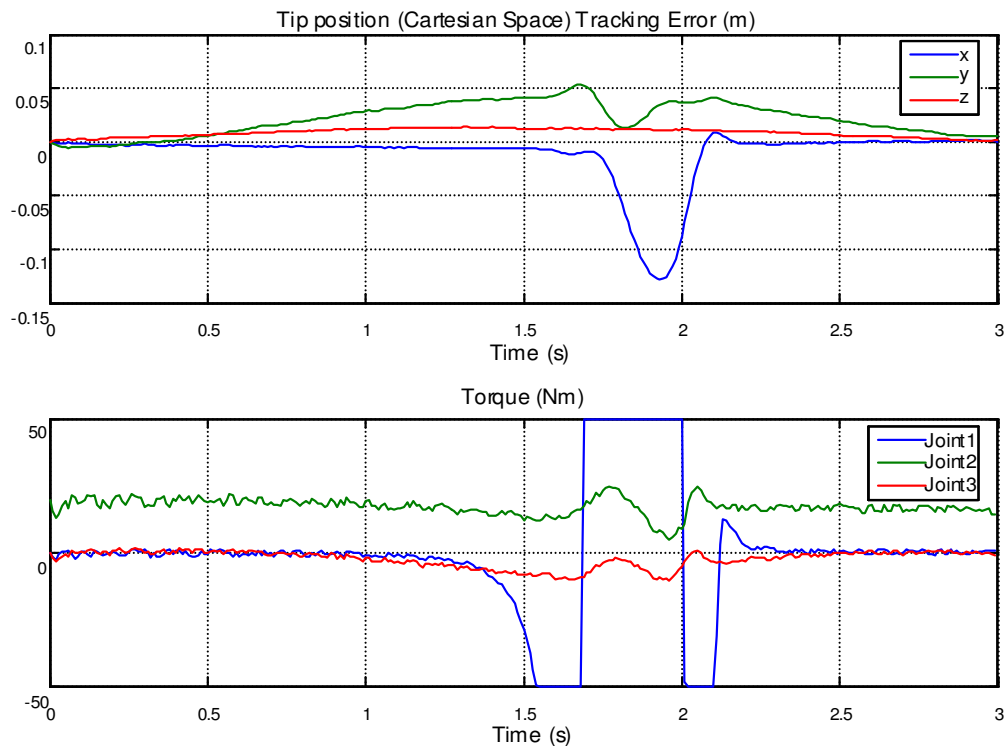


Figure 3.9 Torque of each joint and tip position error in x, y and z directions for Macro trajectory tracking control, with torque limit

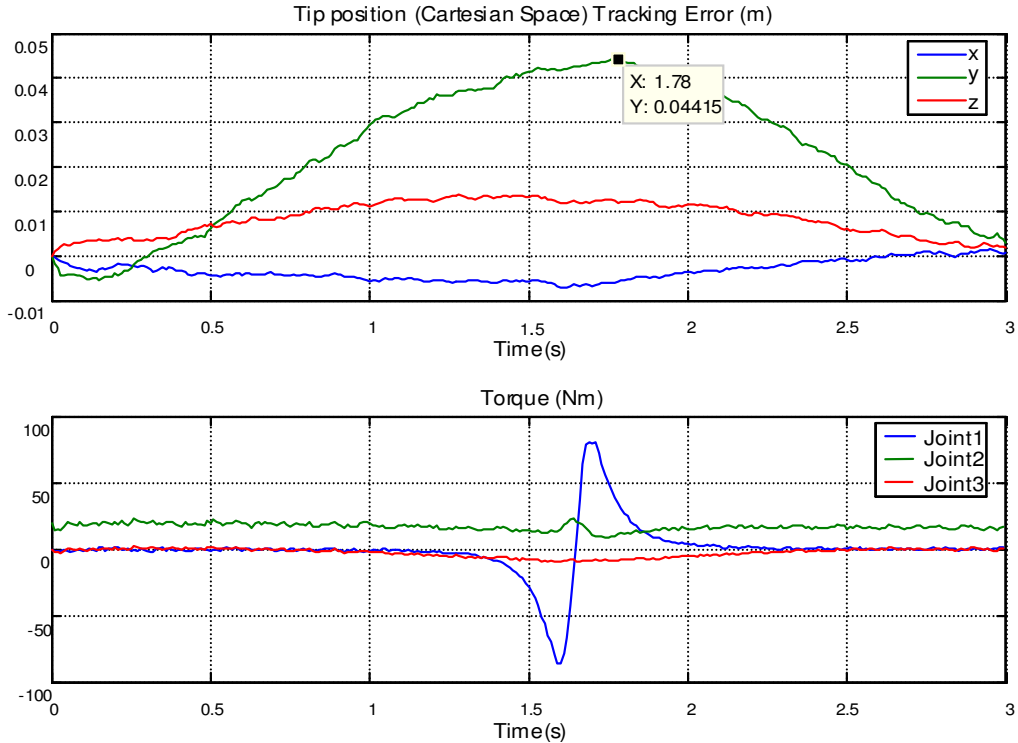


Figure 3.10 Torque of each joint and tip position error in x, y and z directions for Macro trajectory tracking control, without torque limit

Conclusion

In both cases, with or without torque limit, the tip moves along the desired trajectory closely. When the torques applied is limited to 50Nm, maximum tip error ranges from 0.1 to 0.15m. The steady state error is about $0\sim 9\times 10^{-3}$ m.

If there was larger torque limit or no limit imposed on the joints, better control could be achieved, i.e. smaller tip tracking errors are observed. As shown in Figure 3.10, Tip tracking error ranges from 0.007 to 0.044m.

Chapter 4

Kinematics, Dynamics and Control of Mini manipulator

The Mini manipulator is very similar in structure with the Macro manipulator, but has higher accuracy, smaller workspace, and faster response. The same procedures are used to solve for the kinematics and dynamics model of the Mini robot. Results are listed in the following sections. A software model of the Mini manipulator is built on top of the results. Operational space framework is applied for high performance control of the Mini manipulator (goal position and trajectory tracking).

4.1 Kinematic model of the robot

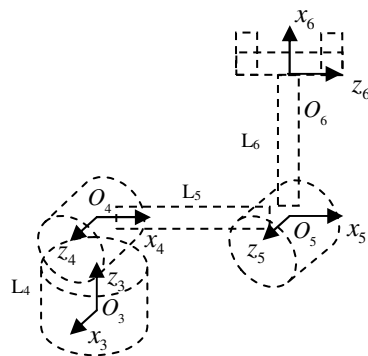


Figure 4.1 Assignment of coordinate frames to the Mini robot at the robot's home position

The numbering for frames attached to the Mini robot is from 3 to 6. Frame 3 serves as

the reference frame of the Mini robot. It refers to the same Frame 3 as in Macro robot frame assignment. The purpose is to be consistent in frame assignments, so that to save computation efforts from transformation from one frame to another. Expression of Frame 6 in Frame 3 is derived as follows,

$${}^3T_6 = {}^3T_4 {}^4T_5 {}^5T_6 \quad (4.1)$$

From the frame assignment in Figure 4.1, we get the values of D-H parameters for the Mini manipulator as follows:

Table 4.1 D-H parameters for the Mini manipulator

Link	θ_i (rad)	d_i (m)	a_i (m)	α_i (rad)
4	$\frac{\pi}{2} + q_4$	L_4	0	$\frac{\pi}{2}$
5	q_5	0	L_5	0
6	$\frac{\pi}{2} + q_6$	0	L_6	$\frac{\pi}{2}$

where q_4 , q_5 and q_6 are the generalized positions for joint 1, 2 and 3, respectively.

Since the Mini manipulator has all revolute joints, they are equal to θ_4 , θ_5 and θ_6 , respectively.

Applying equation (3.2) we have,

$${}^3T_4 = \begin{bmatrix} -s4 & 0 & c4 & 0 \\ c4 & 0 & s4 & 0 \\ 0 & 1 & 0 & 0 \\ 0 & 0 & 0 & 1 \end{bmatrix} \quad {}^4T_5 = \begin{bmatrix} c5 & -s5 & 0 & \frac{1}{10}c5 \\ s5 & c5 & 0 & \frac{1}{10}s5 \\ 0 & 0 & 1 & 0 \\ 0 & 0 & 0 & 1 \end{bmatrix}$$

$${}^5T_6 = \begin{bmatrix} -s_6 & 0 & c_6 & -\frac{1}{10}s_6 \\ c_6 & 0 & s_6 & \frac{1}{10}c_6 \\ 0 & 1 & 0 & 0 \\ 0 & 0 & 0 & 1 \end{bmatrix} \quad {}^3T_5 = \begin{bmatrix} -s_4c_5 & s_4s_5 & c_4 & -\frac{1}{10}s_4c_5 \\ c_4c_5 & -c_4s_5 & s_4 & \frac{1}{10}c_4c_5 \\ s_5 & c_5 & 0 & \frac{1}{10}s_5 \\ 0 & 0 & 0 & 1 \end{bmatrix}$$

Then we have the complete transformation from Frame 6 to Frame 3 as follows,

$${}^3T_6 = \begin{bmatrix} -\frac{1}{2}c_4s_5 + \frac{1}{2}c(4-5-6) & c_4 & -\frac{1}{2}s_4s_5 - \frac{1}{2}s(4-5-6) & -\frac{1}{20}c_4s_5 + \frac{1}{20}c(4-5-6) - \frac{1}{20}s_4s_5 - \frac{1}{20}s(4-5) \\ \frac{1}{2}s(4-5-6) - \frac{1}{2}s_4s_5 & s_4 & \frac{1}{2}c(4-5-6) + \frac{1}{2}c_4s_5 & \frac{1}{20}s(4-5-6) - \frac{1}{20}s_4s_5 + \frac{1}{20}c(4-5) + \frac{1}{20}c_4s_5 \\ c_5s_6 & 0 & s_5s_6 & \frac{1}{10}c_5s_6 + \frac{1}{10}s_5 \\ 0 & 0 & 0 & 1 \end{bmatrix}$$

The following shows the equivalent expressions used in the above result and throughout this thesis.

$$C_4 = \cos(q_4), c_5 = \cos(q_5), c_6 = \cos(q_6), s_4 = \sin(q_4), s_5 = \sin(q_5), s_6 = \sin(q_6)$$

$$c_4s_5 = \cos(q_4+q_5), s_4s_5 = \sin(q_4+q_5), c(4-5) = \cos(q_4-q_5), s(4-5) = \sin(q_4-q_5)$$

$$c_4s_5s_6 = \cos(q_4+q_5+q_6), s_4s_5s_6 = \sin(q_4+q_5+q_6)$$

$$c(4-5-6) = \cos(q_4-q_5-q_6), s(4-5-6) = \sin(q_4-q_5-q_6)$$

Velocity of the end-effector

Applying equation (3.5) to the Mini robot, we have

$${}^3J_m = \begin{pmatrix} Z_3 \times P_{36} & Z_4 \times P_{46} & Z_5 \times P_{56} \\ Z_3 & Z_4 & Z_5 \end{pmatrix} \quad (4.2)$$

$$Z_3 = \begin{bmatrix} 0 \\ 0 \\ 1 \end{bmatrix} \quad Z_4 = \begin{bmatrix} c4 \\ s4 \\ 0 \end{bmatrix} \quad Z_5 = \begin{bmatrix} c4 \\ s4 \\ 0 \end{bmatrix}$$

Then we get the **Basic Jacobian** of Mini manipulator in its Base Frame, i.e. Frame 3, which is denoted by 3J_m .

$${}^3J_m = \begin{bmatrix} \frac{1}{20} s456 - \frac{1}{20} s(4-5-6) - \frac{1}{20} c45 - \frac{1}{20} c(4-5) & \frac{1}{20} s456 + \frac{1}{20} s(4-5-6) - \frac{1}{20} c45 + \frac{1}{20} c(4-5) & \frac{1}{20} s456 + \frac{1}{20} s(4-5-6) \\ -\frac{1}{20} c456 + \frac{1}{20} c(4-5-6) - \frac{1}{20} s45 - \frac{1}{20} s(4-5) & -\frac{1}{20} c456 - \frac{1}{20} c(4-5-6) - \frac{1}{20} s45 + \frac{1}{20} s(4-5) & -\frac{1}{20} c456 - \frac{1}{20} c(4-5-6) \\ 0 & -\frac{1}{10} s56 + \frac{1}{10} c5 & -\frac{1}{10} s56 \\ 0 & c4 & c4 \\ 0 & s4 & s4 \\ 1 & 0 & 0 \end{bmatrix}$$

Linear velocity for the Mini manipulator at its end-effector in its Base Frame, i.e. Frame 3 is denoted by 3v_m ,

$${}^3J_m = \begin{bmatrix} {}^3J_{mv} \\ {}^3J_{m\omega} \end{bmatrix} \quad (4.3)$$

$${}^3v_m = {}^3J_{mv} \dot{q}_m \quad (4.4)$$

$${}^3v_m = \begin{bmatrix} \frac{1}{20} s456 - \frac{1}{20} s(4-5-6) - \frac{1}{20} c45 - \frac{1}{20} c(4-5) & \frac{1}{20} s456 + \frac{1}{20} s(4-5-6) - \frac{1}{20} c45 + \frac{1}{20} c(4-5) & \frac{1}{20} s456 + \frac{1}{20} s(4-5-6) \\ -\frac{1}{20} c456 + \frac{1}{20} c(4-5-6) - \frac{1}{20} s45 - \frac{1}{20} s(4-5) & -\frac{1}{20} c456 - \frac{1}{20} c(4-5-6) - \frac{1}{20} s45 + \frac{1}{20} s(4-5) & -\frac{1}{20} c456 - \frac{1}{20} c(4-5-6) \\ 0 & -\frac{1}{10} s56 + \frac{1}{10} c5 & -\frac{1}{10} s56 \end{bmatrix} \begin{bmatrix} \dot{q}_4 \\ \dot{q}_5 \\ \dot{q}_6 \end{bmatrix}$$

4.2 Dynamic model of the Mini robot

Similar to the Macro robot, dynamic model of the Mini robot is derived as follows,

$$P_{34} = \begin{bmatrix} 0 \\ 0 \\ 0 \end{bmatrix} \quad P_{35} = \begin{bmatrix} -\frac{1}{10}s4c5 \\ \frac{1}{10}c4c5 \\ \frac{1}{10}s5 \end{bmatrix}$$

$$P_{36} = \begin{bmatrix} -\frac{1}{20}c456 + \frac{1}{20}c(4-5-6) - \frac{1}{20}s45 - \frac{1}{20}s(4-5) \\ -\frac{1}{20}s456 + \frac{1}{20}s(4-5-6) + \frac{1}{20}c45 + \frac{1}{20}c(4-5) \\ \frac{1}{10}c56 + \frac{1}{10}s5 \end{bmatrix}$$

$$J_{v_4} = \begin{bmatrix} 0 & 0 & 0 \\ 0 & 0 & 0 \\ 0 & 0 & 0 \end{bmatrix}$$

$$J_{v_5} = \begin{bmatrix} -\frac{1}{10}c4c5 & \frac{1}{10}s4s5 & 0 \\ -\frac{1}{10}s4c5 & -\frac{1}{10}c4s5 & 0 \\ 0 & \frac{1}{10}c5 & 0 \end{bmatrix}$$

$$J_{v_6} = \begin{bmatrix} \frac{1}{20}s456 - \frac{1}{20}s(4-5-6) - \frac{1}{20}c45 - \frac{1}{20}c(4-5) & \frac{1}{20}s456 + \frac{1}{20}s(4-5-6) - \frac{1}{20}c45 + \frac{1}{20}c(4-5) & \frac{1}{20}s456 + \frac{1}{20}s(4-5-6) \\ -\frac{1}{20}c456 + \frac{1}{20}c(4-5-6) - \frac{1}{20}s45 - \frac{1}{20}s(4-5) & -\frac{1}{20}c456 - \frac{1}{20}c(4-5-6) - \frac{1}{20}s45 + \frac{1}{20}s(4-5) & -\frac{1}{20}c456 - \frac{1}{20}c(4-5-6) \\ 0 & -\frac{1}{10}s56 + c5 & -\frac{1}{10}s56 \end{bmatrix}$$

$$J_{\omega_4} = [Z_3 \quad 0 \quad 0] = \begin{bmatrix} 0 & 0 & 0 \\ 0 & 0 & 0 \\ 1 & 0 & 0 \end{bmatrix}$$

$$J_{\omega_5} = [Z_3 \quad Z_4 \quad 0] = \begin{bmatrix} 0 & c4 & 0 \\ 0 & s4 & 0 \\ 1 & 0 & 0 \end{bmatrix}$$

$$J_{\omega_6} = [Z_3 \quad Z_4 \quad Z_5] = \begin{bmatrix} 0 & c4 & c4 \\ 0 & s4 & s4 \\ 1 & 0 & 0 \end{bmatrix}$$

Inertia tensor of link i ($i = 4, 5, 6$) is,

$$I_{Ci} = {}^3R_{Ci} \begin{pmatrix} I_{xxi} & 0 & 0 \\ 0 & I_{yyi} & 0 \\ 0 & 0 & I_{zzi} \end{pmatrix} {}^3R_{Ci}^T \quad (4.5)$$

where I_{xxi} , I_{yyi} , I_{zzi} are the moment of inertia about the principle axis of the hollow cylinder. Since the mass of each link is centered at one single point mass, the moment of inertia of each link is zero.

$$I_{Ci} = {}^3R_{Ci} \begin{pmatrix} I_{xxi} & 0 & 0 \\ 0 & I_{yyi} & 0 \\ 0 & 0 & I_{zzi} \end{pmatrix} {}^3R_{Ci}^T = \begin{pmatrix} 0 & 0 & 0 \\ 0 & 0 & 0 \\ 0 & 0 & 0 \end{pmatrix}$$

Then we have

$$J_{\omega 5}^T {}^3R_{C_5} I_{C_5} {}^3R_{C_5}^T J_{\omega 5} = \begin{bmatrix} 0 & 0 & 0 \\ 0 & 0 & 0 \\ 0 & 0 & 0 \end{bmatrix}$$

$$J_{\omega 6}^T {}^3R_{C_6} I_{C_6} {}^3R_{C_6}^T J_{\omega 6} = \begin{bmatrix} 0 & 0 & 0 \\ 0 & 0 & 0 \\ 0 & 0 & 0 \end{bmatrix}$$

Using Equation (3.17), we have the Inertia Mass Matrix as follows,

$$M(q) = \begin{bmatrix} \frac{3}{2000} - \frac{1}{2000} c(2q_6+2q_5) - \frac{1}{1000} s_6 - \frac{1}{1000} s(q_6+2q_5) + \frac{1}{1000} c(2q_5) & 0 & 0 \\ 0 & \frac{3}{1000} - \frac{1}{500} s_6 & \frac{1}{1000} - \frac{1}{1000} s_6 \\ 0 & -\frac{1}{1000} s_6 + \frac{1}{1000} & \frac{1}{1000} \end{bmatrix}$$

Centrifugal and Coriolis terms

$$B(q) = \begin{bmatrix} -\frac{1}{500} c(q_6+2 \cdot q_5) - \frac{1}{500} s(2 \cdot q_5) + \frac{1}{1000} s(2 \cdot q_6+2 \cdot q_5) & -\frac{1}{1000} c_6 - \frac{1}{1000} c(q_6+2 \cdot q_5) + \frac{1}{1000} s(2 \cdot q_6+2 \cdot q_5) & 0 \\ 0 & 0 & -\frac{1}{500} c_6 \\ 0 & 0 & 0 \end{bmatrix}$$

$$C(q) = \begin{bmatrix} 0 & 0 & 0 \\ \frac{1}{1000}c(q_6+2 \cdot q_5) + \frac{1}{1000}s(2 \cdot q_5) - \frac{1}{2000}s(2 \cdot q_6+2 \cdot q_5) & 0 & -\frac{1}{1000}c_6 \\ \frac{1}{2000}c_6 + \frac{1}{2000}c(q_6+2 \cdot q_5) - \frac{1}{2000}s(2 \cdot q_6+2 \cdot q_5) & \frac{1}{1000}c_6 & 0 \end{bmatrix}$$

Gravity terms

$$G(q) = \begin{bmatrix} 0 \\ 0.1962 \cdot c_5 - 0.0981 \cdot s_5 s_6 \\ -0.0981 \cdot s_5 s_6 \end{bmatrix}$$

With $g = [0 \ 0 \ -9.81]^T$ is specified in Frame 3

Equations of Motion

Apply Equations (3.19) and (3.24) to the Mini robot, we get

$$\begin{bmatrix} \frac{3}{2000} - \frac{1}{2000}c(2q_6+2q_5) - \frac{1}{1000}s_6 - \frac{1}{1000}s(q_6+2q_5) + \frac{1}{1000}c(2q_5) & 0 & 0 \\ 0 & \frac{3}{1000} - \frac{1}{500}s_6 & \frac{1}{1000} - \frac{1}{1000}s_6 \\ 0 & -\frac{1}{1000}s_6 + \frac{1}{1000} & \frac{1}{1000} \end{bmatrix} \begin{bmatrix} \ddot{q}_4 \\ \ddot{q}_5 \\ \ddot{q}_6 \end{bmatrix} + \begin{bmatrix} 0 & 0 & 0 \\ \frac{1}{1000}c(q_6+2 \cdot q_5) + \frac{1}{1000}s(2 \cdot q_5) - \frac{1}{2000}s(2 \cdot q_6+2 \cdot q_5) & 0 & -\frac{1}{1000}c_6 \\ \frac{1}{2000}c_6 + \frac{1}{2000}c(q_6+2 \cdot q_5) - \frac{1}{2000}s(2 \cdot q_6+2 \cdot q_5) & \frac{1}{1000}c_6 & 0 \end{bmatrix} \begin{bmatrix} \dot{q}_4^2 \\ \dot{q}_5^2 \\ \dot{q}_6^2 \end{bmatrix} + \begin{bmatrix} -\frac{1}{500}c(q_6+2 \cdot q_5) - \frac{1}{500}s(2 \cdot q_5) + \frac{1}{1000}s(2 \cdot q_6+2 \cdot q_5) & -\frac{1}{1000}c_6 - \frac{1}{1000}c(q_6+2 \cdot q_5) + \frac{1}{1000}s(2 \cdot q_6+2 \cdot q_5) & 0 \\ 0 & 0 & -\frac{1}{500}c_6 \\ 0 & 0 & 0 \end{bmatrix} \begin{bmatrix} \dot{q}_4 \dot{q}_5 \\ \dot{q}_4 \dot{q}_6 \\ \dot{q}_5 \dot{q}_6 \end{bmatrix} + \begin{bmatrix} 0 \\ 0.1962 \cdot c_5 - 0.0981 \cdot s_5 s_6 \\ -0.0981 \cdot s_5 s_6 \end{bmatrix} = \begin{bmatrix} \tau_4 \\ \tau_5 \\ \tau_6 \end{bmatrix}$$

4.3 Operational space robot control

4.3.1 Goal position

Simulation

The control strategy for Mini manipulator is exactly the same as that of the Macro manipulator. The only differences are the robot and control parameters, i.e. K_p and K_v .

We use the Macro goal position [0.1679 -0.7571 0.4255] times 0.1 as the goal position for Mini manipulator. Maximum continuous torque is 5 (Nm). Each joint error is less than 10^{-5} (rad). Sampling time is 1(ms). The following set of parameters is used for computation of PD gains: $\omega_n = 300, \xi = 1$.

The simulation results using this set of parameters are shown in Figure 4.2.

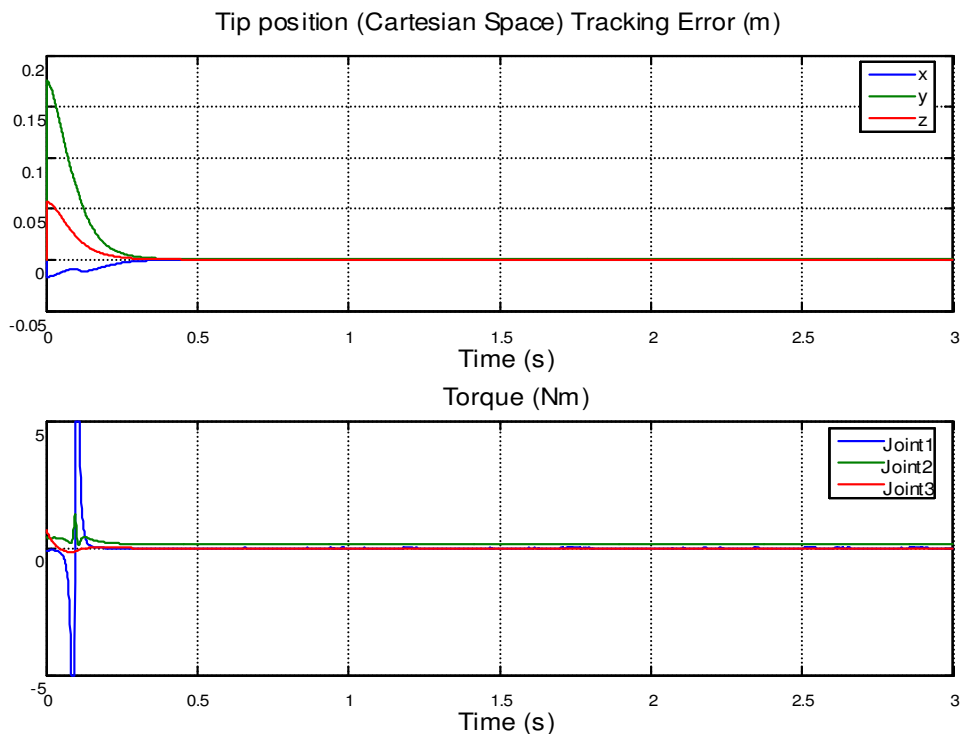


Figure 4.2 Torque of each joint and tip position error in x, y and z directions for Mini manipulator goal position control

Conclusion

The response is similar to a second-order system reference input response. After about 0.3 seconds, the tip reaches the goal position and stays there. We notice that the response of the Mini manipulator is much faster than the Macro.

4.3.2 Trajectory tracking

Simulation

For Mini robot, the end-effector starts at its home position $[0 \ 0.1 \ 0.1]$, ends at an arbitrary position within its workspace. We use the set of numbers chosen for goal position control, $0.1 \times [0.1679 \ -0.7571 \ 0.4255]$, as ending position. All other parameters remain the same as those in goal position control. Figure 4.3 shows the desired trajectory, velocity and acceleration generated from the starting and ending points. The functions have the same appearance as those of the Macro robot, but with a different scale.

Conclusion

Similar as the Macro robot, the Mini robot tip moves along the desired trajectory very closely. Maximum end-effector error ranges from 4×10^{-4} to 8×10^{-4} m. The steady state end-effector error includes deflections of the robot structure, and actuator/servo resolution. It is about 6×10^{-5} m. We notice that the Mini robot has a much smaller errors than the Macro robot.

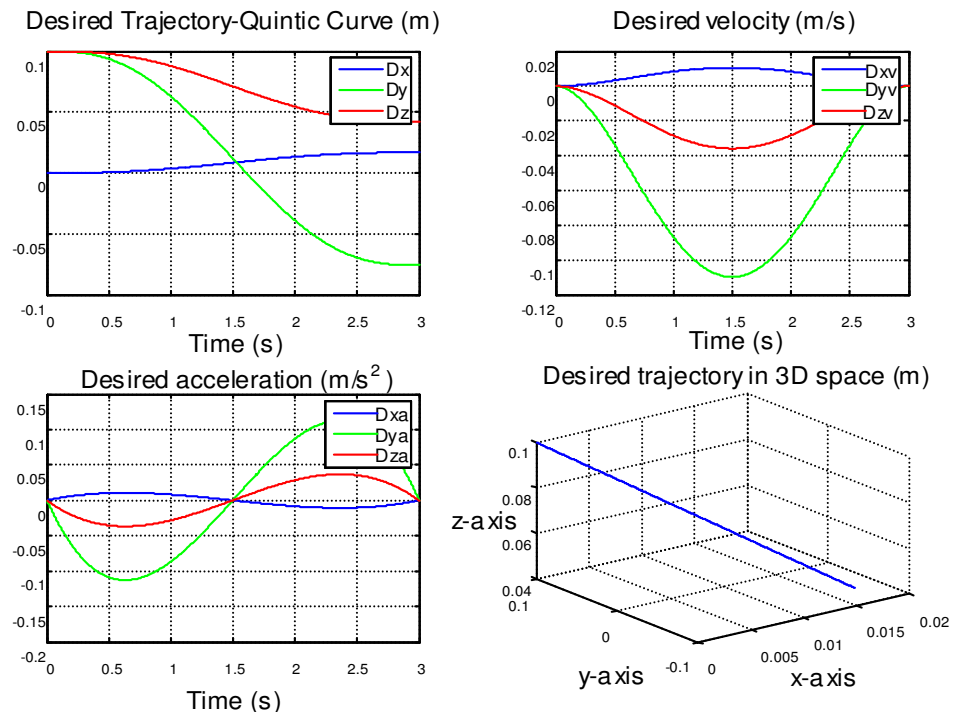


Figure 4.3 Desired trajectory, velocity and acceleration for Mini manipulator

The simulation results using this set of parameters are shown in Figure 4.4.

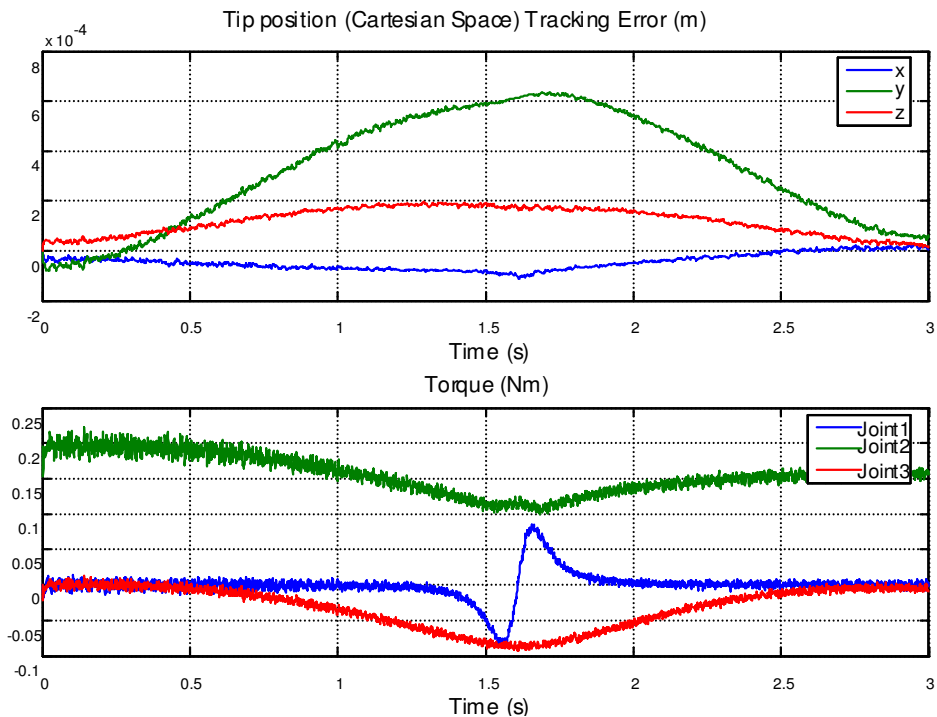


Figure 4.4 Torque of each joint and tip position error in x, y and z directions for Mini manipulator trajectory tracking control

Chapter 5

Overall Control for Combined Macro-Mini manipulator System

With the first few research objectives achieved in Chapter 3 and 4 - high performance control of a 3DOF manipulator with dynamics analysis, an overall control strategy for combined Macro-Mini manipulator system is explored and analyzed in this chapter, based on research findings from the above two chapters.

5.1 Macro-Mini manipulator structure and modeling

The assignment of frames is shown in Figure 5.1. D-H parameters, shown in Table 5.1, for the Macro-Mini manipulator is derived from the assigned frames.

The kinematics and dynamics of the Macro-Mini manipulator system are derived based on this set of parameters. The expressions are much more complicated than the Macro or Mini manipulator system. Computations take several minutes or even longer to finish one round. Such computation speed is obviously impossible to be used in real-time control. Typical sample time for a robot controller is 10ms. The result of the equations of motion is shown in Appendix A. It takes up to several pages on A4 size paper.

5.2 Control structure for Macro-Mini manipulator

Method 1

One proposed method of control for Macro-Mini manipulator is to treat the system as one and derive an overall controller based on the combined system. This method does not use any individual controller for Macro or Mini manipulator. An illustration of control structure is shown in Figure 5.2. In this case, we need to use the overall kinematics and dynamics of the 6DOF Macro-Mini manipulator system. As a conclusion from the above section, this method can be used for lower DOF systems. But for our proposed system, the computations are too slow to be used for real-time control.

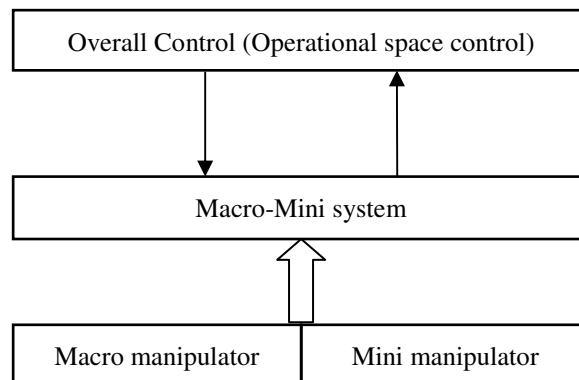


Figure 5.2 Tip position control using an overall control strategy regardless of individual controllers for Macro and Mini manipulators.

Another issue with this method is that the 6DOF robot is redundant with respect to its tasks. The task is to control the tip of Macro-Mini manipulator to reach a goal position or to follow a desired trajectory in 3D space. The tasks only require 3 degrees-of-freedom. We will have to deal with redundancy problem together with the complicated computations in the control. Thus this method may not be the best choice

for control.

Method 2

Another proposed method is to design subsystem controllers independently and connect them to form a combined subsystem controller [2] [30], as shown in Figure 5.3. The Mini manipulator controller is designed to respond very quickly to a static reference input while the Macro controller is designed to position the Macro end-point, which is assumed to be a rigid body, as quickly as possible.

Figure 5.4 illustrates the detailed trajectory determination process in one direction. Firstly, the tip of Macro-Mini manipulator system is given a task to perform, that translates to a desired trajectory for the tip $x(t)$. The Mini robot desired trajectory is a constant value r , which is a user specified value with the only restriction that the Mini robot tip is placed within the workspace of Mini robot. For example, r can be the desired posture for the Mini manipulator. The difference between desired tip position and the current Macro end-point position (expressed in the same frame, typically Frame 0) is controlled to follow the reference r . The desired trajectory for Macro is simply the tip position minus off the Mini reference, expressed in Base Frame.

The desired position for Mini manipulator is defined beforehand, i.e. the Mini manipulator stabilizes itself to the predefined reference throughout the control process while Macro is achieving the tasks. In this case, the subsystems react with their independent closed-loop dynamics.

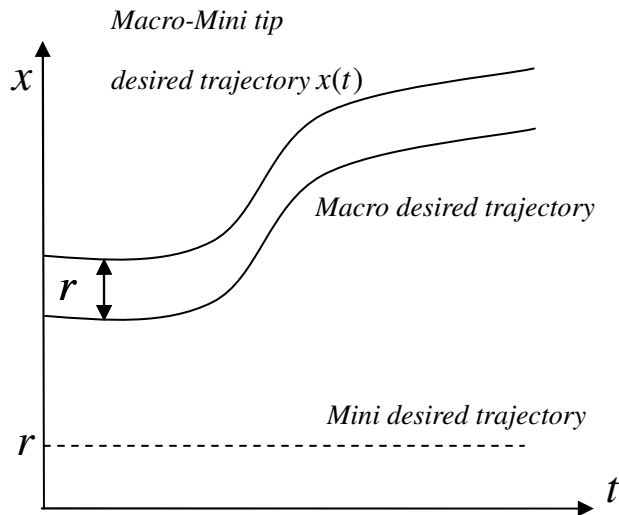


Figure 5.3 Determination of Macro and Mini manipulator trajectories, in x direction

Ballhaus developed independent controllers for a Macro-Mini manipulator system where the Macro is a two-link flexible manipulator. He describes an undesirable interaction between the Macro and Mini manipulators when the gains on the Mini manipulator controller are too large [30], resulting in performance limitations on the overall system. This control method does not take full advantage of the fast response of the Mini manipulator as the Mini manipulator reference input is based on a static value and the Mini cannot compensate for steady-state positioning errors in the Macro subsystem, which dominate the performance.

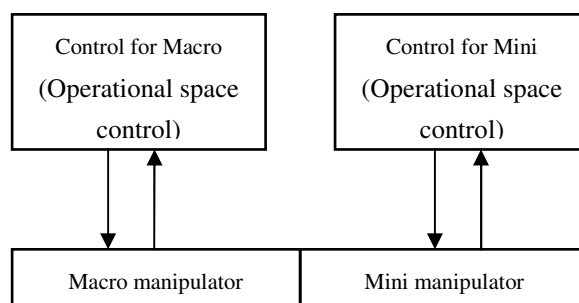


Figure 5.4 Control structure for Macro-Mini manipulator system when the two subsystems are controlled separately

Method 3

We propose a new method of control. Independent controllers of Macro and Mini manipulators are used. Macro and Mini manipulators take turns to move, that is, at any point of time, only a 3DOF robot is moving. The task is three dimensional goal positioning or trajectory tracking, thus the combined system is not redundant with regard to its tasks. There is no redundancy issue with this control strategy.

The desired Macro end-point position follows a given task expressed in the Base Frame. The reference input for Mini manipulator is a dynamic value, which is the difference between desired tip position and the current Macro end-point position (expressed in the same frame, typically Frame 0). If the reference is within the workspace of Mini manipulator, the Mini manipulator moves toward the reference. Otherwise, it holds its current posture. A feedback loop is closed creating an interaction between the Macro and Mini manipulator subsystems. The simulation results are discussed in the next section.

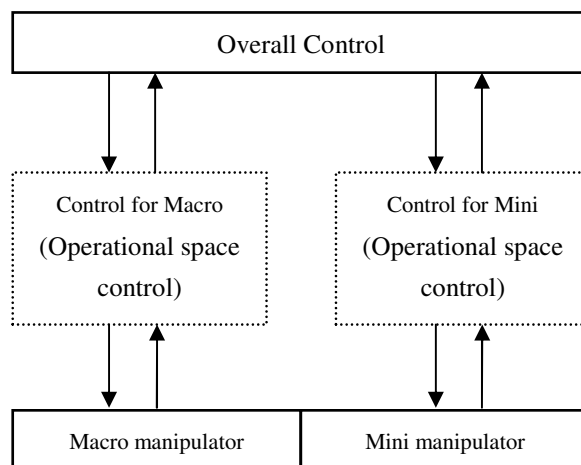


Figure 5.5 Tip position control using an overall control strategy on top of individual controllers for Macro and Mini manipulators.

5.3 Macro-Mini manipulator control simulations

5.3.1 Goal position control with one way coupling

The task is to control the 6DOF Macro-Mini robot tip to reach a goal position within its workspace in 3D space. The robot moves according to the following control steps until the simulation time finishes.

Control steps

1. Use independent Macro controller to make the Macro end-point move toward the goal position, expressed in Frame 0.
2. The Mini manipulator reference input is the difference between goal position and current Macro end-point position, expressed in the same frame.
3. Check whether the Mini manipulator reference input is within the reach of Mini manipulator. If yes, go to step 4; otherwise go to step 1.
4. Use independent Mini manipulator controller to make the Mini manipulator end-point (tip of the Macro-Mini manipulator system) to follow the reference.
5. Go back to step 1.

Figure 5.6 illustrates the control steps.

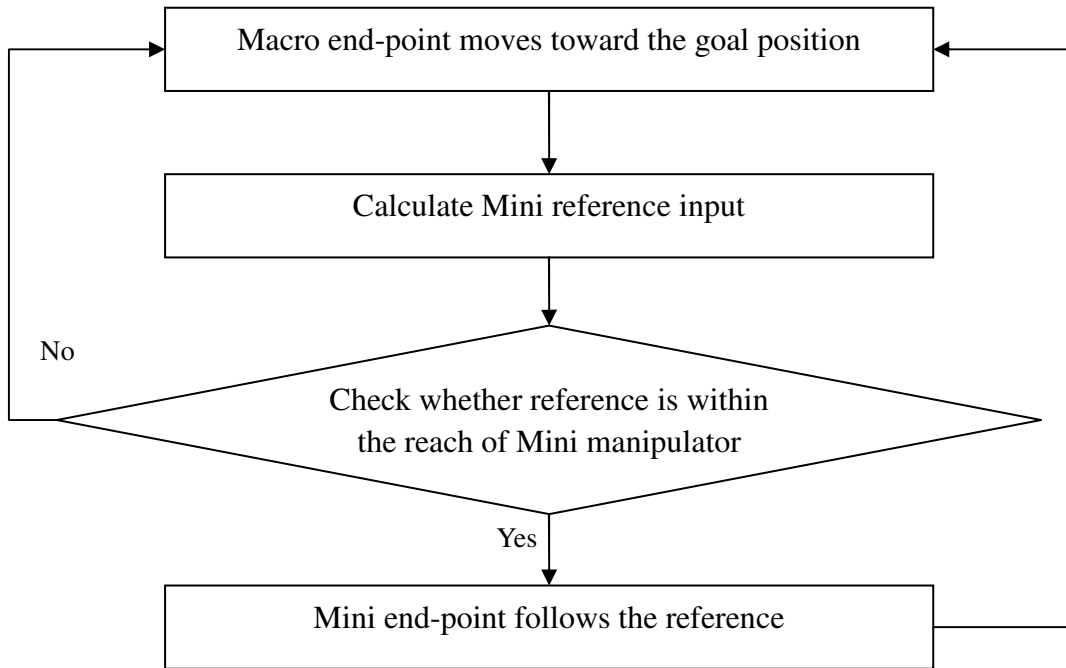


Figure 5.6 Macro-Mini manipulator overall control steps

Figure 5.7 illustrates the control structure.

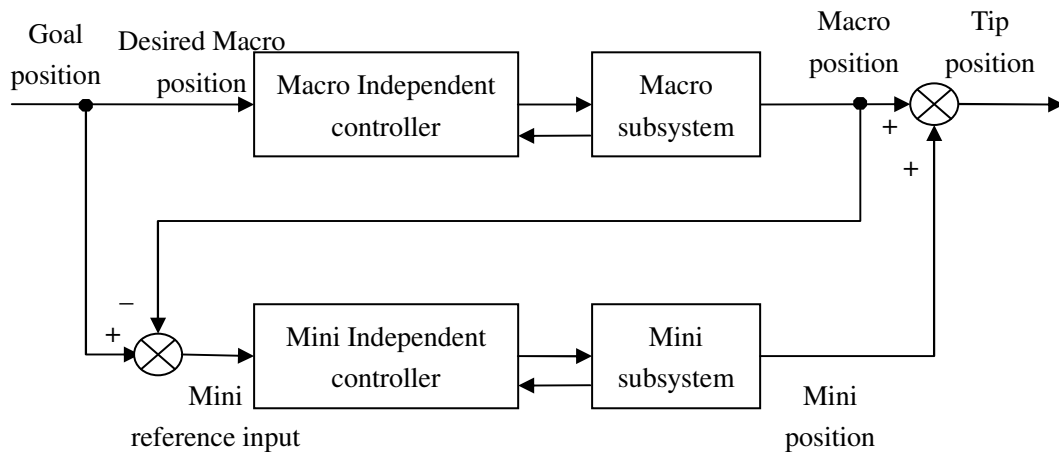


Figure 5.7 Overall control strategies on top of individual controllers for Macro and Mini manipulators (one way coupling)

Simulation

For the purpose of easy comparison, we choose the tip starting point at $[0 \ 1 \ 1] + [0 \ 0.1$

0.1] and goal position at [0.1679 -0.7571 0.4255] + [0 0.1 0.1]. If the Mini robot holds itself still from start to end, the Macro behaves exactly the same as when it moves alone. Maximum continuous torque, joint error, and sampling time remain the same as those in individual controls. The following set of parameters is used for computation of PD gains. For Macro manipulator, $\omega_n = 30, \xi = 1$. For Mini manipulator, $\omega_n = 300, \xi = 1$.

The simulation results using this set of parameters are shown in Figure 5.8.

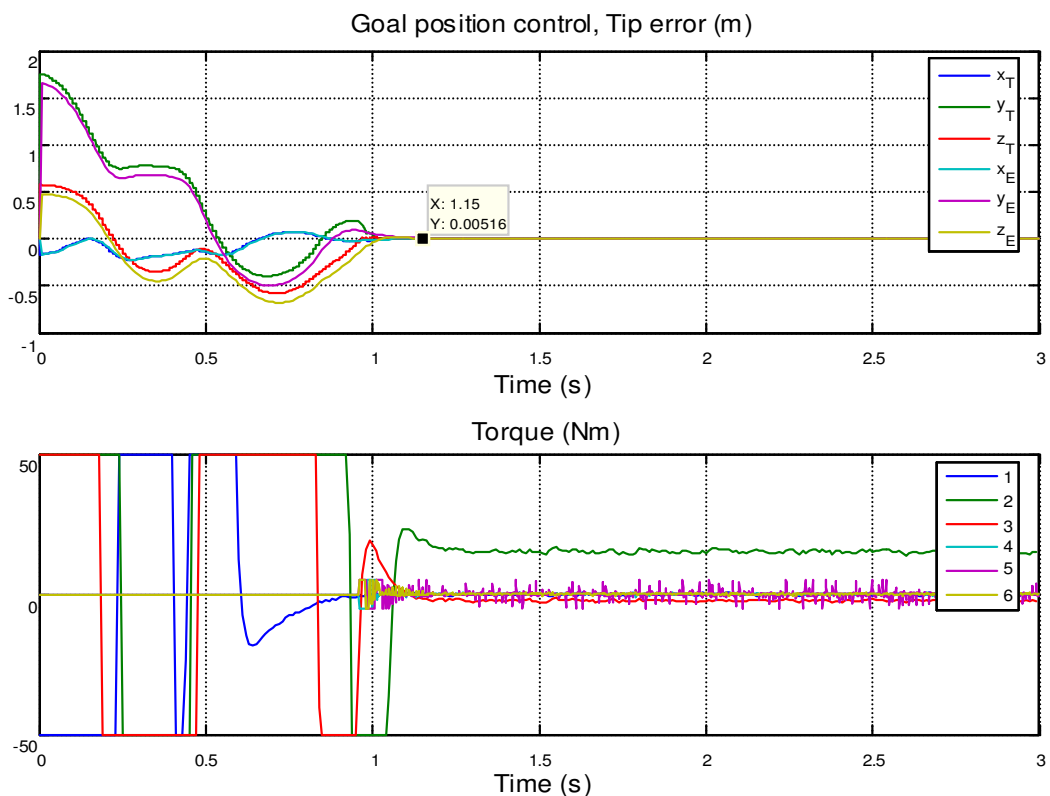


Figure 5.8 Torque of each joint and tip position error in x, y and z directions for Macro-Mini manipulator goal position control with one way coupling

In Figure 5.8, x_E , y_E and z_E are the Macro end-effector errors in x, y and z direction, respectively. x_T , y_T and z_T are the tip errors in x, y and z direction, respectively. The numbers from 1 to 6 are the torques applied to joint 1 to 6 respectively.

Conclusion

The time taken to reach the goal is about 1.0 seconds. As compared to the Macro settling time, 1.4 seconds, the combined system has improved its performance. The Macro is dominating the performance of the combined system. The steady state error is $0 \sim 4 \times 10^{-4}$, which is similar to the Mini manipulator performing alone. The Mini manipulator has improved the overall accuracy of the combined system.

5.3.2 Goal position control with two way coupling

We have also tried to calculate the desired Macro position as the difference of desired tip position (goal position) and Mini manipulator offset, keeping the rest unchanged. This modification on **method 3** creates a two way coupling between the Macro manipulator and Mini manipulator. Figure 5.9 illustrates this control strategy.

Conclusion

The time taken to reach the goal is about 1.5 seconds. As compared to the Macro settling time, 1.4 seconds, the combined system doesn't have any advantage. The steady state error is $0 \sim 9 \times 10^{-4}$, which is close to that of the Mini manipulator. The combined system has better accuracy than the Macro alone.

Compared to the control performance of one way coupling, the combined system has not taken full advantage of the fast response of Mini manipulator.

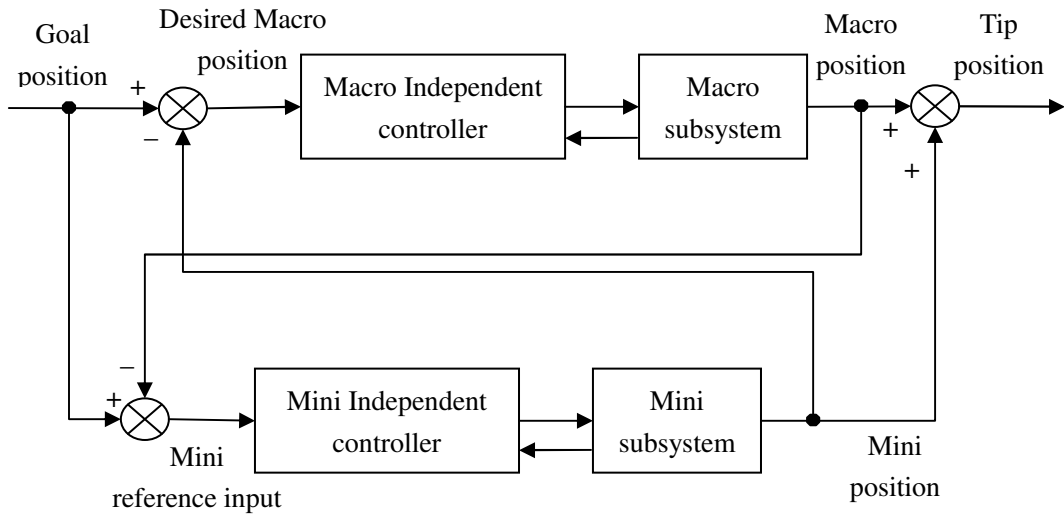


Figure 5.9 Overall control strategies on top of individual controllers for Macro and Mini manipulators (two way coupling)

The simulation results are shown in Figure 5.10. Legends are the same as Figure 5.8.

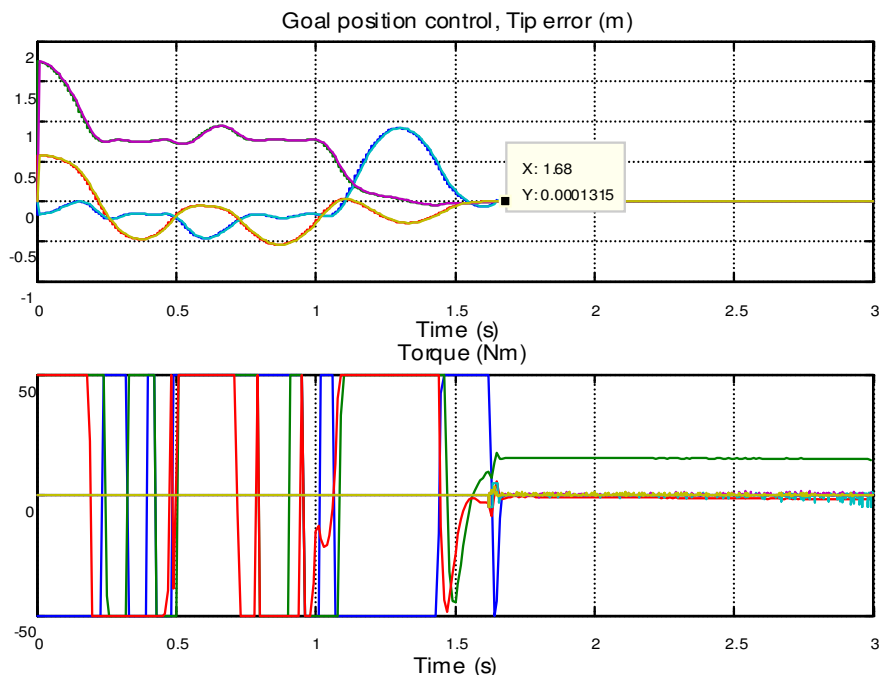


Figure 5.10 Torque of each joint and tip position error in x, y and z directions for Macro-Mini manipulator goal position control with two way coupling

5.3.3 Trajectory tracking control with one way coupling

The task is to control the 6DOF Macro-Mini robot end-effector to follow 3D trajectory. The end-point starts at $[0 \ 1 \ 1] + [0 \ 0.1 \ 0.1]$ and ends at $[0.1679 \ -0.7571 \ 0.4255] + [0 \ 0.1 \ 0.1]$. A fifth order quintic curve is generated between the starting and ending point. Figure 5.11 shows the desired tip trajectory, velocity and acceleration generated. The functions have the same appearance but different scale as those of the Macro or Mini robot.

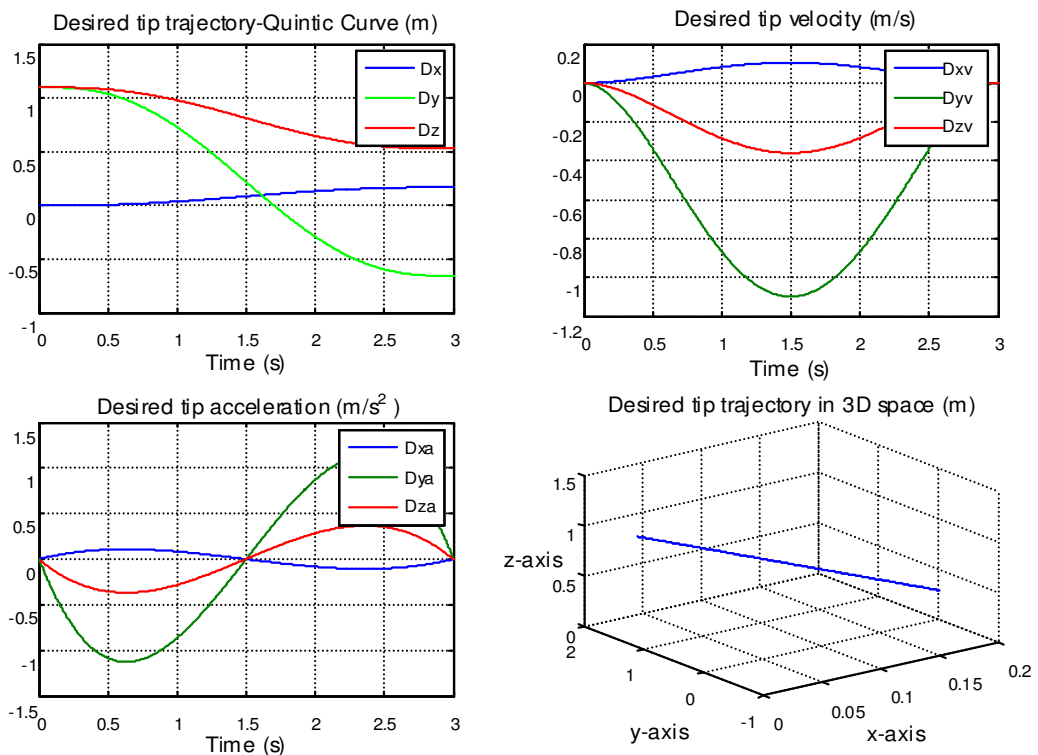


Figure 5.11 Desired tip trajectory, velocity and acceleration for Macro-Mini manipulator

Simulation

The control steps are similar to goal position control. The only difference is that, instead of one goal throughout the control, there is a series of goals, i.e. the trajectory.

The simulation results using this set of parameters are shown in Figure 5.12.

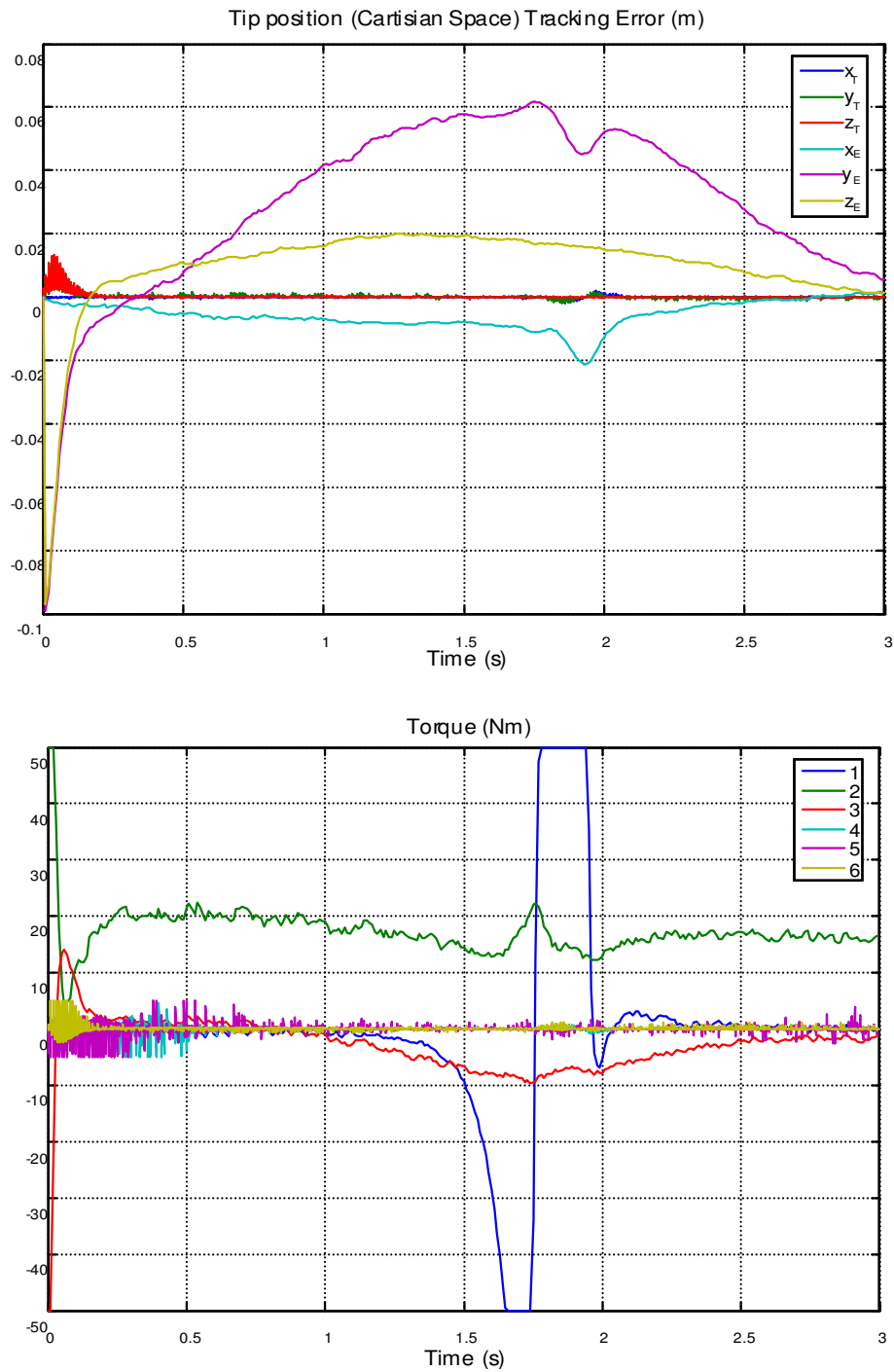


Figure 5.12 Torque of each joint and tip position error in x, y and z directions for Macro-Mini manipulator trajectory tracking control with one way coupling

Conclusion

The steady state error is $0 \sim 5 \times 10^{-4}$, which is similar to the Mini manipulator performing alone. Without the Mini manipulator, the error would be $0 \sim 0.01$, as shown

in Figure 5.12. The Maximum tracking error is 0.01, as compared to the 0.06 when Macro moving alone, the Mini manipulator has improved the overall performance of the combined system.

5.3.4 Trajectory tracking control with two way coupling

Calculate the desired Macro position as the difference of desired tip position and Mini manipulator offset, keeping the rest unchanged. The simulation results are shown in Figure 5.13. Legends are the same as Figure 5.8.

Conclusion

The overall control makes the Mini manipulator stretches to its limit very fast and after which, the Mini manipulator is not able to compensate for the tracking and steady state error. The performance is close to that of the Macro performing alone. This overall control strategy is not making full use of the Mini manipulator to improve the performance of the system.

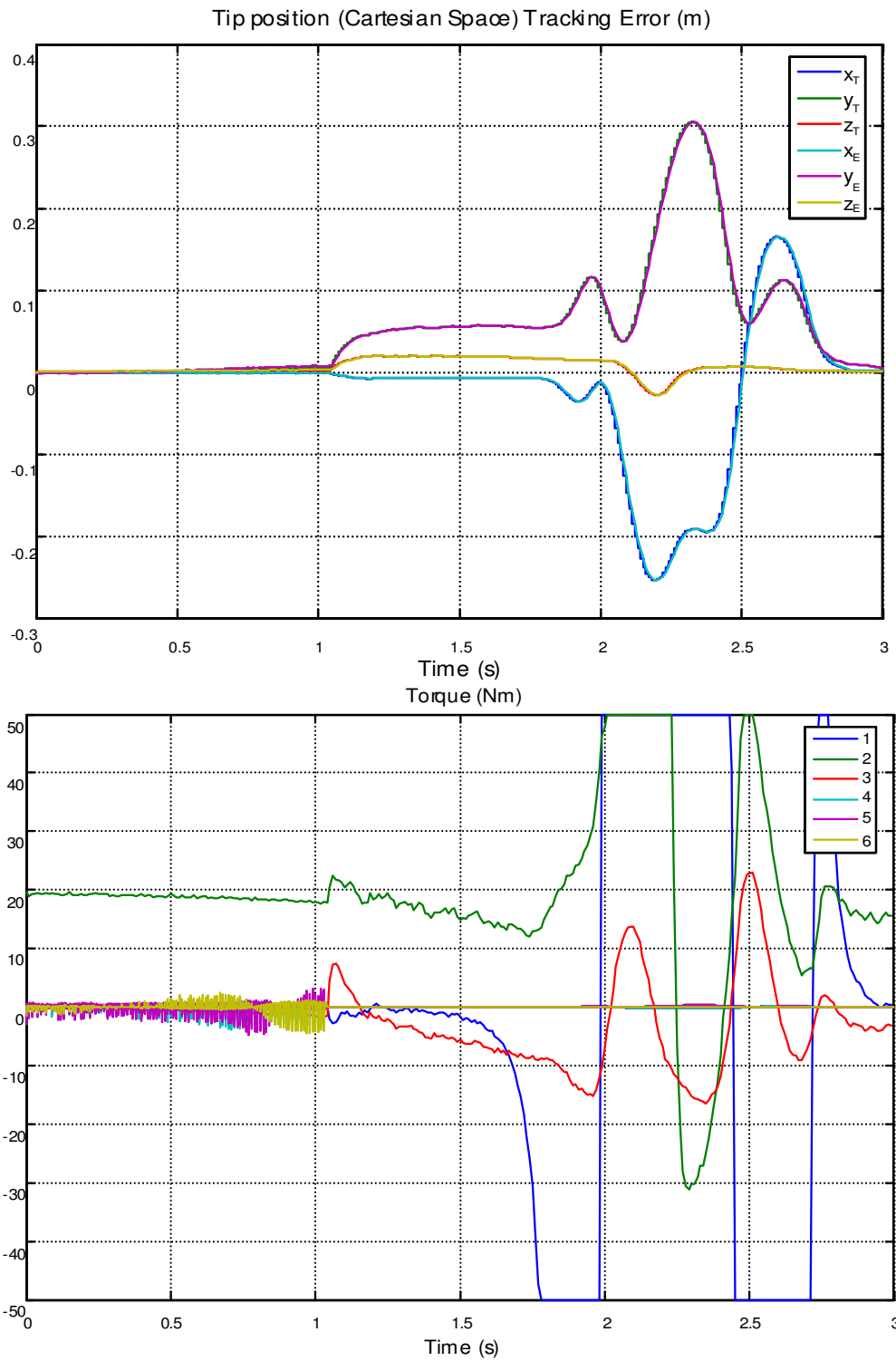


Figure 5.13 Torque of each joint and tip position error in x, y and z directions for Macro-Mini manipulator trajectory tracking control with two way coupling

5.3.5 Summary

In summary, Chapter 5 has discussed the kinematics and dynamics of Macro-Mini manipulator system. Three different methods for overall control are proposed. The first method is not realizable. The second method was tried by other researchers before [2] [30], but it was found that the overall system performance is dominated by the Macro. The benefits of having a Mini manipulator in the system are not taken full advantage of.

A new method is then proposed, the third one, for the overall control. Simulations are done to achieve high performance goal position and trajectory tracking control. The results shown that after adding the Mini manipulator, the Macro manipulator can achieve faster response time in goal position control, smaller tracking error in trajectory tracking control, and smaller steady state error in both.

A modification on **method 3**, the two way coupling control, is also simulated. The overall controller is not taking full advantage of the Mini manipulator, to improve performance of the combined system, in both goal position and trajectory tracking control.

Chapter 6

Conclusions and Future Work

6.1 Conclusions

In conclusion, the results of Macro/Mini manipulator study can be summarized as below.

1. The simulation results show that the Macro manipulator performance can be improved by mounting a Mini manipulator at the end.
2. High performance control of the combined system does not need calculation of full dynamics of the overall system. The overall control is based on independent controllers of Macro manipulator and Mini manipulator.
3. This enables us to achieve better accuracy and faster speed by simply adding a Mini manipulator to a readily available Macro. The manufacturing cost could be much less than that of making a whole new manipulator system at the same performance requirement.
4. This study also enables greater flexibility for different combinations with different manipulation tasks, in the sense that by changing the Mini manipulator part, without any modification on the Macro part, the overall system can perform a different job. Because the original Macro controller remains unchanged in the proposed overall control scheme.
5. The simulation results demonstrated that the control of high degrees-of-freedom

manipulators with dynamics can be realized by breaking them down into two lower degrees-of-freedom manipulators. The computation of dynamics becomes much easier. Thus the controller design would be easier.

6.2 Future work

Following ideas are proposed for future studies using Macro-Mini manipulators

1. Due to the long reach and light weight features in many Macro-Mini applications, the Macro manipulators are structurally flexible. They vibrate with low frequencies, typically within or near the desired bandwidth of the control system. It is mentioned earlier in this thesis, with the Mini manipulator offers a possible solution to account for these low frequency vibration modes, thus maintain stability and ensure desired performance. However, the effects of vibration modes and frictions are not simulated in the software model of both Macro and Mini manipulator. Also, this study did not include the vibrations analysis in the controller design. It would be a great challenge to incorporate these factors in the robot software model and controller design.
2. This control scheme was not implemented real -time. Future work would be to develop a Macro-Mini manipulator system and to achieve high performance control of each subsystem. Then implement the overall control algorithm on the robots. Study the effects which are not modeled in the simulations and try to modify the overall control to compensate for them.

3. This simulation has achieved high performance position control, i.e. goal position and trajectory tracking controls. Extension of this work could be to achieve high performance control of Macro-Mini manipulator with force control or hybrid position/force control. With the same overall control structure, but different sensor information, try to see whether the control scheme still works.
4. Another work would be to explore possibility of high performance control of redundant manipulators which have more than 6DOF and need to be broken down into three or more parts, such as an elephant trunk robot structure studied by Hannan, M.W., Walker, I.D. [10]. The extension to a combined robot with more parts without considering frictions and vibrations is theoretically straightforward; however the modeling and final control law will be more complex.

Bibliography

1. A.J. Koivo, K.S. Lee, Self-tuning control of two-link manipulator with a flexible forearm, *International Journal of Robotics Research* 11 (1992) 383-395.
2. Andre Sharon, Neville Hogan, and David E. Hardt. "The macro/micro manipulator: An improved architecture for robot control" *Robotics and Computer Integrated Manufacturing*, 10(3):209-222, 1993.
3. Armstrong, B., Khatib, O., Burdick, J., The Explicit Dynamic Model and Inertial Parameters of the PUMA 560 Arm, *IEEE Int. Conf. Robotics and Automation*, pp. 510-518, 1986
4. Corke, P. and Armstrong-Hélouvry, B., A meta-study of PUMA 560 dynamics: A critical appraisal of literature data, *Robotica*, vol. 13(3), pp253-258, 1995.
5. Craig, J. "Introduction to Robotics Mechanics and Control", Addison-Wesley Publishing Company, Inc., 1989
6. D. Wang, M. Vidyasagar, Passive control of a flexible link, in: Proceedings of the 1990 IEEE International Conference on *Robotics and Automation*, Cincinnati, 1990, pp. 1432-1437.
7. Denavit, J. and Hartenberg, R. S, A Kinematic Notation for Lower-Pair Mechanisms Based on Matrices, *J. App. Mech.*, vol. 77, pp. 215-221, 1955
8. Fu, K. S., Gonzales, R. C., Lee, C. S. G, *Robotics: Control, Sensing, Vision, and Intelligence*, McGraw-Hill, 1987.
9. H. D. Stevens and L. J. Howy, "The Limitations of Independent Controller Design

- for a Multiple-link Flexible Macro-manipulator Carrying a Rigid Mini-manipulator”, *Robotics for Challenging Environments* (1996), pp. 93-99
10. Hannan, M.W., Walker, I.D., Analysis and experiments with an elephant's trunk robot, *Advanced Robotics*, Volume 15, Number 8, 2001 , pp. 847-858(12)
 11. I. Sharf. Active damping of a large flexible manipulator with a short-reach robot. *American Control Conference*, pages 3329-3333, vol. 5, Seattle WA, June 1995.
 12. J. Carusone, G.M.T. D'Eleuterio, Tracking control for end-effector position and orientation of structurally flexible manipulator, *Journal of Robotic Systems* 10 (1993) 847-870.
 13. J.S. Chen, C.H. Meng, Modelling and adaptive control of a flexible one-link manipulator, *Robotica* 8 (1990) 339-345.
 14. Jae Y. Lew and Dan J. Trudnowski. Vibration control of a micro/macro-manipulator system. *IEEE Control Systems*, 16(1):26-31, February 1996.
 15. Jansen J.F. et al, “Long Reach Manipulation For Waste Storage Tank Remediation,” ASME, DSC-Vol. 31, *Modelling and Control of Compliant and Rigid Motion Systems*, 1991, pp. 67-73.
 16. Khatib O, A unified approach for motion and force control of robot manipulators - the operational space formulation, *IEEE Journal of Robotics and Automation* 3 (1): 43-53 Feb 1987
 17. Khatib O, The Operational Space Framework, *JSME International Journal Series C-Dynamics Control Robotics Design And Manufacturing* 36 (3): 277-287 Sep

1993

18. Khatib, O., Dynamic Control of Manipulators in Operational Space, 6th CISM-IFTToMM Congress on *Theory of Machines and Mechanisms*, New York: Wiley, pp. 1128-1131, 1983
19. Khatib, O., Inertial Properties in Robotic Manipulation: An Object-Level Framework,” *Int. J. of Robotics Research*, vol 14, no.1, pp 19-36, 1995
20. Knape B. and Berger A., “Development of a Remote Tank Inspection (RTI) Robotic System,” Proceedings of the 4th ANS Topical Meeting, *Robotics and Remote Systems*, M. Jamshidi and P. Eicker, editors, Albuquerque, NM, 1991, pp. 470-481.
21. M.M. Svinin, M. Uchiyama, A new compensation scheme for the inverse kinematics tasks of flexible robot arms, in: Proceedings of the IEEE International Conference on *Robotics and Automation*, San Diego, 1994, pp. 315-320.
22. O. Khatib, “Reduced effective inertia in macro-mini manipulator systems,” in Fifth Int. Symp. Robotics Research, 1990, pp. 279-284.
23. Ogata, K., *Modern Control Engineering*, Prentice-Hall., 1988
24. P.P. Lin, H.D. Chiang, X.X. Cui, An improvement method of on-line calculation and compensation of static deflection at a robot end-effector, *Journal of Robotic Systems* 8 (1991) 267-288.
25. Rodrigo S. Jamisola, Full Dynamics Identification and Control of PUMA 560 and Mitsubishi PA-10 Robots, Master’s thesis, National University of Singapore, 2001
26. T. Yosbikawa, K. Hosoda, T. Doi, and H. Murakami, “Quasi-static trajectory

- tracking control of flexible manipulator by macro-micro manipulator system,” in *Proc. 1993 IEEE Int. Conf. on Robotics and Automation*, 1993, pp. 210-214.
27. T. Yoshikawa et al., “Dynamic trajectory tracking control of flexible manipulator by macro-micro manipulator system,” in *Proc. of 1994 IEEE Int. Conf. on Robotics and Automation*, pp. 1804-1809, 1994.
 28. T. Yoshikawa, K. Hosoda, K. Harada, A. Matsumoto, and H. Murakami, “Hybrid position/force control of flexible manipulators by macro-micro manipulator system,” *Proc. 1994 Int. Conf. on Robotics and Automation*, 1994, pp. 2125-2130,
 29. Tsuneo Yoshikawa, Kensuke Harada, and Atsushi Matsumoto, Hybrid Position/Force Control of Flexible-Macro/Rigid-Micro Manipulator Systems, *Transactions on Robotics and Automation*, Vol. 12, No. 4, August 1996
 30. W. L. Ballhaus and S. M. Rock. End-point control of a two-link flexible robotic manipulator with a mini-manipulator: Dynamic coupling issues. In *Proceedings of the ASME Winter Annual Meeting*, Anaheim, CA, November 1992.
 31. X.P. Cheng, R.V. Patel, Neural network based tracking control of a flexible macro–micro manipulator system, *Neural Networks* 16 (2003) 271-286

Appendix: Equations of Motion for Combined Macro-Mini Manipulator System

The following shows the equations of motion for Combined Macro-Mini Manipulator System, i.e. the overall dynamics of a 6DOF manipulator system, based on the parameters assumed in this thesis. The purpose of attaching it here is to show the complexity of a 6DOF serial manipulator system. If the studied system does not have point mass for all links, which is usually true in real-life cases, the equations will be further complicated by the inertia matrix of each link. It is impractical to use such a formulation for real-time control of a manipulator. One can also imagine how complicated the equations of motion for a seven or higher degrees-of-freedom manipulator can become.

T =

$$\begin{aligned}
 & (-1/8000*\sin(2*q5-2*q4+q3+q2)-1/400*\sin(q6+q5+q2+q3+q4)-1/400*\sin(-q6-q5+q2+q3-q4)-1/8000*\sin(-2*q6-2*q5+q3+q2-q4)+1/400*\sin(-q6-q5+q2+q3+q4)+3/8000*\sin(2*q4+q3+q2)+1/200*\cos(-q5+q2+q3+q4)+1/200*\cos(q5+q2+q3+q4)-1/200*\cos(-q5+q2+q3-q4)-1/8000*\sin(-2*q5-2*q4+q3+q2)+1/400*\sin(q6+q5+q2+q3-q4)-1/16000*\sin(-2*q6-2*q5+2*q4+q3+q2)-1/8000*\cos(-2*q5+2*q4+q3+q2-q6)-1/200*\cos(q5+q2+q3-q4)+1/4000*\sin(2*q5+q4+q3+q2)-1/4000*\sin(2*q5-q4+q3+q2)-1/4000*\cos(q6+2*q5-q4+q3+q2)+1/8000*\cos(-q6-2*q4+q3+q2)+1/16000*\sin(2*q6+2*q5-2*q4+q3+q2)+1/4000*\cos(-q6-2*q5+q3+q2+q4)+1/8000*\cos(q6+2*q4+q3+q2)-1/4000*\sin(-2*q5+q4+q3+q2)-1/4000*\cos(-q6-2*q5-q4+q3+q2)+1/8000*\cos(q6+2*q5+2*q4+q3+q2)+1/8000*\sin(-2*q6-2*q5+q3+q2+q4)-1/8000*\sin(2*q6+2*q5+q3+q2+q4)+1/4000*\sin(-2*q5-q4+q3+q2)-1/8000*\cos(-q6+2*q4+q3+q2)+1/8000*\sin(2*q5+2*q4+q3+q2)-1/8000*\cos(2*q5-2*q4+q6+q3+q2)+1/8000*\sin(-2*q5+2*q4+q3+q2)+1/16000*\sin(-2*q6-2*q5-2*q4+q3+q2)+1/8000*\sin(2*q6+2*q5+q3+q2-q4)-3/8000*\sin(-2*q4+q3+q2)-1/8000*\cos(-2*q4+q3+q2+q6)-1/16000*\sin(2*q6+2*q5+2*q4+q3+q2)+1/4000*\cos(q6+2*q5+q4+q3+q2)+1/8000*\cos(-q6-2*q5-2*q4+q3+q2))*q3^2+(1/4000*\sin(2*q6+2*q5+q3+q2)-1/2000*\sin(-2*q5+q3+q2)-1/2000*\cos(q6+q3+q2)-1/2000*\sin(2*q5+q3+q2)-1/2000*\cos(q6+2*q5+q3+q2)+1/2000*\cos(-q6+q3+q2)+1/2000*\cos(-2*q5+q3+q2-q6)+1/4000*\sin(-2*q6-2*q5+q3+q2)-3/2000*\sin(q2+q3)+1/4000*\sin(2*q5-2*q4+q3+q2)+3/4000*\sin(2*q4+q3+q
 \end{aligned}$$

$$\begin{aligned}
& 2)+1/4000*\sin(-2*q5-2*q4+q3+q2)-1/8000*\sin(-2*q6-2*q5+2*q4+q3+q2)-1/4000*\cos(-2*q5+2*q4+q3+q2-q6)-1/4000*\cos(-q6-2*q4+q3+q2)-1/8000*\sin(2*q6+2*q5-2*q4+q3+q2)+1/4000*\cos(q6+2*q4+q3+q2)+1/4000*\cos(q6+2*q5+2*q4+q3+q2)-1/4000*\cos(-q6+2*q4+q3+q2)+1/4000*\sin(2*q5+2*q4+q3+q2)+1/4000*\cos(2*q5-2*q4+q6+q3+q2)+1/4000*\sin(-2*q5+2*q4+q3+q2)-1/8000*\sin(-2*q6-2*q5-2*q4+q3+q2)+3/4000*\sin(-2*q4+q3+q2)+1/4000*\cos(-2*q4+q3+q2+q6)-1/8000*\sin(2*q6+2*q5+2*q4+q3+q2)-1/4000*\cos(-q6-2*q5-2*q4+q3+q2))*qv3*qv4+(-1/400*\sin(q6+q5+q2+q3-q4)-1/400*\sin(-q6-q5+q2+q3+q4)+1/400*\sin(q6+q5+q2+q3+q4)+1/400*\cos(-q6-q5+q4+q2)+1/400*\cos(-q6-q5+q4-q2)+1/400*\sin(-q6-q5+q2+q3-q4)+1/4000*\cos(-q6+q3+q2+q4)+1/4000*\cos(q6+q4+q3+q2)-1/4000*\cos(-q6-q4+q3+q2)-1/400*\cos(q6+q5+q4+q2)-1/400*\cos(q6+q5+q4-q2)-1/4000*\cos(q6+q3+q2-q4))*qv6^2+(-1/2000*\cos(q6+q3+q2-q4)+3/2000*\sin(q2+q3+q4)-1/4000*\sin(2*q5-2*q4+q3+q2)+1/4000*\sin(-2*q6-2*q5+q3+q2-q4)+1/4000*\sin(-2*q5-2*q4+q3+q2)+1/8000*\sin(-2*q6-2*q5+2*q4+q3+q2)+1/4000*\cos(-2*q5+2*q4+q3+q2-q6)+1/2000*\sin(2*q5+q4+q3+q2)-1/2000*\sin(2*q5-q4+q3+q2)-1/2000*\cos(q6+2*q5-q4+q3+q2)-3/2000*\sin(q2+q3-q4)+1/8000*\sin(2*q6+2*q5-2*q4+q3+q2)-1/2000*\cos(-q6-2*q5+q3+q2+q4)+1/2000*\sin(-2*q5+q4+q3+q2)+1/2000*\cos(-q6-2*q5-q4+q3+q2)+1/4000*\cos(q6+2*q5+2*q4+q3+q2)-1/4000*\sin(-2*q6-2*q5+q3+q2+q4)-1/4000*\sin(2*q6+2*q5+q3+q2+q4)-1/2000*\sin(-2*q5-q4+q3+q2)-1/2000*\cos(-q6+q3+q2+q4)+1/4000*\sin(2*q5+2*q4+q3+q2)-1/4000*\cos(2*q5-2*q4+q6+q3+q2)+1/2000*\cos(q6+q4+q3+q2)-1/4000*\sin(-2*q5+2*q4+q3+q2)-1/8000*\sin(-2*q6-2*q5-2*q4+q3+q2)+1/4000*\sin(2*q6+2*q5+q3+q2-q4)+1/2000*\cos(-q6-q4+q3+q2)-1/8000*\sin(2*q6+2*q5+2*q4+q3+q2)+1/2000*\cos(q6+2*q5+q4+q3+q2)-1/4000*\cos(-q6-2*q5-2*q4+q3+q2))*qv3*qv5+(-1/400*\cos(-q6-q5+q4+q3)+1/4000*\sin(2*q6+2*q5+2*q3+2*q2-q4)+1/8000*\sin(-2*q5+2*q4+2*q3+2*q2)+3/4000*\sin(-2*q5+2*q3+2*q2)+1/200*\cos(-q6-q5+q3+2*q2)+1/200*\sin(-q5-q4+q3+2*q2)-1/200*\cos(2*q3+2*q2+q5+q4)+1/4000*\sin(2*q5+2*q4)+1/16000*\sin(2*q6+2*q5-2*q4+2*q3+2*q2)-1/16000*\sin(-2*q6-2*q5+2*q4+2*q3+2*q2)-1/400*\cos(q6+q5+q4+q3+2*q2)-1/8000*\cos(-q6-2*q5+2*q4+2*q3+2*q2)-1/100*\cos(2*q3+2*q2+q5)+1/2000*\cos(-q6-2*q5-q4+2*q3+2*q2)+1/50*\cos(q5)-1/8000*\sin(2*q6+2*q5+2*q4)+1/4000*\cos(2*q5+2*q4+q6)-1/2000*\sin(2*q5-q4+2*q3+2*q2)-1/100*\sin(q5+q3+2*q2)-1/8000*\cos(-q6-2*q5-2*q4+2*q3+2*q2)-1/100*\sin(q3-q5)-1/200*\cos(2*q3+2*q2+q5-q4)-1/2000*\sin(2*q5)-1/200*\sin(q5+q4+q3+2*q2)-3/4000*\cos(q6+2*q5+2*q3+2*q2)-1/100*\sin(q6+q5)-1/100*\cos(2*q3+2*q2-q5)-1/8000*\sin(2*q5+2*q4+2*q3+2*q2)+1/400*\sin(2*q3+2*q2+q6+q5-q4)+1/400*\sin(2*q3+2*q2-q6-q5-q4)-1/200*\cos(q6+q5+q3)-3/4000*\sin(2*q5+2*q3+2*q2)+1/40000*\sin(2*q6+2*q5)+1/200*\cos(2*q3+2*q2-q5+q4)+1/4000*\cos(-2*q5+2*q4-q6)+1/400*\sin(2*q3+2*q2+q6+q5+q4)+1/400*\sin(2*q3+2*q2-q6-q5+q4)+1/8000*\sin(-2*q6-2*q5+2*q4)+1/200*\cos(2*q3+2*q2-q5-q4)-1/400*\cos(q6+q5-q4+q3)-1/400*\cos(-q6-q5-q4+q3)-1/200*\sin(2*q3+2*q2-q6-q5)-1/400*\cos(q6+q5+q4+q3)-1/2000*\cos(q6+2*q5+2*q3+2*q2-q4)+1/200*\sin(2*q3+2*q2+q6+q5)-1/2000*\sin(2*q5+q4+2*q3+2*q2)+1/4000*\sin(2*q6+2*q5+q4+2*q3+2*q2)-1/100*\sin(q3+q5)-1/8000*\cos(q6+2*q5-2*q4+2*q3+2*q2)+1/200*\sin(-q5+q4+q3+2*q2)-1/2000*\cos(q6+2*q5)-3/40000*\cos(-q6-2*q5+2*q3+2*q2)+1/200*\sin(-q5-q4+q3)+1/4000*\sin(-2*q6-2*q5+q4+2*q3+2*q2)-1/400*\cos(-q6-q5+q4+q3+2*q2)-1/200*\cos(q6+q5+q3+2*q2)+3/8000*\sin(2*q6+2*q5+2*q3+2*q2)-1/16000*\sin(-2*q6-2*q5-2*q4+2*q3+2*q2)-1/200*\sin(q5-q4+q3+2*q2)-1/100*\sin(-q5+q3+2*q2)-1/4000*\sin(-2*q5+2*q4)+1/4000*\sin(-2*q6-2*q5+2*q3+2*q2-q4)+1/200*\cos(-q6-q5+q3)-1/2000*\sin(q5+q4+q3)-3/8000*\sin(-2*q6-2*q5+2*q3+2*q2)+1/16000*\sin(2*q6+2*q5+2*q4+2*q3+2*q2)+1/2000*\cos(-q6-2*q5+q4+2*q3+2*q2)-1/2000*\sin(-2*q5+q4+2*q3+2*q2)-1/400*\cos(q6+q5-q4+q3+2*q2)-1/2000*\cos(q6+2*q5+2*q3+2*q2+q4)-1/200*\sin(q5-q4+q3)+1/200*\sin(-q5+q4+q3)-1/8000*\sin(2*q5-2*q4+2*q3+2*q2)+1/8000*\sin(-2*q5-2*q4+2*q3+2*q2)-1/2000*\sin(-2*q5-q4+2*q3+2*q2)-1/400*\cos(-q6-q5-q4+q3+2*q2)-1/8000*\cos(2*q5+2*q4+2*q3+2*q2+q6))*qv1*qv5+
\end{aligned}$$

$$\begin{aligned}
& -1/4000*\cos(q6+q3+q2-q4)+1/2000*\sin(q2+q3+q4)+1/4000*\sin(-2*q6-2*q5+q3+q2-q4)+1/8000*s \\
& \sin(-2*q6-2*q5+2*q4+q3+q2)+1/8000*\cos(-2*q5+2*q4+q3+q2-q6)-1/4000*\cos(q6+2*q5-q4+q3+q \\
& 2)-1/2000*\sin(q2+q3-q4)-1/8000*\cos(-q6-2*q4+q3+q2)+1/8000*\sin(2*q6+2*q5-2*q4+q3+q2)-1/4 \\
& 000*\cos(-q6-2*q5+q3+q2+q4)+1/8000*\cos(q6+2*q4+q3+q2)+1/4000*\cos(-q6-2*q5-q4+q3+q2)+1 \\
& /8000*\cos(q6+2*q5+2*q4+q3+q2)-1/4000*\sin(-2*q6-2*q5+q3+q2+q4)-1/4000*\sin(2*q6+2*q5+q \\
& 3+q2+q4)+1/8000*\cos(-q6+2*q4+q3+q2)-1/4000*\cos(-q6+q3+q2+q4)-1/8000*\cos(2*q5-2*q4+q6 \\
& +q3+q2)+1/4000*\cos(q6+q4+q3+q2)-1/8000*\sin(-2*q6-2*q5-2*q4+q3+q2)+1/4000*\sin(2*q6+2* \\
& q5+q3+q2-q4)+1/4000*\cos(-q6-q4+q3+q2)-1/8000*\cos(-2*q4+q3+q2+q6)-1/8000*\sin(2*q6+2*q5 \\
& +2*q4+q3+q2)+1/4000*\cos(q6+2*q5+q4+q3+q2)-1/8000*\cos(-q6-2*q5-2*q4+q3+q2))*qv3*qv6+ \\
& (1/400*\cos(-q6-q5+q4+q3)+1/4000*\sin(2*q6+2*q5+2*q3+2*q2-q4)-1/8000*\sin(-2*q5+2*q4+2*q \\
& 3+2*q2)-3/4000*\sin(-2*q5+2*q3+2*q2)-1/200*\cos(-q6-q5+q3+2*q2)-1/8000*\cos(-2*q4+2*q3+2* \\
& q2+q6)-1/200*\sin(-q5-q4+q3+2*q2)-1/100*\cos(2*q3+2*q2+q5+q4)+1/16000*\sin(2*q6+2*q5-2*q \\
& 4+2*q3+2*q2)-6/5*\cos(q3)+1/16000*\sin(-2*q6-2*q5+2*q4+2*q3+2*q2)-1/400*\cos(q6+q5+q4+q \\
& 3+2*q2)+1/8000*\cos(-q6-2*q5+2*q4+2*q3+2*q2)-1/50*\cos(2*q3+2*q2+q5)-1/2000*\cos(-q6-2*q \\
& 5-q4+2*q3+2*q2)-1/2000*\sin(2*q5-q4+2*q3+2*q2)-1/100*\sin(q5+q3+2*q2)+1/8000*\cos(-q6-2*q \\
& 5-2*q4+2*q3+2*q2)+1/100*\sin(q3-q5)-1/100*\cos(2*q3+2*q2+q5-q4)-1/200*\sin(q5+q4+q3+2*q2 \\
&)-3/4000*\cos(q6+2*q5+2*q3+2*q2)+1/50*\cos(2*q3+2*q2-q5)-1/8000*\sin(2*q5+2*q4+2*q3+2*q \\
& 2)-6/5*\cos(q3+2*q2)+1/200*\sin(2*q3+2*q2+q6+q5-q4)-1/200*\sin(2*q3+2*q2-q6-q5-q4)-1/200*c \\
& \cos(q6+q5+q3)-3/4000*\sin(2*q5+2*q3+2*q2)-1/100*\cos(2*q3+2*q2-q5+q4)+1/200*\sin(2*q3+2*q \\
& 2+q6+q5+q4)-1/200*\sin(2*q3+2*q2-q6-q5+q4)+1/4000*\cos(2*q3+2*q2+q6)-1/100*\cos(2*q3+2* \\
& q2-q5-q4)-1/400*\cos(q6+q5-q4+q3)+1/400*\cos(-q6-q5-q4+q3)+1/100*\sin(2*q3+2*q2-q6-q5)-1/4 \\
& 00*\cos(q6+q5+q4+q3)-1/2000*\cos(q6+2*q5+2*q3+2*q2-q4)+1/8000*\cos(-q6+2*q4+2*q3+2*q2) \\
& +1/100*\sin(2*q3+2*q2+q6+q5)-1/2000*\sin(2*q5+q4+2*q3+2*q2)+1/4000*\sin(2*q6+2*q5+q4+2 \\
& *q3+2*q2)-1/100*\sin(q3+q5)-1/8000*\cos(q6+2*q5-2*q4+2*q3+2*q2)-1/200*\sin(-q5+q4+q3+2*q \\
& 2)+1/8000*\cos(-q6-2*q4+2*q3+2*q2)+3/4000*\cos(-q6-2*q5+2*q3+2*q2)-1/200*\sin(-q5-q4+q3)- \\
& 1/4000*\sin(-2*q6-2*q5+q4+2*q3+2*q2)+1/400*\cos(-q6-q5+q4+q3+2*q2)-1/200*\cos(q6+q5+q3+ \\
& 2*q2)-3/8000*\sin(-2*q4+2*q3+2*q2)+3/8000*\sin(2*q6+2*q5+2*q3+2*q2)+4803/4000*\sin(2*q3 \\
& +2*q2)+1/16000*\sin(-2*q6-2*q5-2*q4+2*q3+2*q2)-1/200*\sin(q5-q4+q3+2*q2)+1/100*\sin(-q5+q \\
& 3+2*q2)-1/4000*\sin(-2*q6-2*q5+2*q3+2*q2-q4)-1/200*\cos(-q6-q5+q3)-1/200*\sin(q5+q4+q3)+3/ \\
& 8000*\sin(-2*q6-2*q5+2*q3+2*q2)+1/16000*\sin(2*q6+2*q5+2*q4+2*q3+2*q2)-1/2000*\cos(-q6- \\
& 2*q5+q4+2*q3+2*q2)+1/2000*\sin(-2*q5+q4+2*q3+2*q2)-1/400*\cos(q6+q5-q4+q3+2*q2)-1/200 \\
& 0*\cos(q6+2*q5+2*q3+2*q2+q4)-1/8000*\cos(q6+2*q4+2*q3+2*q2)-3/8000*\sin(2*q4+2*q3+2*q2 \\
&)-1/200*\sin(q5-q4+q3)-1/200*\sin(-q5+q4+q3)-1/8000*\sin(2*q5-2*q4+2*q3+2*q2)-1/8000*\sin(-2* \\
& q5-2*q4+2*q3+2*q2)-1/4000*\cos(-q6+2*q3+2*q2)+1/2000*\sin(-2*q5-q4+2*q3+2*q2)+1/400*co \\
& s(-q6-q5-q4+q3+2*q2)-1/8000*\cos(2*q5+2*q4+2*q3+2*q2+q6))*qv1*qv3+(-1/8000*\sin(2*q5-2* \\
& q4+q3+q2)-1/400*\sin(q6+q5+q2+q3+q4)-1/400*\sin(-q6-q5+q2+q3-q4)-1/8000*\sin(-2*q6-2*q5+q \\
& 3+q2-q4)+1/400*\sin(-q6-q5+q2+q3+q4)+3/8000*\sin(2*q4+q3+q2)+1/200*\cos(-q5+q2+q3+q4)+1/ \\
& 200*\cos(q5+q2+q3+q4)-1/200*\cos(-q5+q2+q3-q4)-1/8000*\sin(-2*q5-2*q4+q3+q2)+1/400*\sin(q6 \\
& +q5+q2+q3-q4)-1/16000*\sin(-2*q6-2*q5+2*q4+q3+q2)-1/8000*\cos(-2*q5+2*q4+q3+q2-q6)+1/4 \\
& 00*\cos(q6+q5+q4+q2)-1/200*\cos(q5+q2+q3-q4)+1/400*\cos(q6+q5+q4-q2)+1/4000*\sin(2*q5+q4 \\
& +q3+q2)-1/4000*\sin(2*q5-q4+q3+q2)-1/4000*\cos(q6+2*q5-q4+q3+q2)+1/200*\sin(-q5+q4-q2)+1/ \\
& 8000*\cos(-q6-2*q4+q3+q2)+1/16000*\sin(2*q6+2*q5-2*q4+q3+q2)-1/400*\cos(-q6-q5+q4-q2)+1/ \\
& 4000*\cos(-q6-2*q5+q3+q2+q4)+1/8000*\cos(q6+2*q4+q3+q2)-1/4000*\sin(-2*q5+q4+q3+q2)-1/4 \\
& 000*\cos(-q6-2*q5-q4+q3+q2)+1/200*\sin(q5+q4-q2)+1/8000*\cos(q6+2*q5+2*q4+q3+q2)+1/8000 \\
& *\sin(-2*q6-2*q5+q3+q2+q4)+1/200*\sin(q5+q4+q2)-1/8000*\sin(2*q6+2*q5+q3+q2+q4)+1/4000*s
\end{aligned}$$

$$\begin{aligned}
& \sin(-2*q5-q4+q3+q2)-1/8000*\cos(-q6+2*q4+q3+q2)-1/400*\cos(-q6-q5+q4+q2)+1/8000*\sin(2*q5+ \\
& 2*q4+q3+q2)-1/8000*\cos(2*q5-2*q4+q6+q3+q2)+1/8000*\sin(-2*q5+2*q4+q3+q2)+1/16000*\sin(\\
& -2*q6-2*q5-2*q4+q3+q2)+1/8000*\sin(2*q6+2*q5+q3+q2-q4)-3/8000*\sin(-2*q4+q3+q2)+1/200*s \\
& \sin(-q5+q4+q2)-1/8000*\cos(-2*q4+q3+q2+q6)-1/16000*\sin(2*q6+2*q5+2*q4+q3+q2)+1/4000*\cos \\
& (q6+2*q5+q4+q3+q2)+1/8000*\cos(-q6-2*q5-2*q4+q3+q2))*qv2^2+(-1/400*\cos(-q6-q5+q4+q3)+ \\
& 1/4000*\sin(2*q6+2*q5+2*q3+2*q2-q4)+1/200*\cos(-q6-q5+q3+2*q2)-1/16000*\cos(-2*q4+2*q3+ \\
& 2*q2+q6)+1/16000*\sin(2*q6+2*q5-2*q4+2*q3+2*q2)+1/8000*\cos(2*q4-q6)-1/16000*\sin(-2*q6- \\
& 2*q5+2*q4+2*q3+2*q2)-1/400*\cos(q6+q5+q4+q3+2*q2)-1/16000*\cos(-q6-2*q5+2*q4+2*q3+2* \\
& q2)+1/4000*\cos(-q6-2*q5-q4+2*q3+2*q2)-1/8000*\sin(2*q6+2*q5+2*q4)+1/8000*\cos(2*q5+2*q4 \\
& +q6)-1/8000*\cos(q6)-1/16000*\cos(-q6-2*q5-2*q4+2*q3+2*q2)-3/8000*\cos(q6+2*q5+2*q3+2*q2)- \\
& 1/100*\sin(q6+q5)+1/400*\sin(2*q3+2*q2+q6+q5-q4)+1/400*\sin(2*q3+2*q2-q6-q5-q4)-1/200*\cos(\\
& q6+q5+q3)+1/4000*\sin(2*q6+2*q5)+1/8000*\cos(-2*q5+2*q4-q6)+1/400*\sin(2*q3+2*q2+q6+q5+ \\
& q4)+1/400*\sin(2*q3+2*q2-q6-q5+q4)+1/8000*\cos(2*q3+2*q2+q6)+1/8000*\sin(-2*q6-2*q5+2*q4 \\
&)-1/400*\cos(q6+q5-q4+q3)-1/400*\cos(-q6-q5-q4+q3)-1/200*\sin(2*q3+2*q2-q6-q5)-1/400*\cos(q6 \\
& +q5+q4+q3)-1/4000*\cos(q6+2*q5+2*q3+2*q2-q4)-1/16000*\cos(-q6+2*q4+2*q3+2*q2)+1/200*si \\
& n(2*q3+2*q2+q6+q5)+1/4000*\sin(2*q6+2*q5+q4+2*q3+2*q2)-1/16000*\cos(q6+2*q5-2*q4+2*q \\
& 3+2*q2)-1/16000*\cos(-q6-2*q4+2*q3+2*q2)-1/4000*\cos(q6+2*q5)+1/8000*\cos(q6+2*q4)-3/800 \\
& 0*\cos(-q6-2*q5+2*q3+2*q2)+1/4000*\sin(-2*q6-2*q5+q4+2*q3+2*q2)-1/400*\cos(-q6-q5+q4+q3+ \\
& 2*q2)-1/200*\cos(q6+q5+q3+2*q2)+3/8000*\sin(2*q6+2*q5+2*q3+2*q2)-1/16000*\sin(-2*q6-2*q5 \\
& -2*q4+2*q3+2*q2)+1/4000*\sin(-2*q6-2*q5+2*q3+2*q2-q4)+1/200*\cos(-q6-q5+q3)-3/8000*\sin(- \\
& 2*q6-2*q5+2*q3+2*q2)+1/16000*\sin(2*q6+2*q5+2*q4+2*q3+2*q2)+1/4000*\cos(-q6-2*q5+q4+ \\
& 2*q3+2*q2)-1/400*\cos(q6+q5-q4+q3+2*q2)-1/4000*\cos(q6+2*q5+2*q3+2*q2+q4)-1/16000*\cos(\\
& q6+2*q4+2*q3+2*q2)+1/8000*\cos(-q6+2*q3+2*q2)-1/400*\cos(-q6-q5-q4+q3+2*q2)-1/16000*co \\
& s(2*q5+2*q4+2*q3+2*q2+q6))*qv1*qv6+(1/400*\cos(-q6-q5+q4+q3)-1/8000*\sin(2*q6+2*q5+2*q \\
& 3+2*q2-q4)-1/8000*\sin(-2*q5+2*q4+2*q3+2*q2)+1/8000*\cos(-2*q4+2*q3+2*q2+q6)+1/200*\sin(\\
& -q5-q4+q3+2*q2)-1/200*\cos(2*q3+2*q2+q5+q4)+1/4000*\sin(2*q5+2*q4)-1/16000*\sin(2*q6+2*q \\
& 5-2*q4+2*q3+2*q2)-1/4000*\cos(2*q4-q6)+1/16000*\sin(-2*q6-2*q5+2*q4+2*q3+2*q2)-1/400*co \\
& s(q6+q5+q4+q3+2*q2)+1/8000*\cos(-q6-2*q5+2*q4+2*q3+2*q2)+1/4000*\cos(-q6-2*q5-q4+2*q3 \\
& +2*q2)-1/8000*\sin(2*q6+2*q5+2*q4)+1/4000*\cos(2*q5+2*q4+q6)+1/4000*\sin(2*q5-q4+2*q3+2 \\
& *q2)-1/8000*\cos(-q6-2*q5-2*q4+2*q3+2*q2)+1/200*\cos(2*q3+2*q2+q5-q4)-1/200*\sin(q5+q4+q \\
& 3+2*q2)-1/8000*\sin(2*q5+2*q4+2*q3+2*q2)-1/400*\sin(2*q3+2*q2+q6+q5-q4)+1/400*\sin(2*q3+ \\
& 2*q2-q6-q5-q4)-1/200*\cos(2*q3+2*q2-q5+q4)-1/4000*\cos(-2*q5+2*q4-q6)+1/400*\sin(2*q3+2*q \\
& 2+q6+q5+q4)-1/400*\sin(2*q3+2*q2-q6-q5+q4)-1/8000*\sin(-2*q6-2*q5+2*q4)+1/200*\cos(2*q3+ \\
& 2*q2-q5-q4)+1/400*\cos(q6+q5-q4+q3)-1/400*\cos(-q6-q5-q4+q3)-1/400*\cos(q6+q5+q4+q3)+1/40 \\
& 00*\cos(q6+2*q5+2*q3+2*q2-q4)+1/8000*\cos(-q6+2*q4+2*q3+2*q2)-1/4000*\sin(2*q5+q4+2*q3 \\
& +2*q2)+1/8000*\sin(2*q6+2*q5+q4+2*q3+2*q2)+1/8000*\cos(q6+2*q5-2*q4+2*q3+2*q2)-1/200* \\
& \sin(-q5+q4+q3+2*q2)-1/8000*\cos(-q6-2*q4+2*q3+2*q2)+1/4000*\cos(q6+2*q4)+1/200*\sin(-q5-q \\
& 4+q3)-1/8000*\sin(-2*q6-2*q5+q4+2*q3+2*q2)+1/400*\cos(-q6-q5+q4+q3+2*q2)+3/8000*\sin(-2* \\
& q4+2*q3+2*q2)-1/16000*\sin(-2*q6-2*q5-2*q4+2*q3+2*q2)+1/200*\sin(q5-q4+q3+2*q2)+1/4000 \\
& *\sin(-2*q5+2*q4)+1/8000*\sin(-2*q6-2*q5+2*q3+2*q2-q4)-1/200*\sin(q5+q4+q3)+1/16000*\sin(2* \\
& q6+2*q5+2*q4+2*q3+2*q2)-1/4000*\cos(-q6-2*q5+q4+2*q3+2*q2)+1/4000*\sin(-2*q5+q4+2*q3+ \\
& 2*q2)+3/4000*\sin(2*q4)+1/400*\cos(q6+q5-q4+q3+2*q2)-1/4000*\cos(q6+2*q5+2*q3+2*q2+q4)- \\
& 1/8000*\cos(q6+2*q4+2*q3+2*q2)-3/8000*\sin(2*q4+2*q3+2*q2)+1/200*\sin(q5-q4+q3)-1/200*\sin \\
& (-q5+q4+q3)+1/8000*\sin(2*q5-2*q4+2*q3+2*q2)+1/8000*\sin(-2*q5-2*q4+2*q3+2*q2)-1/4000*s \\
& \sin(-2*q5-q4+2*q3+2*q2)-1/400*\cos(-q6-q5-q4+q3+2*q2)-1/8000*\cos(2*q5+2*q4+2*q3+2*q2+q
\end{aligned}$$

$$\begin{aligned}
& 6)) * qv1 * qv4 + (-1/200 * \sin(q6 + q5 + q2 + q3 - q4) - 1/200 * \sin(-q6 - q5 + q2 + q3 + q4) + 1/200 * \sin(q6 + q5 + q2 + \\
& q3 + q4) + 1/200 * \cos(-q6 - q5 + q4 + q2) + 1/200 * \cos(-q6 - q5 + q4 - q2) + 1/200 * \sin(-q6 - q5 + q2 + q3 - q4) + 1/20 \\
& 00 * \cos(-q6 + q3 + q2 + q4) + 1/2000 * \cos(q6 + q4 + q3 + q2) - 1/2000 * \cos(-q6 - q4 + q3 + q2) - 1/200 * \cos(q6 + q5 \\
& + q4 + q2) - 1/200 * \cos(q6 + q5 + q4 - q2) - 1/2000 * \cos(q6 + q3 + q2 - q4)) * qv5 * qv6 + (-1/200 * \sin(q5 + q4 + q2) - \\
& 1/400 * \sin(q6 + q5 + q2 + q3 - q4) - 1/400 * \sin(-q6 - q5 + q2 + q3 + q4) + 1/400 * \sin(q6 + q5 + q2 + q3 + q4) + 1/400 * \\
& \cos(-q6 - q5 + q4 + q2) - 1/200 * \sin(-q5 + q4 + q2) + 1/400 * \cos(-q6 - q5 + q4 - q2) + 1/400 * \sin(-q6 - q5 + q2 + q3 - q \\
& 4) + 1/200 * \cos(q5 + q2 + q3 - q4) + 1/200 * \cos(-q5 + q2 + q3 - q4) - 1/200 * \cos(q5 + q2 + q3 + q4) - 1/200 * \cos(-q5 \\
& + q2 + q3 + q4) - 1/400 * \cos(q6 + q5 + q4 + q2) - 1/200 * \sin(-q5 + q4 - q2) - 1/400 * \cos(q6 + q5 + q4 - q2) - 1/200 * \sin \\
& (q5 + q4 - q2)) * qv5^2 + (1/400 * \sin(q6 + q5 + q2 + q3 + q4) + 1/400 * \sin(-q6 - q5 + q2 + q3 - q4) + 1/8000 * \sin(-2 * \\
& q6 - 2 * q5 + q3 + q2 - q4) - 1/400 * \sin(-q6 - q5 + q2 + q3 + q4) - 1/200 * \cos(-q5 + q2 + q3 + q4) - 1/200 * \cos(q5 + q2 + \\
& q3 + q4) + 1/200 * \cos(-q5 + q2 + q3 - q4) - 1/400 * \sin(q6 + q5 + q2 + q3 - q4) - 1/400 * \cos(q6 + q5 + q4 + q2) + 1/200 \\
& * \cos(q5 + q2 + q3 - q4) - 1/400 * \cos(q6 + q5 + q4 - q2) - 1/4000 * \sin(2 * q5 + q4 + q3 + q2) + 1/4000 * \sin(2 * q5 - q4 + \\
& q3 + q2) + 1/4000 * \cos(q6 + 2 * q5 - q4 + q3 + q2) - 1/200 * \sin(-q5 + q4 - q2) + 1/400 * \cos(-q6 - q5 + q4 - q2) - 1/4000 \\
& * \cos(-q6 - 2 * q5 + q3 + q2 + q4) + 1/4000 * \sin(-2 * q5 + q4 + q3 + q2) + 1/4000 * \cos(-q6 - 2 * q5 - q4 + q3 + q2) - 1/20 \\
& 0 * \sin(q5 + q4 - q2) - 1/8000 * \sin(-2 * q6 - 2 * q5 + q3 + q2 + q4) - 1/200 * \sin(q5 + q4 + q2) + 1/8000 * \sin(2 * q6 + 2 * \\
& q5 + q3 + q2 + q4) - 1/4000 * \sin(-2 * q5 - q4 + q3 + q2) + 1/400 * \cos(-q6 - q5 + q4 + q2) - 1/8000 * \sin(2 * q6 + 2 * q5 + \\
& q3 + q2 - q4) - 1/200 * \sin(-q5 + q4 + q2) - 1/4000 * \cos(q6 + 2 * q5 + q4 + q3 + q2)) * qv4^2 + (1/2000 * \cos(q6 + q3 + \\
& q2 - q4) + 1/2000 * \sin(2 * q6 + 2 * q5 + q3 + q2) + 1/1000 * \sin(-2 * q5 + q3 + q2) - 1/1000 * \sin(2 * q5 + q3 + q2) + 3/2 \\
& 000 * \sin(q2 + q3 + q4) - 1/1000 * \cos(q6 + 2 * q5 + q3 + q2) - 1/1000 * \cos(-2 * q5 + q3 + q2 - q6) - 1/2000 * \sin(-2 * q \\
& 6 - 2 * q5 + q3 + q2) + 1/200 * \sin(q6 + q5 + q2 + q3 + q4) + 1/200 * \sin(-q6 - q5 + q2 + q3 - q4) + 1/4000 * \sin(-2 * q6 - 2 \\
& * q5 + q3 + q2 - q4) + 1/200 * \sin(-q6 - q5 + q2 + q3 + q4) + 1/100 * \cos(-q5 + q2 + q3 + q4) - 1/100 * \cos(q5 + q2 + q3 + \\
& q4) + 1/100 * \cos(-q5 + q2 + q3 - q4) + 1/200 * \sin(q6 + q5 + q2 + q3 - q4) - 1/200 * \cos(q6 + q5 + q4 + q2) - 1/100 * \cos \\
& (q5 + q2 + q3 - q4) - 1/200 * \cos(q6 + q5 + q4 - q2) - 1/2000 * \sin(2 * q5 + q4 + q3 + q2) - 1/2000 * \sin(2 * q5 - q4 + q3 + q \\
& 2) - 1/2000 * \cos(q6 + 2 * q5 - q4 + q3 + q2) + 3/2000 * \sin(q2 + q3 - q4) + 1/100 * \sin(-q5 + q4 - q2) - 1/200 * \cos(-q6 - \\
& q5 + q4 - q2) + 1/2000 * \cos(-q6 - 2 * q5 + q3 + q2 + q4) - 1/2000 * \sin(-2 * q5 + q4 + q3 + q2) + 1/2000 * \cos(-q6 - 2 * q \\
& 5 - q4 + q3 + q2) - 1/100 * \sin(q5 + q4 - q2) + 1/4000 * \sin(-2 * q6 - 2 * q5 + q3 + q2 + q4) - 1/100 * \sin(q5 + q4 + q2) + 1/ \\
& 4000 * \sin(2 * q6 + 2 * q5 + q3 + q2 + q4) - 1/2000 * \sin(-2 * q5 - q4 + q3 + q2) - 1/200 * \cos(-q6 - q5 + q4 + q2) - 1/2000 \\
& * \cos(-q6 + q3 + q2 + q4) + 1/2000 * \cos(q6 + q4 + q3 + q2) + 1/4000 * \sin(2 * q6 + 2 * q5 + q3 + q2 - q4) + 1/100 * \sin(- \\
& q5 + q4 + q2) - 1/2000 * \cos(-q6 - q4 + q3 + q2) - 1/2000 * \cos(q6 + 2 * q5 + q4 + q3 + q2)) * qv4 * qv5 + (1/4000 * \sin(\\
& 2 * q6 + 2 * q5 + q3 + q2) - 1/2000 * \sin(-2 * q5 + q3 + q2) - 1/2000 * \cos(q6 + q3 + q2) - 1/2000 * \sin(2 * q5 + q3 + q2) - \\
& 1/2000 * \cos(q6 + 2 * q5 + q3 + q2) + 1/2000 * \cos(-q6 + q3 + q2) + 1/2000 * \cos(-2 * q5 + q3 + q2 - q6) + 1/4000 * \sin \\
& (-2 * q6 - 2 * q5 + q3 + q2) - 3/2000 * \sin(q2 + q3) + 1/4000 * \sin(2 * q5 - 2 * q4 + q3 + q2) + 3/4000 * \sin(2 * q4 + q3 + q \\
& 2) + 1/4000 * \sin(-2 * q5 - 2 * q4 + q3 + q2) - 1/8000 * \sin(-2 * q6 - 2 * q5 + 2 * q4 + q3 + q2) - 1/4000 * \cos(-2 * q5 + 2 * q \\
& 4 + q3 + q2 - q6) - 1/4000 * \cos(-q6 - 2 * q4 + q3 + q2) - 1/8000 * \sin(2 * q6 + 2 * q5 - 2 * q4 + q3 + q2) + 1/4000 * \cos(q6 \\
& + 2 * q4 + q3 + q2) + 1/4000 * \cos(q6 + 2 * q5 + 2 * q4 + q3 + q2) - 1/4000 * \cos(-q6 + 2 * q4 + q3 + q2) + 1/4000 * \sin(2 \\
& * q5 + 2 * q4 + q3 + q2) + 1/4000 * \cos(2 * q5 - 2 * q4 + q6 + q3 + q2) + 1/4000 * \sin(-2 * q5 + 2 * q4 + q3 + q2) - 1/8000 * \\
& \sin(-2 * q6 - 2 * q5 - 2 * q4 + q3 + q2) + 3/4000 * \sin(-2 * q4 + q3 + q2) + 1/4000 * \cos(-2 * q4 + q3 + q2 + q6) - 1/8000 * s \\
& \sin(2 * q6 + 2 * q5 + 2 * q4 + q3 + q2) - 1/4000 * \cos(-q6 - 2 * q5 - 2 * q4 + q3 + q2)) * qv2 * qv4 + (3/16000 * \cos(-2 * q4 \\
& + 2 * q3 + 2 * q2) - 3/16000 * \cos(2 * q6 + 2 * q5 + 2 * q3 + 2 * q2) - 4803/8000 * \cos(2 * q3 + 2 * q2) - 1/32000 * \cos(-2 \\
& * q6 - 2 * q5 - 2 * q4 + 2 * q3 + 2 * q2) + 1/200 * \cos(q5 - q4 + q3 + 2 * q2) + 1/8000 * \cos(-2 * q6 - 2 * q5 + 2 * q3 + 2 * q2 - q \\
& 4) - 1/8000 * \cos(2 * q5 + 2 * q4) - 1/200 * \sin(2 * q3 + 2 * q2 - q5 - q4) - 1/32000 * \cos(2 * q6 + 2 * q5 + 2 * q4 + 2 * q3 + 2 \\
& * q2) - 1/4000 * \sin(-q6 - 2 * q5 + q4 + 2 * q3 + 2 * q2) + 1/200 * \cos(-q5 - q4 + q3) - 1/400 * \sin(q6 + q5 - q4 + q3 + 2 * q2 \\
&) - 1/200 * \sin(-q6 - q5 + q3) - 1/4000 * \sin(q6 + 2 * q5 + 2 * q3 + 2 * q2 + q4) - 1/16000 * \sin(q6 + 2 * q4 + 2 * q3 + 2 * q2) \\
& - 6/5 * \sin(q3) + 3/16000 * \cos(2 * q4 + 2 * q3 + 2 * q2) - 1/200 * \sin(2 * q3 + 2 * q2 + q5 + q4) + 1/400 * \cos(2 * q3 + 2 * \\
& q2 - q6 - q5 + q4) + 1/100 * \sin(2 * q3 + 2 * q2 - q5) + 1/200 * \cos(q5 - q4 + q3) + 1/16000 * \cos(2 * q5 - 2 * q4 + 2 * q3 + 2
\end{aligned}$$

$$\begin{aligned}
& *q_2)+1/16000*\cos(-2*q_5-2*q_4+2*q_3+2*q_2)+1/400*\sin(-q_6-q_5-q_4+q_3+2*q_2)+1/16000*\cos(2*q_6+ \\
& 2*q_5+2*q_4)+1/50*\sin(q_5)+1/200*\cos(-q_5+q_4+q_3)-1/8000*\cos(-2*q_5+2*q_4)-1/16000*\sin(2*q_5+2 \\
& *q_4+2*q_3+2*q_2+q_6)+1/200*\cos(-q_5-q_4+q_3+2*q_2)+1/100*\cos(q_6+q_5)-3/8000*\cos(2*q_4)-1/800*si \\
& n(q_6)-1/4000*\sin(-q_6-2*q_5-q_4+2*q_3+2*q_2)+1/4000*\cos(2*q_5-q_4+2*q_3+2*q_2)+1/100*\cos(q_3+q_5) \\
& -1/8000*\sin(2*q_4-q_6)+1/100*\cos(q_5+q_3+2*q_2)-1/400*\sin(q_6+q_5-q_4+q_3)+1/16000*\sin(-q_6-2*q_4+ \\
& 2*q_3+2*q_2)+3/8000*\cos(-2*q_5+2*q_3+2*q_2)-1/200*\sin(-q_6-q_5+q_3+2*q_2)+1/400*\sin(-q_6-q_5-q_4+q \\
& 3)+1/4000*\cos(2*q_5)-1/8000*\cos(2*q_6+2*q_5)-1/32000*\cos(2*q_6+2*q_5-2*q_4+2*q_3+2*q_2)+1/800 \\
& 0*\sin(2*q_5+2*q_4+q_6)+3/8000*\cos(2*q_5+2*q_3+2*q_2)+2723/1600-1/100*\cos(-q_5+q_3+2*q_2)+1/20 \\
& 0*\cos(q_5+q_4+q_3)+1/16000*\cos(2*q_5+2*q_4+2*q_3+2*q_2)-6/5*\sin(q_3+2*q_2)-1/8000*\sin(-q_6+2*q_3 \\
& +2*q_2)-1/4000*\cos(-2*q_5-q_4+2*q_3+2*q_2)-1/200*\sin(q_6+q_5+q_3)-1/4000*\sin(q_6+2*q_5)-1/8000*co \\
& s(2*q_6+2*q_5+2*q_3+2*q_2-q_4)+1/16000*\sin(-q_6+2*q_4+2*q_3+2*q_2)+1/4000*\cos(2*q_5+q_4+2*q_3+ \\
& 2*q_2)-1/400*\cos(2*q_3+2*q_2+q_6+q_5-q_4)-1/8000*\cos(2*q_6+2*q_5+q_4+2*q_3+2*q_2)-1/200*\cos(2*q \\
& 3+2*q_2+q_6+q_5)-3/16000*\cos(-2*q_6-2*q_5+2*q_3+2*q_2)+1/16000*\sin(-q_6-2*q_5-2*q_4+2*q_3+2*q_2) \\
& -1/400*\cos(2*q_3+2*q_2+q_6+q_5+q_4)+1/16000*\cos(-2*q_5+2*q_4+2*q_3+2*q_2)+1/200*\cos(q_5+q_4+q_3 \\
& +2*q_2)-3/8000*\sin(q_6+2*q_5+2*q_3+2*q_2)-1/32000*\cos(-2*q_6-2*q_5+2*q_4+2*q_3+2*q_2)-1/400*\sin \\
& (q_6+q_5+q_4+q_3+2*q_2)+1/16000*\sin(-q_6-2*q_5+2*q_4+2*q_3+2*q_2)-1/4000*\sin(q_6+2*q_5+2*q_3+2*q \\
& 2-q_4)-1/200*\sin(2*q_3+2*q_2-q_5+q_4)+3/8000*\sin(-q_6-2*q_5+2*q_3+2*q_2)-1/8000*\sin(-2*q_5+2*q_4-q \\
& 6)+1/400*\sin(-q_6-q_5+q_4+q_3+2*q_2)-1/400*\sin(q_6+q_5+q_4+q_3)-1/200*\cos(2*q_3+2*q_2-q_6-q_5)-1/200 \\
& *\sin(q_6+q_5+q_3+2*q_2)-1/100*\cos(q_3-q_5)-1/16000*\sin(-2*q_4+2*q_3+2*q_2+q_6)-1/16000*\sin(q_6+2* \\
& q_5-2*q_4+2*q_3+2*q_2)-1/100*\sin(2*q_3+2*q_2+q_5)+1/200*\cos(-q_5+q_4+q_3+2*q_2)+1/16000*\cos(-2* \\
& q_6-2*q_5+2*q_4)+1/8000*\cos(-2*q_6-2*q_5+q_4+2*q_3+2*q_2)+1/400*\sin(-q_6-q_5+q_4+q_3)+11/10*\cos(2 \\
& *q_2)+1/400*\cos(2*q_3+2*q_2-q_6-q_5-q_4)+1/8000*\sin(q_6+2*q_4)-1/200*\sin(2*q_3+2*q_2+q_5-q_4)-1/40 \\
& 00*\cos(-2*q_5+q_4+2*q_3+2*q_2)+1/8000*\sin(2*q_3+2*q_2+q_6))*q_1+(-3/8000*\cos(2*q_4+q_3+q_2)-1/2 \\
& 00*\cos(q_5+q_4+q_2)-1/400*\cos(q_6+q_5+q_2+q_3-q_4)-1/8000*\sin(-q_6+2*q_4+q_3+q_2)-1/400*\cos(-q_6-q_5 \\
& +q_2+q_3+q_4)+1/400*\cos(q_6+q_5+q_2+q_3+q_4)-1/400*\sin(-q_6-q_5+q_4+q_2)+3/8000*\cos(-2*q_4+q_3+q_2) \\
& -1/200*\cos(-q_5+q_4+q_2)-1/8000*\sin(-2*q_4+q_3+q_2+q_6)+1/16000*\cos(2*q_6+2*q_5+2*q_4+q_3+q_2)+1 \\
& /8000*\cos(2*q_5-2*q_4+q_3+q_2)+1/400*\sin(-q_6-q_5+q_4-q_2)+1/4000*\sin(-q_6-2*q_5+q_3+q_2+q_4)+1/400 \\
& *\cos(-q_6-q_5+q_2+q_3-q_4)+1/4000*\cos(-2*q_5+q_4+q_3+q_2)-1/4000*\sin(-q_6-2*q_5-q_4+q_3+q_2)-1/200*si \\
& n(q_5+q_2+q_3-q_4)+1/8000*\sin(q_6+2*q_5+2*q_4+q_3+q_2)-1/8000*\sin(2*q_5-2*q_4+q_6+q_3+q_2)-1/200*si \\
& n(-q_5+q_2+q_3-q_4)-1/8000*\cos(-2*q_5+2*q_4+q_3+q_2)+1/16000*\cos(-2*q_6-2*q_5+2*q_4+q_3+q_2)+1/20 \\
& 00*\sin(q_5+q_2+q_3+q_4)+1/4000*\cos(2*q_5-q_4+q_3+q_2)+1/200*\sin(-q_5+q_2+q_3+q_4)-1/4000*\sin(q_6+2* \\
& q_5-q_4+q_3+q_2)-1/8000*\cos(-2*q_6-2*q_5+q_3+q_2+q_4)+1/8000*\cos(2*q_6+2*q_5+q_3+q_2+q_4)-1/4000*c \\
& os(-2*q_5-q_4+q_3+q_2)-1/8000*\cos(2*q_5+2*q_4+q_3+q_2)-1/8000*\sin(-2*q_5+2*q_4+q_3+q_2-q_6)+1/400* \\
& sin(q_6+q_5+q_4+q_2)+1/200*\cos(-q_5+q_4-q_2)+1/8000*\sin(-q_6-2*q_4+q_3+q_2)+1/4000*\sin(q_6+2*q_5+q \\
& 4+q_3+q_2)+1/8000*\sin(-q_6-2*q_5-2*q_4+q_3+q_2)+1/8000*\cos(-2*q_6-2*q_5+q_3+q_2-q_4)-1/4000*\cos(2 \\
& *q_5+q_4+q_3+q_2)-1/400*\sin(q_6+q_5+q_4-q_2)-1/16000*\cos(2*q_6+2*q_5-2*q_4+q_3+q_2)+1/8000*\sin(q_6 \\
& +2*q_4+q_3+q_2)+1/8000*\cos(-2*q_5-2*q_4+q_3+q_2)+1/200*\cos(q_5+q_4-q_2)-1/16000*\cos(-2*q_6-2*q_5- \\
& 2*q_4+q_3+q_2)-1/8000*\cos(2*q_6+2*q_5+q_3+q_2-q_4))*q_2+(-3/8000*\cos(2*q_4+q_3+q_2)-1/400*\cos(q_6 \\
& +q_5+q_2+q_3-q_4)-1/8000*\sin(-q_6+2*q_4+q_3+q_2)-1/400*\cos(-q_6-q_5+q_2+q_3+q_4)+1/400*\cos(q_6+q_5+q \\
& 2+q_3+q_4)+3/8000*\cos(-2*q_4+q_3+q_2)-1/8000*\sin(-2*q_4+q_3+q_2+q_6)+1/16000*\cos(2*q_6+2*q_5+2* \\
& q_4+q_3+q_2)+1/8000*\cos(2*q_5-2*q_4+q_3+q_2)+1/4000*\sin(-q_6-2*q_5+q_3+q_2+q_4)+1/400*\cos(-q_6-q_5 \\
& +q_2+q_3-q_4)+1/4000*\cos(-2*q_5+q_4+q_3+q_2)-1/4000*\sin(-q_6-2*q_5-q_4+q_3+q_2)-1/200*\sin(q_5+q_2+q \\
& 3-q_4)+1/8000*\sin(q_6+2*q_5+2*q_4+q_3+q_2)-1/8000*\sin(2*q_5-2*q_4+q_6+q_3+q_2)-1/200*\sin(-q_5+q_2+ \\
& q_3-q_4)-1/8000*\cos(-2*q_5+2*q_4+q_3+q_2)+1/16000*\cos(-2*q_6-2*q_5+2*q_4+q_3+q_2)+1/200*\sin(q_5+q \\
& 2+q_3+q_4)+1/4000*\cos(2*q_5-q_4+q_3+q_2)+1/200*\sin(-q_5+q_2+q_3+q_4)-1/4000*\sin(q_6+2*q_5-q_4+q_3+
\end{aligned}$$

$$\begin{aligned}
& q_2) - 1/8000 * \cos(-2 * q_6 - 2 * q_5 + q_3 + q_2 + q_4) + 1/8000 * \cos(2 * q_6 + 2 * q_5 + q_3 + q_2 + q_4) - 1/4000 * \cos(-2 * q_5 - q_4 + q_3 + q_2) - 1/8000 * \cos(2 * q_5 + 2 * q_4 + q_3 + q_2) - 1/8000 * \sin(-2 * q_5 + 2 * q_4 + q_3 + q_2 - q_6) + 1/8000 * \sin(-q_6 - 2 * q_4 + q_3 + q_2) + 1/4000 * \sin(q_6 + 2 * q_5 + q_4 + q_3 + q_2) + 1/8000 * \sin(-q_6 - 2 * q_5 - 2 * q_4 + q_3 + q_2) + 1/8000 * \cos(-2 * q_6 - 2 * q_5 + q_3 + q_2 - q_4) - 1/4000 * \cos(2 * q_5 + q_4 + q_3 + q_2) - 1/16000 * \cos(2 * q_6 + 2 * q_5 - 2 * q_4 + q_3 + q_2) + 1/8000 * \sin(q_6 + 2 * q_4 + q_3 + q_2) + 1/8000 * \cos(-2 * q_5 - 2 * q_4 + q_3 + q_2) - 1/16000 * \cos(-2 * q_6 - 2 * q_5 - 2 * q_4 + q_3 + q_2) - 1/8000 * \cos(2 * q_6 + 2 * q_5 + q_3 + q_2 - q_4) * q_a3 + (1/200 * \cos(q_5 + q_4 + q_2) - 1/400 * \cos(q_6 + q_5 + q_2 + q_3 - q_4) + 1/400 * \cos(-q_6 - q_5 + q_2 + q_3 + q_4) - 1/400 * \cos(q_6 + q_5 + q_2 + q_3 + q_4) + 1/400 * \sin(-q_6 - q_5 + q_4 + q_2) - 1/4000 * \cos(2 * q_6 + 2 * q_5 + q_3 + q_2) + 1/2000 * \cos(-2 * q_5 + q_3 + q_2) + 1/200 * \cos(-q_5 + q_4 + q_2) + 1/400 * \sin(-q_6 - q_5 + q_4 - q_2) - 1/4000 * \sin(-q_6 - 2 * q_5 + q_3 + q_2 + q_4) + 1/400 * \cos(-q_6 - q_5 + q_2 + q_3 - q_4) - 1/4000 * \cos(-2 * q_5 + q_4 + q_3 + q_2) + 3/2000 * \cos(q_2 + q_3) - 1/4000 * \sin(-q_6 - 2 * q_5 - q_4 + q_3 + q_2) - 1/200 * \sin(q_5 + q_2 + q_3 - q_4) - 1/200 * \sin(-q_5 + q_2 + q_3 - q_4) - 1/200 * \sin(q_5 + q_2 + q_3 + q_4) + 1/4000 * \cos(2 * q_5 - q_4 + q_3 + q_2) + 1/2000 * \cos(2 * q_5 + q_3 + q_2) - 1/200 * \sin(-q_5 + q_2 + q_3 + q_4) - 1/4000 * \sin(q_6 + 2 * q_5 - q_4 + q_3 + q_2) + 1/8000 * \cos(-2 * q_6 - 2 * q_5 + q_3 + q_2 + q_4) - 1/2000 * \sin(q_6 + q_3 + q_2) - 1/8000 * \cos(2 * q_6 + 2 * q_5 + q_3 + q_2 + q_4) - 1/4000 * \cos(-2 * q_5 - q_4 + q_3 + q_2) + 1/2000 * \sin(-q_6 + q_3 + q_2) - 1/2000 * \sin(q_6 + 2 * q_5 + q_3 + q_2) - 1/400 * \sin(q_6 + q_5 + q_4 + q_2) + 1/200 * \cos(-q_5 + q_4 - q_2) - 1/4000 * \sin(q_6 + 2 * q_5 + q_4 + q_3 + q_2) + 1/8000 * \cos(-2 * q_6 - 2 * q_5 + q_3 + q_2 - q_4) + 1/4000 * \cos(2 * q_5 + q_4 + q_3 + q_2) - 1/4000 * \sin(q_6 + q_5 + q_4 - q_2) + 1/2000 * \sin(-2 * q_5 + q_3 + q_2 - q_6) + 1/200 * \cos(q_5 + q_4 - q_2) - 1/4000 * \cos(-2 * q_6 - 2 * q_5 + q_3 + q_2) - 1/8000 * \cos(2 * q_6 + 2 * q_5 + q_3 + q_2 - q_4) * q_a4 + (1/200 * \cos(q_5 + q_4 + q_2) + 1/400 * \cos(q_6 + q_5 + q_2 + q_3 - q_4) - 1/400 * \cos(-q_6 - q_5 + q_2 + q_3 + q_4) - 1/400 * \cos(q_6 + q_5 + q_2 + q_3 + q_4) - 1/400 * \sin(-q_6 - q_5 + q_4 + q_2) - 1/2000 * \cos(-q_5 + q_4 + q_2) - 1/400 * \sin(-q_6 - q_5 + q_4 - q_2) + 1/400 * \cos(-q_6 - q_5 + q_2 + q_3 - q_4) + 1/200 * \sin(q_5 + q_2 + q_3 - q_4) - 1/2000 * \sin(-q_6 + q_3 + q_2 + q_4) + 1/2000 * \sin(q_6 + q_4 + q_3 + q_2) - 1/200 * \sin(-q_5 + q_2 + q_3 - q_4) + 3/2000 * \cos(q_2 + q_3 - q_4) - 3/2000 * \cos(q_2 + q_3 + q_4) - 1/200 * \sin(q_5 + q_2 + q_3 + q_4) + 1/200 * \sin(-q_5 + q_2 + q_3 + q_4) + 1/2000 * \sin(-q_6 - q_4 + q_3 + q_2) - 1/400 * \sin(q_6 + q_5 + q_4 + q_2) - 1/200 * \cos(-q_5 + q_4 - q_2) - 1/400 * \sin(q_6 + q_5 + q_4 - q_2) + 1/200 * \cos(q_5 + q_4 - q_2) - 1/2000 * \sin(q_6 + q_3 + q_2 - q_4) * q_a5 + (-1/4000 * \cos(q_6 + q_3 + q_2 - q_4) + 1/2000 * \sin(q_2 + q_3 + q_4) + 1/4000 * \sin(-2 * q_6 - 2 * q_5 + q_3 + q_2 - q_4) + 1/8000 * \sin(-2 * q_6 - 2 * q_5 + 2 * q_4 + q_3 + q_2) + 1/8000 * \cos(-2 * q_5 + 2 * q_4 + q_3 + q_2 - q_6) - 1/4000 * \cos(q_6 + 2 * q_5 - q_4 + q_3 + q_2) - 1/2000 * \sin(q_2 + q_3 - q_4) - 1/8000 * \cos(-q_6 - 2 * q_4 + q_3 + q_2) + 1/8000 * \sin(2 * q_6 + 2 * q_5 - 2 * q_4 + q_3 + q_2) - 1/4000 * \cos(-q_6 - 2 * q_5 + q_3 + q_2 + q_4) + 1/8000 * \cos(q_6 + 2 * q_4 + q_3 + q_2) + 1/4000 * \cos(-q_6 - 2 * q_5 - q_4 + q_3 + q_2) + 1/8000 * \cos(q_6 + 2 * q_5 + 2 * q_4 + q_3 + q_2) - 1/4000 * \sin(-2 * q_6 - 2 * q_5 + q_3 + q_2 + q_4) - 1/4000 * \sin(2 * q_6 + 2 * q_5 + q_3 + q_2 + q_4) + 1/8000 * \cos(-q_6 + 2 * q_4 + q_3 + q_2) - 1/4000 * \cos(-q_6 + q_3 + q_2 + q_4) - 1/8000 * \cos(2 * q_5 - 2 * q_4 + q_6 + q_3 + q_2) + 1/4000 * \cos(q_6 + q_4 + q_3 + q_2) - 1/8000 * \sin(-2 * q_6 - 2 * q_5 - 2 * q_4 + q_3 + q_2) + 1/4000 * \sin(2 * q_6 + 2 * q_5 + q_3 + q_2 - q_4) + 1/4000 * \cos(-q_6 - q_4 + q_3 + q_2) - 1/8000 * \cos(-2 * q_4 + q_3 + q_2 + q_6) - 1/8000 * \sin(2 * q_6 + 2 * q_5 + 2 * q_4 + q_3 + q_2) + 1/4000 * \cos(q_6 + 2 * q_5 + q_4 + q_3 + q_2) - 1/8000 * \cos(-q_6 - 2 * q_5 - 2 * q_4 + q_3 + q_2) * q_v2 * q_v6 + (1/4000 * \cos(q_6 + q_3 + q_2 - q_4) + 1/2000 * \sin(2 * q_6 + 2 * q_5 + q_3 + q_2) - 1/2000 * \cos(q_6 + q_3 + q_2) + 1/2000 * \sin(q_2 + q_3 + q_4) - 1/2000 * \cos(q_6 + 2 * q_5 + q_3 + q_2) - 1/2000 * \cos(-q_6 + q_3 + q_2) - 1/2000 * \cos(-2 * q_5 + q_3 + q_2 - q_6) - 1/2000 * \sin(-2 * q_6 - 2 * q_5 + q_3 + q_2) + 1/200 * \sin(q_6 + q_5 + q_2 + q_3 + q_4) + 1/200 * \sin(-q_6 - q_5 + q_2 + q_3 - q_4) + 1/4000 * \sin(-2 * q_6 - 2 * q_5 + q_3 + q_2 - q_4) + 1/200 * \sin(-q_6 - q_5 + q_2 + q_3 + q_4) + 1/200 * \sin(q_6 + q_5 + q_2 + q_3 - q_4) - 1/200 * \cos(q_6 + q_5 + q_4 + q_2) - 1/200 * \cos(q_6 + q_5 + q_4 - q_2) - 1/4000 * \cos(q_6 + 2 * q_5 - q_4 + q_3 + q_2) + 1/2000 * \sin(q_2 + q_3 - q_4) - 1/200 * \cos(-q_6 - q_5 + q_4 - q_2) + 1/4000 * \cos(-q_6 - 2 * q_5 + q_3 + q_2 + q_4) + 1/4000 * \cos(-q_6 - 2 * q_5 - q_4 + q_3 + q_2) + 1/4000 * \sin(-2 * q_6 - 2 * q_5 + q_3 + q_2 + q_4) + 1/4000 * \sin(2 * q_6 + 2 * q_5 + q_3 + q_2 + q_4) - 1/200 * \cos(-q_6 - q_5 + q_4 + q_2) - 1/4000 * \cos(-q_6 + q_3 + q_2 + q_4) + 1/4000 * \cos(q_6 + q_4 + q_3 + q_2) + 1/4000 * \sin(2 * q_6 + 2 * q_5 + q_3 + q_2 - q_4) - 1/4000 * \cos(-q_6 - q_4 + q_3 + q_2) - 1/4000 * \cos(q_6 + 2 * q_5 + q_4 + q_3 + q_2) * q_v4 * q_v6 + (1/400 * \cos(q_6 + q_5 + q_2 + q_3 - q_4) - 1/400 * \cos(-q_6 - q_5 + q_2 + q_3 + q_4) - 1/400 * \cos(q_6 + q_5 + q_2 + q_3 + q_4) - 1/400 * \sin(-q_6 - q_5 + q_4 + q_2) - 1/400 * \sin(-q_6 - q_5 + q_4 - q_2) + 1/400 * \cos(-q_6 - q_5 + q_2 + q_3 - q_4) - 1/4000 * \sin(-q_6 + q_3 + q_2 + q_4) + 1/4000 * \sin(q_6 + q_4 + q_3 + q_2) + 1/2000 * \cos(q_2 + q_3 - q_4) - 1/2000 * \cos(q_2 + q_3 + q_4) + 1/4000 * \sin(-q_6 - q_4 + q_3 + q_2) - 1/400 * \sin(q_6 + q_5 + q_4 + q_2) - 1/400 * \sin(q_6 + q_5 + q_4 - q_2) - 1/4000 * \sin(q_6 + q_3 + q_2 - q_4) * q_a6 + (-1/2000 * \cos(q_6 + q_3 + q_2 - q_4) + 3/2000 * \sin(q_2 + q_3 + q_4) - 1/4000 * s
\end{aligned}$$

$$\begin{aligned}
& \sin(2*q5-2*q4+q3+q2)+1/4000*\sin(-2*q6-2*q5+q3+q2-q4)+1/4000*\sin(-2*q5-2*q4+q3+q2)+1/80 \\
& 00*\sin(-2*q6-2*q5+2*q4+q3+q2)+1/4000*\cos(-2*q5+2*q4+q3+q2-q6)+1/2000*\sin(2*q5+q4+q3+ \\
& q2)-1/2000*\sin(2*q5-q4+q3+q2)-1/2000*\cos(q6+2*q5-q4+q3+q2)-3/2000*\sin(q2+q3-q4)+1/8000 \\
& *sin(2*q6+2*q5-2*q4+q3+q2)-1/2000*\cos(-q6-2*q5+q3+q2+q4)+1/2000*\sin(-2*q5+q4+q3+q2)+ \\
& 1/2000*\cos(-q6-2*q5-q4+q3+q2)+1/4000*\cos(q6+2*q5+2*q4+q3+q2)-1/4000*\sin(-2*q6-2*q5+q3 \\
& +q2+q4)-1/4000*\sin(2*q6+2*q5+q3+q2+q4)-1/2000*\sin(-2*q5-q4+q3+q2)-1/2000*\cos(-q6+q3+q \\
& 2+q4)+1/4000*\sin(2*q5+2*q4+q3+q2)-1/4000*\cos(2*q5-2*q4+q6+q3+q2)+1/2000*\cos(q6+q4+q \\
& 3+q2)-1/4000*\sin(-2*q5+2*q4+q3+q2)-1/8000*\sin(-2*q6-2*q5-2*q4+q3+q2)+1/4000*\sin(2*q6+2 \\
& *q5+q3+q2-q4)+1/2000*\cos(-q6-q4+q3+q2)-1/8000*\sin(2*q6+2*q5+2*q4+q3+q2)+1/2000*\cos(q \\
& 6+2*q5+q4+q3+q2)-1/4000*\cos(-q6-2*q5-2*q4+q3+q2))*qv2*qv5+(1/4000*\sin(2*q6+2*q5+2*q3 \\
& +2*q2-q4)-1/8000*\sin(-2*q5+2*q4+2*q3+2*q2)-3/4000*\sin(-2*q5+2*q3+2*q2)-1/100*cos(-q6-q \\
& 5+q3+2*q2)-1/8000*cos(-2*q4+2*q3+2*q2+q6)-1/100*sin(-q5-q4+q3+2*q2)-1/100*cos(2*q3+2* \\
& q2+q5+q4)+1/16000*\sin(2*q6+2*q5-2*q4+2*q3+2*q2)+1/16000*\sin(-2*q6-2*q5+2*q4+2*q3+2* \\
& q2)-1/200*cos(q6+q5+q4+q3+2*q2)+1/8000*cos(-q6-2*q5+2*q4+2*q3+2*q2)-1/50*cos(2*q3+2* \\
& q2+q5)-1/2000*cos(-q6-2*q5-q4+2*q3+2*q2)-1/2000*\sin(2*q5-q4+2*q3+2*q2)-1/50*sin(q5+q3+ \\
& 2*q2)+1/8000*cos(-q6-2*q5-2*q4+2*q3+2*q2)-1/100*cos(2*q3+2*q2+q5-q4)-1/100*sin(q5+q4+ \\
& q3+2*q2)-3/4000*cos(q6+2*q5+2*q3+2*q2)+1/50*cos(2*q3+2*q2-q5)-1/8000*\sin(2*q5+2*q4+2 \\
& *q3+2*q2)-12/5*cos(q3+2*q2)+1/200*sin(2*q3+2*q2+q6+q5-q4)-1/200*sin(2*q3+2*q2-q6-q5-q4 \\
&)-3/4000*sin(2*q5+2*q3+2*q2)-1/100*cos(2*q3+2*q2-q5+q4)+1/200*sin(2*q3+2*q2+q6+q5+q4) \\
& -1/200*sin(2*q3+2*q2-q6-q5+q4)+1/4000*cos(2*q3+2*q2+q6)-1/100*cos(2*q3+2*q2-q5-q4)+1/1 \\
& 00*sin(2*q3+2*q2-q6-q5)-1/2000*cos(q6+2*q5+2*q3+2*q2-q4)+1/8000*cos(-q6+2*q4+2*q3+2* \\
& q2)+1/100*sin(2*q3+2*q2+q6+q5)-1/2000*sin(2*q5+q4+2*q3+2*q2)+1/4000*sin(2*q6+2*q5+q4 \\
& +2*q3+2*q2)-1/8000*cos(q6+2*q5-2*q4+2*q3+2*q2)-1/100*sin(-q5+q4+q3+2*q2)+1/8000*cos(- \\
& q6-2*q4+2*q3+2*q2)+3/4000*cos(-q6-2*q5+2*q3+2*q2)-1/4000*sin(-2*q6-2*q5+q4+2*q3+2*q2 \\
&)+1/200*cos(-q6-q5+q4+q3+2*q2)-1/100*cos(q6+q5+q3+2*q2)-3/8000*sin(-2*q4+2*q3+2*q2)+3 \\
& /8000*sin(2*q6+2*q5+2*q3+2*q2)+4803/4000*sin(2*q3+2*q2)+1/16000*sin(-2*q6-2*q5-2*q4+2 \\
& *q3+2*q2)-1/100*sin(q5-q4+q3+2*q2)+1/50*sin(-q5+q3+2*q2)-1/4000*sin(-2*q6-2*q5+2*q3+2* \\
& q2-q4)+3/8000*sin(-2*q6-2*q5+2*q3+2*q2)+1/16000*sin(2*q6+2*q5+2*q4+2*q3+2*q2)-1/2000 \\
& *cos(-q6-2*q5+q4+2*q3+2*q2)-11/5*sin(2*q2)+1/2000*sin(-2*q5+q4+2*q3+2*q2)-1/200*cos(q6 \\
& +q5-q4+q3+2*q2)-1/2000*cos(q6+2*q5+2*q3+2*q2+q4)-1/8000*cos(q6+2*q4+2*q3+2*q2)-3/80 \\
& 00*sin(2*q4+2*q3+2*q2)-1/8000*sin(2*q5-2*q4+2*q3+2*q2)-1/8000*sin(-2*q5-2*q4+2*q3+2*q \\
& 2)-1/4000*cos(-q6+2*q3+2*q2)+1/2000*sin(-2*q5-q4+2*q3+2*q2)+1/200*cos(-q6-q5-q4+q3+2* \\
& q2)-1/8000*cos(2*q5+2*q4+2*q3+2*q2+q6))*qv1*qv2+(-1/4000*sin(2*q5-2*q4+q3+q2)-1/200*s \\
& in(q6+q5+q2+q3+q4)-1/200*sin(-q6-q5+q2+q3-q4)-1/4000*sin(-2*q6-2*q5+q3+q2-q4)+1/200*sin \\
& (-q6-q5+q2+q3+q4)+3/4000*sin(2*q4+q3+q2)+1/100*cos(-q5+q2+q3+q4)+1/100*cos(q5+q2+q3+ \\
& q4)-1/100*cos(-q5+q2+q3-q4)-1/4000*sin(-2*q5-2*q4+q3+q2)+1/200*sin(q6+q5+q2+q3-q4)-1/80 \\
& 00*sin(-2*q6-2*q5+2*q4+q3+q2)-1/4000*cos(-2*q5+2*q4+q3+q2-q6)-1/100*cos(q5+q2+q3-q4)+ \\
& 1/2000*sin(2*q5+q4+q3+q2)-1/2000*sin(2*q5-q4+q3+q2)-1/2000*cos(q6+2*q5-q4+q3+q2)+1/40 \\
& 00*cos(-q6-2*q4+q3+q2)+1/8000*sin(2*q6+2*q5-2*q4+q3+q2)+1/2000*cos(-q6-2*q5+q3+q2+q4 \\
&)+1/4000*cos(q6+2*q4+q3+q2)-1/2000*sin(-2*q5+q4+q3+q2)-1/2000*cos(-q6-2*q5-q4+q3+q2)+ \\
& 1/4000*cos(q6+2*q5+2*q4+q3+q2)+1/4000*sin(-2*q6-2*q5+q3+q2+q4)-1/4000*sin(2*q6+2*q5+ \\
& q3+q2+q4)+1/2000*sin(-2*q5-q4+q3+q2)-1/4000*cos(-q6+2*q4+q3+q2)+1/4000*sin(2*q5+2*q4 \\
& +q3+q2)-1/4000*cos(2*q5-2*q4+q6+q3+q2)+1/4000*sin(-2*q5+2*q4+q3+q2)+1/8000*sin(-2*q6- \\
& 2*q5-2*q4+q3+q2)+1/4000*sin(2*q6+2*q5+q3+q2-q4)-3/4000*sin(-2*q4+q3+q2)-1/4000*cos(-2 \\
& *q4+q3+q2+q6)-1/8000*sin(2*q6+2*q5+2*q4+q3+q2)+1/2000*cos(q6+2*q5+q4+q3+q2)+1/4000
\end{aligned}$$

$$*\cos(-q_6-2*q_5-2*q_4+q_3+q_2))*q_2*q_3$$

$$\begin{aligned} & -2943/250*\sin(q_2+q_3)+(-1/200*\cos(-q_6-q_5+q_3)-1/400*\cos(q_6+q_5-q_4+q_3)+1/400*\cos(-q_6-q_5-q_4+q_3) \\ & -1/2000*\cos(-q_6+q_4)-1/2000*\cos(q_6+q_4)-1/200*\sin(q_6+q_5+q_4)-1/200*\cos(q_6+q_5+q_3)+1/200*\sin(-q_6-q_5+q_4) \\ & -1/400*\cos(q_6+q_5+q_4+q_3)+1/400*\cos(-q_6-q_5+q_4+q_3))*q_6^2+10791/500*\cos(q_2)-981/40000*\sin(q_6+q_5+q_2+q_3+q_4) \\ & -981/10000*\cos(q_2+q_3-q_5)+981/10000*\cos(q_2+q_3+q_5)+(1/100*\cos(-q_6-q_5+q_3)+1/4000*\sin(2*q_6+2*q_5+2*q_4) \\ & -1/50*\sin(q_6+q_5)-3/2000*\cos(q_6)-1/4000*\cos(2*q_4-q_6)-1/200*\cos(q_6+q_5-q_4+q_3) \\ & -1/200*\cos(-q_6-q_5-q_4+q_3)-1/2000*\sin(2*q_6+2*q_5)-1/4000*\cos(2*q_5+2*q_4+q_6) \\ & -1/100*\cos(q_6+q_5+q_3)+1/2000*\cos(q_6+2*q_5)-1/4000*\cos(-2*q_5+2*q_4-q_6)-1/200*\cos(q_6+q_5+q_4+q_3) \\ & -1/4000*\sin(-2*q_6-2*q_5+2*q_4)-1/200*\cos(-q_6-q_5+q_4+q_3)-1/4000*\cos(q_6+2*q_4))*q_3*q_6+ \\ & (-1/2000*\sin(2*q_5+2*q_4)+1/100*\sin(-q_5-q_4+q_3)+1/100*\cos(-q_6-q_5+q_3)-1/100*\sin(q_5-q_4+q_3) \\ & +1/4000*\sin(2*q_6+2*q_5+2*q_4)+1/25*\cos(q_5)+1/100*\sin(-q_5+q_4+q_3)+1/2000*\sin(-2*q_5+2*q_4) \\ & -1/50*\sin(q_6+q_5)-1/50*\sin(q_3+q_5)-1/200*\cos(q_6+q_5-q_4+q_3)-1/200*\cos(-q_6-q_5-q_4+q_3)+1/1000*\sin(2*q_5) \\ & -1/2000*\sin(2*q_6+2*q_5)-1/2000*\cos(2*q_5+2*q_4+q_6)-1/100*\sin(q_5+q_4+q_3)-1/100*\cos(q_6+q_5+q_3) \\ & +1/1000*\cos(q_6+2*q_5)-1/2000*\cos(-2*q_5+2*q_4-q_6)-1/200*\cos(q_6+q_5+q_4+q_3)-1/50*\sin(q_3-q_5) \\ & -1/4000*\sin(-2*q_6-2*q_5+2*q_4)-1/200*\cos(-q_6-q_5+q_4+q_3))*q_2*q_5+981/40000*\sin(-q_6-q_5+q_2+q_3-q_4) \\ & +(1/2000*\cos(q_6+q_3+q_2-q_4)-3/2000*\sin(q_2+q_3+q_4)-1/4000*\sin(2*q_5-2*q_4+q_3+q_2)-1/200*\sin(q_6+q_5+q_2+q_3+q_4) \\ & +1/200*\sin(-q_6-q_5+q_2+q_3-q_4)+1/4000*\sin(-2*q_6-2*q_5+q_3+q_2-q_4)-1/200*\sin(-q_6-q_5+q_2+q_3+q_4) \\ & -1/100*\cos(-q_5+q_2+q_3+q_4)+1/100*\cos(q_5+q_2+q_3+q_4)+1/100*\cos(-q_5+q_2+q_3-q_4)+1/4000*\sin(-2*q_5-2*q_4+q_3+q_2) \\ & +1/200*\sin(q_6+q_5+q_2+q_3-q_4)+1/8000*\sin(-2*q_6-2*q_5+2*q_4+q_3+q_2)+1/4000*\cos(-2*q_5+2*q_4+q_3+q_2-q_6) \\ & +1/200*\cos(q_6+q_5+q_4+q_2)-1/100*\cos(q_5+q_2+q_3-q_4)-1/200*\cos(q_6+q_5+q_4-q_2)+1/2000*\sin(2*q_5+q_4+q_3+q_2) \\ & -1/2000*\sin(2*q_5-q_4+q_3+q_2)-1/2000*\cos(q_6+2*q_5-q_4+q_3+q_2)+3/2000*\sin(q_2+q_3-q_4)+1/100*\sin(-q_5+q_4-q_2) \\ & +1/8000*\sin(2*q_6+2*q_5-2*q_4+q_3+q_2)-1/200*\cos(-q_6-q_5+q_4-q_2)-1/2000*\cos(-q_6-2*q_5+q_3+q_2+q_4) \\ & +1/2000*\sin(-2*q_5+q_4+q_3+q_2)+1/2000*\cos(-q_6-2*q_5-q_4+q_3+q_2)-1/100*\sin(q_5+q_4-q_2)+1/4000*\cos(q_6+2*q_5+2*q_4+q_3+q_2) \\ & -1/4000*\sin(-2*q_6-2*q_5+q_3+q_2+q_4)+1/100*\sin(q_5+q_4+q_2)-1/4000*\sin(2*q_6+2*q_5+q_3+q_2+q_4) \\ & -1/2000*\sin(-2*q_5-q_4+q_3+q_2)+1/200*\cos(-q_6-q_5+q_4+q_2)+1/2000*\cos(-q_6+q_3+q_2+q_4)+1/4000*\sin(2*q_5+2*q_4+q_3+q_2) \\ & -1/4000*\cos(2*q_5-2*q_4+q_6+q_3+q_2)-1/2000*\cos(q_6+q_4+q_3+q_2)-1/4000*\sin(-2*q_5+2*q_4+q_3+q_2) \\ & -1/8000*\sin(-2*q_6-2*q_5-2*q_4+q_3+q_2)+1/4000*\sin(2*q_6+2*q_5+q_3+q_2-q_4)-1/100*\sin(-q_5+q_4+q_2) \\ & -1/2000*\cos(-q_6-q_4+q_3+q_2)-1/8000*\sin(2*q_6+2*q_5+2*q_4+q_3+q_2)+1/2000*\cos(q_6+2*q_5+q_4+q_3+q_2) \\ & -1/4000*\cos(-q_6-2*q_5-2*q_4+q_3+q_2))*q_1*q_5+(-1/200*\sin(-q_5-q_4+q_3)-1/200*\cos(-q_6-q_5+q_3) \\ & -6/5*\cos(q_3)-1/200*\sin(q_5-q_4+q_3)-1/200*\sin(-q_5+q_4+q_3)-1/100*\sin(q_3+q_5)-1/400*\cos(q_6+q_5-q_4+q_3) \\ & +1/400*\cos(-q_6-q_5-q_4+q_3)-1/200*\sin(q_5+q_4+q_3)-1/200*\cos(q_6+q_5+q_3)-1/400*\cos(q_6+q_5+q_4+q_3) \\ & +1/100*\sin(q_3-q_5)+1/400*\cos(-q_6-q_5+q_4+q_3))*q_3^2+(-1/200*\sin(-q_5-q_4+q_3)-1/200*\cos(-q_6-q_5+q_3) \\ & -1/200*\sin(q_5-q_4+q_3)-1/200*\sin(-q_5+q_4+q_3)-1/100*\sin(q_3+q_5)-1/400*\cos(q_6+q_5-q_4+q_3) \\ & +1/400*\cos(-q_6-q_5-q_4+q_3)+1/100*\cos(q_5+q_4)-1/200*\sin(q_5+q_4+q_3)-1/200*\sin(q_6+q_5+q_4) \\ & -1/200*\cos(q_6+q_5+q_3)+1/200*\sin(-q_6-q_5+q_4)+1/100*\cos(-q_5+q_4)-1/400*\cos(q_6+q_5+q_4+q_3) \\ & +1/100*\sin(q_3-q_5)+1/400*\cos(-q_6-q_5+q_4+q_3))*q_5^2+(1/4000*\sin(-2*q_6-2*q_5+q_4)-1/200*\sin(-q_5-q_4+q_3) \\ & +1/2000*\cos(q_6+2*q_5+q_4)-1/200*\sin(q_5-q_4+q_3)-1/200*\sin(-q_5+q_4+q_3)+1/2000*\sin(2*q_5+q_4) \\ & -1/400*\cos(q_6+q_5-q_4+q_3)-1/2000*\sin(-2*q_5+q_4)+1/400*\cos(-q_6-q_5-q_4+q_3)+1/100*\cos(q_5+q_4) \\ & -1/200*\sin(q_5+q_4+q_3)-1/200*\sin(q_6+q_5+q_4)+1/200*\sin(-q_6-q_5+q_4)+1/100*\cos(-q_5+q_4)+1/2000*\cos(-q_6-2*q_5+q_4) \\ & -1/400*\cos(q_6+q_5+q_4+q_3)+1/400*\cos(-q_6-q_5+q_4+q_3)-1/4000*\sin(2*q_6+2*q_5+q_4))*q_4^2+981/40000*\sin(-q_6-q_5+q_2+q_3+q_4) \\ & +(-1/200*\cos(-q_6-q_5+q_4+q_3)-3/1000*\sin(q_4)-1/2000*\sin(-2*q_6-2*q_5+q_4)+1/1000*\cos(q_6+2*q_5+q_4)+1/1000*\cos(-q_6+q_4) \\ & -1/1000*\cos(q_6+q_4)+1/1000*\sin(2*q_5+q_4)-1/100*\sin(-q_6-q_5+q_4)+1/200*\cos(q_6+q_5-q_4+q_3)+1/200*c \end{aligned}$$

$$\begin{aligned}
& \cos(-q_6-q_5-q_4+q_3)-1/100*\sin(q_6+q_5+q_4)+1/50*\cos(q_5+q_4)-1/200*\cos(q_6+q_5+q_4+q_3)+1/1000*\sin(-2*q_5+q_4)-1/50*\cos(-q_5+q_4)-1/100*\sin(-q_5-q_4+q_3)-1/1000*\cos(-q_6-2*q_5+q_4)-1/100*\sin(q_5+q_4+q_3)-1/2000*\sin(2*q_6+2*q_5+q_4)+1/100*\sin(q_5-q_4+q_3)+1/100*\sin(-q_5+q_4+q_3))*q_v4*q_v5+(1/100*\cos(-q_6-q_5+q_3)+1/4000*\sin(2*q_6+2*q_5+2*q_4)-1/50*\sin(q_6+q_5)-3/2000*\cos(q_6)-1/4000*\cos(2*q_4-q_6)-1/200*\cos(q_6+q_5-q_4+q_3)-1/200*\cos(-q_6-q_5-q_4+q_3)-1/2000*\sin(2*q_6+2*q_5)-1/4000*\cos(2*q_5+2*q_4+q_6)-1/100*\cos(q_6+q_5+q_3)+1/2000*\cos(q_6+2*q_5)-1/4000*\cos(-2*q_5+2*q_4-q_6)-1/200*\cos(q_6+q_5+q_4+q_3)-1/4000*\sin(-2*q_6-2*q_5+2*q_4)-1/200*\cos(-q_6-q_5+q_4+q_3)-1/4000*\cos(q_6+2*q_4))*q_v2*q_v6+981/20000*\cos(-q_5+q_2+q_3+q_4)+981/20000*\cos(q_5+q_2+q_3+q_4)+981/20000*\cos(-q_5+q_2+q_3-q_4)+(-1/2000*\sin(2*q_5+2*q_4)+1/100*\sin(-q_5-q_4+q_3)+1/100*\sin(q_5-q_4+q_3)+1/4000*\sin(2*q_6+2*q_5+2*q_4)-1/100*\sin(-q_5+q_4+q_3)-1/2000*\sin(-2*q_5+2*q_4)-3/2000*\sin(2*q_4)+1/2000*\cos(2*q_4-q_6)+1/200*\cos(q_6+q_5-q_4+q_3)-1/200*\cos(-q_6-q_5-q_4+q_3)-1/2000*\cos(2*q_5+2*q_4+q_6)-1/100*\sin(q_5+q_4+q_3)+1/2000*\cos(-2*q_5+2*q_4-q_6)-1/200*\cos(q_6+q_5+q_4+q_3)+1/4000*\sin(-2*q_6-2*q_5+2*q_4)+1/200*\cos(-q_6-q_5+q_4+q_3)-1/2000*\cos(q_6+2*q_4))*q_v3*q_v4-981/40000*\sin(q_6+q_5+q_2+q_3-q_4)-981/20000*\sin(q_6+q_2+q_3+q_5)-981/20000*\sin(-q_6+q_2+q_3-q_5)+981/20000*\cos(q_5+q_2+q_3-q_4)+(-1/2000*\sin(2*q_5+2*q_4)+1/100*\sin(-q_5-q_4+q_3)+1/100*\sin(q_5-q_4+q_3)+1/4000*\sin(2*q_6+2*q_5+2*q_4)-1/100*\sin(-q_5+q_4+q_3)-1/2000*\sin(-2*q_5+2*q_4)-3/2000*\sin(2*q_4)+1/2000*\cos(2*q_4-q_6)+1/200*\cos(q_6+q_5-q_4+q_3)-1/200*\cos(-q_6-q_5-q_4+q_3)-1/2000*\cos(2*q_5+2*q_4+q_6)-1/100*\sin(q_5+q_4+q_3)+1/2000*\cos(-2*q_5+2*q_4-q_6)-1/200*\cos(q_6+q_5+q_4+q_3)+1/4000*\sin(-2*q_6-2*q_5+2*q_4)+1/200*\cos(-q_6-q_5+q_4+q_3)-1/2000*\cos(q_6+2*q_4))*q_v2*q_v4+(-1/2000*\sin(2*q_5+2*q_4)+1/100*\sin(-q_5-q_4+q_3)+1/100*\cos(-q_6-q_5+q_3)-1/100*\sin(q_5-q_4+q_3)+1/4000*\sin(2*q_6+2*q_5+2*q_4)+1/25*\cos(q_5)+1/100*\sin(-q_5+q_4+q_3)+1/2000*\sin(-2*q_5+2*q_4)-1/50*\sin(q_6+q_5)-1/50*\sin(q_3+q_5)-1/200*\cos(q_6+q_5-q_4+q_3)-1/200*\cos(-q_6-q_5-q_4+q_3)+1/1000*\sin(2*q_5)-1/2000*\sin(2*q_6+2*q_5)-1/2000*\cos(2*q_5+2*q_4+q_6)-1/100*\sin(q_5+q_4+q_3)-1/100*\cos(q_6+q_5+q_3)+1/1000*\cos(q_6+2*q_5)-1/2000*\cos(-2*q_5+2*q_4-q_6)-1/200*\cos(q_6+q_5+q_4+q_3)-1/50*\sin(q_3-q_5)-1/4000*\sin(-2*q_6-2*q_5+2*q_4)-1/200*\cos(-q_6-q_5+q_4+q_3))*q_v3*q_v5+(-3/8000*\cos(2*q_4+q_3+q_2)-1/200*\cos(q_5+q_4+q_2)-1/400*\cos(q_6+q_5+q_2+q_3-q_4)-1/8000*\sin(-q_6+2*q_4+q_3+q_2)-1/400*\cos(-q_6-q_5+q_2+q_3+q_4)+1/400*\cos(q_6+q_5+q_2+q_3+q_4)-1/400*\sin(-q_6-q_5+q_4+q_2)+3/8000*\cos(-2*q_4+q_3+q_2)-1/200*\cos(-q_5+q_4+q_2)-1/8000*\sin(-2*q_4+q_3+q_2+q_6)+1/16000*\cos(2*q_6+2*q_5+2*q_4+q_3+q_2)+1/8000*\cos(2*q_5-2*q_4+q_3+q_2)+1/400*\sin(-q_6-q_5+q_4-q_2)+1/4000*\sin(-q_6-2*q_5+q_3+q_2+q_4)+1/400*\cos(-q_6-q_5+q_2+q_3-q_4)+1/4000*\cos(-2*q_5+q_4+q_3+q_2)-1/4000*\sin(-q_6-2*q_5-q_4+q_3+q_2)-1/200*\sin(q_5+q_2+q_3-q_4)+1/8000*\sin(q_6+2*q_5+2*q_4+q_3+q_2)-1/8000*\sin(2*q_5-2*q_4+q_6+q_3+q_2)-1/200*\sin(-q_5+q_2+q_3-q_4)-1/8000*\cos(-2*q_5+2*q_4+q_3+q_2)+1/16000*\cos(-2*q_6-2*q_5+2*q_4+q_3+q_2)+1/200*\sin(q_5+q_2+q_3+q_4)+1/4000*\cos(2*q_5-q_4+q_3+q_2)+1/200*\sin(-q_5+q_2+q_3+q_4)-1/4000*\sin(q_6+2*q_5-q_4+q_3+q_2)-1/8000*\cos(-2*q_6-2*q_5+q_3+q_2+q_4)+1/8000*\cos(2*q_6+2*q_5+q_3+q_2+q_4)-1/4000*\cos(-2*q_5-q_4+q_3+q_2)-1/8000*\cos(2*q_5+2*q_4+q_3+q_2)-1/8000*\sin(-2*q_5+2*q_4+q_3+q_2-q_6)+1/400*\sin(q_6+q_5+q_4+q_2)+1/200*\cos(-q_5+q_4-q_2)+1/8000*\sin(-q_6-2*q_4+q_3+q_2)+1/4000*\sin(q_6+2*q_5+q_4+q_3+q_2)+1/8000*\sin(-q_6-2*q_5-2*q_4+q_3+q_2)+1/8000*\cos(-2*q_6-2*q_5+q_3+q_2-q_4)-1/4000*\cos(2*q_5+q_4+q_3+q_2)-1/400*\sin(q_6+q_5+q_4-q_2)-1/16000*\cos(2*q_6+2*q_5-2*q_4+q_3+q_2)+1/8000*\sin(q_6+2*q_4+q_3+q_2)+1/8000*\cos(-2*q_5-2*q_4+q_3+q_2)+1/200*\cos(q_5+q_4-q_2)-1/16000*\cos(-2*q_6-2*q_5-2*q_4+q_3+q_2)-1/8000*\cos(2*q_6+2*q_5+q_3+q_2-q_4))*q_a1+(-1/2000*\sin(-2*q_6-2*q_5+q_4)+1/2000*\cos(q_6+2*q_5+q_4)+1/200*\cos(q_6+q_5-q_4+q_3)+1/200*\cos(-q_6-q_5-q_4+q_3)-1/100*\sin(q_6+q_5+q_4)-1/100*\sin(-q_6-q_5+q_4)-1/2000*\cos(-q_6-2*q_5+q_4)-1/200*\cos(q_6+q_5+q_4+q_3)-1/200*\cos(-q_6-q_5+q_4+q_3)-1/2000*\sin(2*q_6+2*q_5+q_4)-1/1000*\sin(q_4)+1/2000*\cos(-q_6+q_4)-1/2000*\cos(q_6+q_4))*q_v4*q_v6+(1/4000*\cos(q_6+q_3+q_2-q_4)-1/2000*\sin(q_2+q_3+q_4)-1/200*\sin(q_6+q_5+q_2+q_3+q_4)+1/200*\sin(-q_6-q_5+q_2+q_3-q_4)+1/4000*\sin(-2*q_6-2*q_5+q_3+q_2-q_4)-1/200*\sin(-q_6-q_5+q_2+q_3+q_4)+1/200*\sin(q_6+q_5+q_2+q_3-q_4)+1/8000*\sin(-2*q_6-2*q_5+2*q_4+q
\end{aligned}$$

$$\begin{aligned}
& 3+q2)+1/8000*\cos(-2*q5+2*q4+q3+q2-q6)+1/200*\cos(q6+q5+q4+q2)-1/200*\cos(q6+q5+q4-q2)- \\
& 1/4000*\cos(q6+2*q5-q4+q3+q2)+1/2000*\sin(q2+q3-q4)-1/8000*\cos(-q6-2*q4+q3+q2)+1/8000*\sin \\
& n(2*q6+2*q5-2*q4+q3+q2)-1/200*\cos(-q6-q5+q4-q2)-1/4000*\cos(-q6-2*q5+q3+q2+q4)+1/8000* \\
& \cos(q6+2*q4+q3+q2)+1/4000*\cos(-q6-2*q5-q4+q3+q2)+1/8000*\cos(q6+2*q5+2*q4+q3+q2)-1/40 \\
& 00*\sin(-2*q6-2*q5+q3+q2+q4)-1/4000*\sin(2*q6+2*q5+q3+q2+q4)+1/8000*\cos(-q6+2*q4+q3+q2 \\
&)+1/200*\cos(-q6-q5+q4+q2)+1/4000*\cos(-q6+q3+q2+q4)-1/8000*\cos(2*q5-2*q4+q6+q3+q2)-1/4 \\
& 000*\cos(q6+q4+q3+q2)-1/8000*\sin(-2*q6-2*q5-2*q4+q3+q2)+1/4000*\sin(2*q6+2*q5+q3+q2-q4) \\
& -1/4000*\cos(-q6-q4+q3+q2)-1/8000*\cos(-2*q4+q3+q2+q6)-1/8000*\sin(2*q6+2*q5+2*q4+q3+q2) \\
& +1/4000*\cos(q6+2*q5+q4+q3+q2)-1/8000*\cos(-q6-2*q5-2*q4+q3+q2))*qv1*qv6+(13609/4000+1 \\
& /4000*\cos(2*q5+2*q4)+1/100*\cos(-q5-q4+q3)-1/100*\sin(-q6-q5+q3)-12/5*\sin(q3)+1/100*\cos(q5- \\
& q4+q3)-1/8000*\cos(2*q6+2*q5+2*q4)+1/25*\sin(q5)+1/100*\cos(-q5+q4+q3)+1/4000*\cos(-2*q5+ \\
& 2*q4)+1/50*\cos(q6+q5)+3/4000*\cos(2*q4)-3/2000*\sin(q6)+1/50*\cos(q3+q5)+1/4000*\sin(2*q4-q \\
& 6)-1/200*\sin(q6+q5-q4+q3)+1/200*\sin(-q6-q5-q4+q3)-1/2000*\cos(2*q5)+1/4000*\cos(2*q6+2*q5 \\
&)-1/4000*\sin(2*q5+2*q4+q6)+1/100*\cos(q5+q4+q3)-1/100*\sin(q6+q5+q3)+1/2000*\sin(q6+2*q5) \\
& +1/4000*\sin(-2*q5+2*q4-q6)-1/200*\sin(q6+q5+q4+q3)-1/50*\cos(q3-q5)-1/8000*\cos(-2*q6-2*q5 \\
& +2*q4)+1/200*\sin(-q6-q5+q4+q3)-1/4000*\sin(q6+2*q4))*qa2+(1/4000*\cos(2*q5+2*q4)+1/200*c \\
& \cos(-q5-q4+q3)-1/200*\sin(-q6-q5+q3)-6/5*\sin(q3)+4809/4000+1/200*\cos(q5-q4+q3)-1/8000*\cos(2 \\
& *q6+2*q5+2*q4)+1/25*\sin(q5)+1/200*\cos(-q5+q4+q3)+1/4000*\cos(-2*q5+2*q4)+1/50*\cos(q6+q \\
& 5)+3/4000*\cos(2*q4)-3/2000*\sin(q6)+1/100*\cos(q3+q5)+1/4000*\sin(2*q4-q6)-1/400*\sin(q6+q5- \\
& q4+q3)+1/400*\sin(-q6-q5-q4+q3)-1/2000*\cos(2*q5)+1/4000*\cos(2*q6+2*q5)-1/4000*\sin(2*q5+2 \\
& *q4+q6)+1/200*\cos(q5+q4+q3)-1/200*\sin(q6+q5+q3)+1/2000*\sin(q6+2*q5)+1/4000*\sin(-2*q5+2 \\
& *q4-q6)-1/400*\sin(q6+q5+q4+q3)-1/100*\cos(q3-q5)-1/8000*\cos(-2*q6-2*q5+2*q4)+1/400*\sin(-q \\
& 6-q5+q4+q3)-1/4000*\sin(q6+2*q4))*qa3+(-1/4000*\cos(-2*q6-2*q5+q4)-1/200*\cos(-q5-q4+q3)+1 \\
& /2000*\sin(q6+2*q5+q4)-1/200*\cos(q5-q4+q3)+1/200*\cos(-q5+q4+q3)-1/2000*\cos(2*q5+q4)+1/4 \\
& 000*\sin(q6+q5-q4+q3)+1/2000*\cos(-2*q5+q4)-1/400*\sin(-q6-q5-q4+q3)+1/100*\sin(q5+q4)+1/200 \\
& *cos(q5+q4+q3)+1/200*cos(q6+q5+q4)-1/200*cos(-q6-q5+q4)+1/100*sin(-q5+q4)+1/2000*sin(-q \\
& 6-2*q5+q4)-1/400*sin(q6+q5+q4+q3)+1/400*sin(-q6-q5+q4+q3)+1/4000*cos(2*q6+2*q5+q4))*q \\
& a4+(-1/200*cos(-q5-q4+q3)+1/200*sin(-q6-q5+q3)+1/200*cos(q5-q4+q3)+3/1000*cos(q4)-1/200* \\
& \cos(-q5+q4+q3)+1/100*cos(q3+q5)-1/400*sin(q6+q5-q4+q3)-1/400*sin(-q6-q5-q4+q3)+1/100*sin \\
& (q5+q4)+1/1000*sin(-q6+q4)+1/200*cos(q5+q4+q3)-1/1000*sin(q6+q4)+1/200*cos(q6+q5+q4)-1/ \\
& 200*sin(q6+q5+q3)+1/200*cos(-q6-q5+q4)-1/100*sin(-q5+q4)-1/400*sin(q6+q5+q4+q3)+1/100*c \\
& \cos(q3-q5)-1/400*sin(-q6-q5+q4+q3))*qa5+(1/200*sin(-q6-q5+q3)+1/1000*cos(q4)-1/400*sin(q6+ \\
& q5-q4+q3)-1/400*sin(-q6-q5-q4+q3)+1/2000*sin(-q6+q4)-1/2000*sin(q6+q4)+1/200*cos(q6+q5+q \\
& 4)-1/200*sin(q6+q5+q3)+1/200*cos(-q6-q5+q4)-1/400*sin(q6+q5+q4+q3)-1/400*sin(-q6-q5+q4+ \\
& q3))*qa6+(-1/100*cos(-q6-q5+q3)-1/200*cos(q6+q5-q4+q3)+1/200*cos(-q6-q5-q4+q3)-1/1000*co \\
& s(-q6+q4)-1/1000*cos(q6+q4)-1/100*sin(q6+q5+q4)-1/100*cos(q6+q5+q3)+1/100*sin(-q6-q5+q4) \\
& -1/200*cos(q6+q5+q4+q3)+1/200*cos(-q6-q5+q4+q3))*qv5*qv6+(-1/100*sin(-q5-q4+q3)-1/100*c \\
& \cos(-q6-q5+q3)-12/5*cos(q3)-1/100*sin(q5-q4+q3)-1/100*sin(-q5+q4+q3)-1/50*sin(q3+q5)-1/200* \\
& \cos(q6+q5-q4+q3)+1/200*cos(-q6-q5-q4+q3)-1/100*sin(q5+q4+q3)-1/100*cos(q6+q5+q3)-1/200* \\
& \cos(q6+q5+q4+q3)+1/50*sin(q3-q5)+1/200*cos(-q6-q5+q4+q3))*qv2*qv3+(-1/4000*sin(2*q6+2* \\
& q5+q3+q2)+1/2000*sin(-2*q5+q3+q2)+1/2000*cos(q6+q3+q2)+1/2000*sin(2*q5+q3+q2)+1/2000 \\
& *cos(q6+2*q5+q3+q2)-1/2000*cos(-q6+q3+q2)-1/2000*cos(-2*q5+q3+q2-q6)-1/4000*sin(-2*q6-2 \\
& *q5+q3+q2)+3/2000*sin(q2+q3)+1/4000*sin(2*q5-2*q4+q3+q2)-1/200*sin(q6+q5+q2+q3+q4)+1/ \\
& 200*sin(-q6-q5+q2+q3-q4)+1/4000*sin(-2*q6-2*q5+q3+q2-q4)+1/200*sin(-q6-q5+q2+q3+q4)+3/ \\
& 4000*sin(2*q4+q3+q2)+1/100*cos(-q5+q2+q3+q4)+1/100*cos(q5+q2+q3+q4)+1/100*cos(-q5+q2
\end{aligned}$$

$$\begin{aligned}
&+q_3-q_4)+1/4000*\sin(-2*q_5-2*q_4+q_3+q_2)-1/200*\sin(q_6+q_5+q_2+q_3-q_4)-1/8000*\sin(-2*q_6-2*q_5+2 \\
&*q_4+q_3+q_2)-1/4000*\cos(-2*q_5+2*q_4+q_3+q_2-q_6)+1/200*\cos(q_6+q_5+q_4+q_2)+1/100*\cos(q_5+q_2+q \\
&3-q_4)-1/200*\cos(q_6+q_5+q_4-q_2)+1/2000*\sin(2*q_5+q_4+q_3+q_2)+1/2000*\sin(2*q_5-q_4+q_3+q_2)+1/20 \\
&00*\cos(q_6+2*q_5-q_4+q_3+q_2)-1/100*\sin(-q_5+q_4-q_2)-1/4000*\cos(-q_6-2*q_4+q_3+q_2)-1/8000*\sin(2*q \\
&6+2*q_5-2*q_4+q_3+q_2)+1/200*\cos(-q_6-q_5+q_4-q_2)+1/2000*\cos(-q_6-2*q_5+q_3+q_2+q_4)+1/4000*\cos(\\
&q_6+2*q_4+q_3+q_2)-1/2000*\sin(-2*q_5+q_4+q_3+q_2)+1/2000*\cos(-q_6-2*q_5-q_4+q_3+q_2)-1/100*\sin(q_5+ \\
&q_4-q_2)+1/4000*\cos(q_6+2*q_5+2*q_4+q_3+q_2)+1/4000*\sin(-2*q_6-2*q_5+q_3+q_2+q_4)+1/100*\sin(q_5+q \\
&4+q_2)-1/4000*\sin(2*q_6+2*q_5+q_3+q_2+q_4)-1/2000*\sin(-2*q_5-q_4+q_3+q_2)-1/4000*\cos(-q_6+2*q_4+q \\
&3+q_2)-1/200*\cos(-q_6-q_5+q_4+q_2)+1/4000*\sin(2*q_5+2*q_4+q_3+q_2)+1/4000*\cos(2*q_5-2*q_4+q_6+q_3 \\
&+q_2)+1/4000*\sin(-2*q_5+2*q_4+q_3+q_2)-1/8000*\sin(-2*q_6-2*q_5-2*q_4+q_3+q_2)-1/4000*\sin(2*q_6+2* \\
&q_5+q_3+q_2-q_4)+3/4000*\sin(-2*q_4+q_3+q_2)+1/100*\sin(-q_5+q_4+q_2)+1/4000*\cos(-2*q_4+q_3+q_2+q_6)- \\
&1/8000*\sin(2*q_6+2*q_5+2*q_4+q_3+q_2)+1/2000*\cos(q_6+2*q_5+q_4+q_3+q_2)-1/4000*\cos(-q_6-2*q_5-2* \\
&q_4+q_3+q_2))*q_v1*q_v4+(-1/8000*\sin(2*q_6+2*q_5+2*q_3+2*q_2-q_4)+1/16000*\sin(-2*q_5+2*q_4+2*q_3 \\
&+2*q_2)+3/8000*\sin(-2*q_5+2*q_3+2*q_2)+1/200*\cos(-q_6-q_5+q_3+2*q_2)+1/16000*\cos(-2*q_4+2*q_3+ \\
&2*q_2+q_6)+1/200*\sin(-q_5-q_4+q_3+2*q_2)+1/200*\cos(2*q_3+2*q_2+q_5+q_4)-1/32000*\sin(2*q_6+2*q_5- \\
&*q_4+2*q_3+2*q_2)-1/32000*\sin(-2*q_6-2*q_5+2*q_4+2*q_3+2*q_2)+1/400*\cos(q_6+q_5+q_4+q_3+2*q_2)-1 \\
&/16000*\cos(-q_6-2*q_5+2*q_4+2*q_3+2*q_2)+1/100*\cos(2*q_3+2*q_2+q_5)+1/4000*\cos(-q_6-2*q_5-q_4+2 \\
&*q_3+2*q_2)+1/4000*\sin(2*q_5-q_4+2*q_3+2*q_2)+1/100*\sin(q_5+q_3+2*q_2)-1/16000*\cos(-q_6-2*q_5-2* \\
&q_4+2*q_3+2*q_2)+1/200*\cos(2*q_3+2*q_2+q_5-q_4)+1/200*\sin(q_5+q_4+q_3+2*q_2)+3/8000*\cos(q_6+2*q \\
&5+2*q_3+2*q_2)-1/100*\cos(2*q_3+2*q_2-q_5)+1/16000*\sin(2*q_5+2*q_4+2*q_3+2*q_2)+6/5*\cos(q_3+2*q \\
&2)-1/400*\sin(2*q_3+2*q_2+q_6+q_5-q_4)+1/400*\sin(2*q_3+2*q_2-q_6-q_5-q_4)+3/8000*\sin(2*q_5+2*q_3+2 \\
&*q_2)+1/200*\cos(2*q_3+2*q_2-q_5+q_4)-1/400*\sin(2*q_3+2*q_2+q_6+q_5+q_4)+1/400*\sin(2*q_3+2*q_2-q_6- \\
&q_5+q_4)-1/8000*\cos(2*q_3+2*q_2+q_6)+1/200*\cos(2*q_3+2*q_2-q_5-q_4)-1/200*\sin(2*q_3+2*q_2-q_6-q_5)+ \\
&1/4000*\cos(q_6+2*q_5+2*q_3+2*q_2-q_4)-1/16000*\cos(-q_6+2*q_4+2*q_3+2*q_2)-1/200*\sin(2*q_3+2*q_2 \\
&+q_6+q_5)+1/4000*\sin(2*q_5+q_4+2*q_3+2*q_2)-1/8000*\sin(2*q_6+2*q_5+q_4+2*q_3+2*q_2)+1/16000*co \\
&s(q_6+2*q_5-2*q_4+2*q_3+2*q_2)+1/200*\sin(-q_5+q_4+q_3+2*q_2)-1/16000*\cos(-q_6-2*q_4+2*q_3+2*q_2)- \\
&3/8000*\cos(-q_6-2*q_5+2*q_3+2*q_2)+1/8000*\sin(-2*q_6-2*q_5+q_4+2*q_3+2*q_2)-1/400*\cos(-q_6-q_5+q \\
&4+q_3+2*q_2)+1/200*\cos(q_6+q_5+q_3+2*q_2)+3/16000*\sin(-2*q_4+2*q_3+2*q_2)-3/16000*\sin(2*q_6+2* \\
&q_5+2*q_3+2*q_2)-4803/8000*\sin(2*q_3+2*q_2)-1/32000*\sin(-2*q_6-2*q_5-2*q_4+2*q_3+2*q_2)+1/200*s \\
&in(q_5-q_4+q_3+2*q_2)-1/100*\sin(-q_5+q_3+2*q_2)+1/8000*\sin(-2*q_6-2*q_5+2*q_3+2*q_2-q_4)-3/16000*si \\
&n(-2*q_6-2*q_5+2*q_3+2*q_2)-1/32000*\sin(2*q_6+2*q_5+2*q_4+2*q_3+2*q_2)+1/4000*\cos(-q_6-2*q_5+q_4 \\
&+2*q_3+2*q_2)+11/10*\sin(2*q_2)-1/4000*\sin(-2*q_5+q_4+2*q_3+2*q_2)+1/400*\cos(q_6+q_5-q_4+q_3+2*q \\
&2)+1/4000*\cos(q_6+2*q_5+2*q_3+2*q_2+q_4)+1/16000*\cos(q_6+2*q_4+2*q_3+2*q_2)+3/16000*\sin(2*q_4 \\
&+2*q_3+2*q_2)+1/16000*\sin(2*q_5-2*q_4+2*q_3+2*q_2)+1/16000*\sin(-2*q_5-2*q_4+2*q_3+2*q_2)+1/800 \\
&0*\cos(-q_6+2*q_3+2*q_2)-1/4000*\sin(-2*q_5-q_4+2*q_3+2*q_2)-1/400*\cos(-q_6-q_5-q_4+q_3+2*q_2)+1/160 \\
&00*\cos(2*q_5+2*q_4+2*q_3+2*q_2+q_6))*q_v1^2
\end{aligned}$$

$$\begin{aligned}
&-2943/250*\sin(q_2+q_3)+(1/4000*\sin(-2*q_6-2*q_5+q_4)+1/2000*\cos(q_6+2*q_5+q_4)+1/2000*\sin(2*q_5 \\
&+q_4)-1/2000*\sin(-2*q_5+q_4)+1/100*\cos(q_5+q_4)-1/200*\sin(q_6+q_5+q_4)+1/200*\sin(-q_6-q_5+q_4)+1/10 \\
&0*\cos(-q_5+q_4)+1/2000*\cos(-q_6-2*q_5+q_4)-1/4000*\sin(2*q_6+2*q_5+q_4))*q_v4^2+(1/4000*\sin(2*q_6 \\
&+2*q_5+2*q_4)-1/50*\sin(q_6+q_5)-3/2000*\cos(q_6)-1/4000*\cos(2*q_4-q_6)-1/2000*\sin(2*q_6+2*q_5)-1/4 \\
&000*\cos(2*q_5+2*q_4+q_6)+1/2000*\cos(q_6+2*q_5)-1/4000*\cos(-2*q_5+2*q_4-q_6)-1/4000*\sin(-2*q_6-2 \\
&*q_5+2*q_4)-1/4000*\cos(q_6+2*q_4))*q_v2*q_v6+(-1/2000*\sin(2*q_5+2*q_4)+1/4000*\sin(2*q_6+2*q_5+2 \\
&*q_4)-1/2000*\sin(-2*q_5+2*q_4)-3/2000*\sin(2*q_4)+1/2000*\cos(2*q_4-q_6)-1/2000*\cos(2*q_5+2*q_4+q \\
&6)+1/2000*\cos(-2*q_5+2*q_4-q_6)+1/4000*\sin(-2*q_6-2*q_5+2*q_4)-1/2000*\cos(q_6+2*q_4))*q_v3*q_v4-
\end{aligned}$$

$$\begin{aligned}
& 981/40000*\sin(q6+q5+q2+q3+q4)-981/10000*\cos(q2+q3-q5)+981/10000*\cos(q2+q3+q5)+(-1/200 \\
& 0*\sin(2*q5+2*q4)+1/4000*\sin(2*q6+2*q5+2*q4)+1/25*\cos(q5)+1/2000*\sin(-2*q5+2*q4)-1/50*si \\
& n(q6+q5)+1/1000*\sin(2*q5)-1/2000*\sin(2*q6+2*q5)-1/2000*\cos(2*q5+2*q4+q6)+1/1000*\cos(q6 \\
& +2*q5)-1/2000*\cos(-2*q5+2*q4-q6)-1/4000*\sin(-2*q6-2*q5+2*q4))*qv3*qv5+(1/4000*\sin(2*q6 \\
& +2*q5+2*q4)-1/50*\sin(q6+q5)-3/2000*\cos(q6)-1/4000*\cos(2*q4-q6)-1/2000*\sin(2*q6+2*q5)-1/4 \\
& 000*\cos(2*q5+2*q4+q6)+1/2000*\cos(q6+2*q5)-1/4000*\cos(-2*q5+2*q4-q6)-1/4000*\sin(-2*q6-2 \\
& *q5+2*q4)-1/4000*\cos(q6+2*q4))*qv3*qv6+(-1/800*\cos(-q6-q5+q4+q3)-1/8000*\sin(2*q6+2*q5+ \\
& 2*q3+2*q2-q4)+1/16000*\sin(-2*q5+2*q4+2*q3+2*q2)+3/8000*\sin(-2*q5+2*q3+2*q2)+1/400*co \\
& s(-q6-q5+q3+2*q2)+1/16000*\cos(-2*q4+2*q3+2*q2+q6)+1/400*\sin(-q5-q4+q3+2*q2)+1/200*cos \\
& (2*q3+2*q2+q5+q4)-1/32000*\sin(2*q6+2*q5-2*q4+2*q3+2*q2)+3/5*\cos(q3)-1/32000*\sin(-2*q6- \\
& 2*q5+2*q4+2*q3+2*q2)+1/800*\cos(q6+q5+q4+q3+2*q2)-1/16000*\cos(-q6-2*q5+2*q4+2*q3+2* \\
& q2)+1/100*\cos(2*q3+2*q2+q5)+1/4000*\cos(-q6-2*q5-q4+2*q3+2*q2)+1/4000*\sin(2*q5-q4+2*q \\
& 3+2*q2)+1/200*\sin(q5+q3+2*q2)-1/16000*\cos(-q6-2*q5-2*q4+2*q3+2*q2)-1/200*\sin(q3-q5)+1/ \\
& 200*\cos(2*q3+2*q2+q5-q4)+1/400*\sin(q5+q4+q3+2*q2)+3/8000*\cos(q6+2*q5+2*q3+2*q2)-1/1 \\
& 000*\cos(2*q3+2*q2-q5)+1/16000*\sin(2*q5+2*q4+2*q3+2*q2)+3/5*\cos(q3+2*q2)-1/400*\sin(2*q3 \\
& +2*q2+q6+q5-q4)+1/400*\sin(2*q3+2*q2-q6-q5-q4)+1/400*\cos(q6+q5+q3)+3/8000*\sin(2*q5+2* \\
& q3+2*q2)+1/200*\cos(2*q3+2*q2-q5+q4)-1/400*\sin(2*q3+2*q2+q6+q5+q4)+1/400*\sin(2*q3+2*q \\
& 2-q6-q5+q4)-1/8000*\cos(2*q3+2*q2+q6)+1/200*\cos(2*q3+2*q2-q5-q4)+1/800*\cos(q6+q5-q4+q3 \\
&)-1/800*\cos(-q6-q5-q4+q3)-1/200*\sin(2*q3+2*q2-q6-q5)+1/800*\cos(q6+q5+q4+q3)+1/4000*\cos(\\
& q6+2*q5+2*q3+2*q2-q4)-1/16000*\cos(-q6+2*q4+2*q3+2*q2)-1/200*\sin(2*q3+2*q2+q6+q5)+1/ \\
& 4000*\sin(2*q5+q4+2*q3+2*q2)-1/8000*\sin(2*q6+2*q5+q4+2*q3+2*q2)+1/200*\sin(q3+q5)+1/16 \\
& 000*\cos(q6+2*q5-2*q4+2*q3+2*q2)+1/400*\sin(-q5+q4+q3+2*q2)-1/16000*\cos(-q6-2*q4+2*q3+ \\
& 2*q2)-3/8000*\cos(-q6-2*q5+2*q3+2*q2)+1/400*\sin(-q5-q4+q3)+1/8000*\sin(-2*q6-2*q5+q4+2*q \\
& 3+2*q2)-1/800*\cos(-q6-q5+q4+q3+2*q2)+1/400*\cos(q6+q5+q3+2*q2)+3/16000*\sin(-2*q4+2*q3 \\
& +2*q2)-3/16000*\sin(2*q6+2*q5+2*q3+2*q2)-4803/8000*\sin(2*q3+2*q2)-1/32000*\sin(-2*q6-2*q \\
& 5-2*q4+2*q3+2*q2)+1/400*\sin(q5-q4+q3+2*q2)-1/200*\sin(-q5+q3+2*q2)+1/8000*\sin(-2*q6-2*q \\
& 5+2*q3+2*q2-q4)+1/400*\cos(-q6-q5+q3)+1/400*\sin(q5+q4+q3)-3/16000*\sin(-2*q6-2*q5+2*q3+ \\
& 2*q2)-1/32000*\sin(2*q6+2*q5+2*q4+2*q3+2*q2)+1/4000*\cos(-q6-2*q5+q4+2*q3+2*q2)-1/4000 \\
& *\sin(-2*q5+q4+2*q3+2*q2)+1/800*\cos(q6+q5-q4+q3+2*q2)+1/4000*\cos(q6+2*q5+2*q3+2*q2+ \\
& q4)+1/16000*\cos(q6+2*q4+2*q3+2*q2)+3/16000*\sin(2*q4+2*q3+2*q2)+1/400*\sin(q5-q4+q3)+1 \\
& /400*\sin(-q5+q4+q3)+1/16000*\sin(2*q5-2*q4+2*q3+2*q2)+1/16000*\sin(-2*q5-2*q4+2*q3+2*q2 \\
&)+1/8000*\cos(-q6+2*q3+2*q2)-1/4000*\sin(-2*q5-q4+2*q3+2*q2)-1/800*\cos(-q6-q5-q4+q3+2*q2 \\
&)+1/16000*\cos(2*q5+2*q4+2*q3+2*q2+q6))*qv1^2+981/40000*\sin(-q6-q5+q2+q3-q4)+(1/4000* \\
& cos(q6+q3+q2-q4)-1/2000*\sin(q2+q3+q4)-1/200*\sin(q6+q5+q2+q3+q4)+1/200*\sin(-q6-q5+q2+q3 \\
& -q4)+1/4000*\sin(-2*q6-2*q5+q3+q2-q4)-1/200*\sin(-q6-q5+q2+q3+q4)+1/200*\sin(q6+q5+q2+q3- \\
& q4)+1/8000*\sin(-2*q6-2*q5+2*q4+q3+q2)+1/8000*\cos(-2*q5+2*q4+q3+q2-q6)-1/4000*\cos(q6+2 \\
& *q5-q4+q3+q2)+1/2000*\sin(q2+q3-q4)-1/8000*\cos(-q6-2*q4+q3+q2)+1/8000*\sin(2*q6+2*q5-2* \\
& q4+q3+q2)-1/4000*\cos(-q6-2*q5+q3+q2+q4)+1/8000*\cos(q6+2*q4+q3+q2)+1/4000*\cos(-q6-2*q \\
& 5-q4+q3+q2)+1/8000*\cos(q6+2*q5+2*q4+q3+q2)-1/4000*\sin(-2*q6-2*q5+q3+q2+q4)-1/4000*si \\
& n(2*q6+2*q5+q3+q2+q4)+1/8000*\cos(-q6+2*q4+q3+q2)+1/4000*\cos(-q6+q3+q2+q4)-1/8000*co \\
& s(2*q5-2*q4+q6+q3+q2)-1/4000*\cos(q6+q4+q3+q2)-1/8000*\sin(-2*q6-2*q5-2*q4+q3+q2)+1/400 \\
& 0*\sin(2*q6+2*q5+q3+q2-q4)-1/4000*\cos(-q6-q4+q3+q2)-1/8000*\cos(-2*q4+q3+q2+q6)-1/8000*s \\
& in(2*q6+2*q5+2*q4+q3+q2)+1/4000*\cos(q6+2*q5+q4+q3+q2)-1/8000*\cos(-q6-2*q5-2*q4+q3+q \\
& 2))*qv1*qv6+(-1/2000*\sin(2*q5+2*q4)+1/4000*\sin(2*q6+2*q5+2*q4)-1/2000*\sin(-2*q5+2*q4)- \\
& 3/2000*\sin(2*q4)+1/2000*\cos(2*q4-q6)-1/2000*\cos(2*q5+2*q4+q6)+1/2000*\cos(-2*q5+2*q4-q6
\end{aligned}$$

$$\begin{aligned}
&)+1/4000*\sin(-2*q6-2*q5+2*q4)-1/2000*\cos(q6+2*q4))*qv2*qv4+981/40000*\sin(-q6-q5+q2+q3+q4)+981/20000*\cos(-q5+q2+q3+q4)+981/20000*\cos(q5+q2+q3+q4)+981/20000*\cos(-q5+q2+q3-q4)-981/40000*\sin(q6+q5+q2+q3-q4)-981/20000*\sin(q6+q2+q3+q5)-981/20000*\sin(-q6+q2+q3-q5)+981/20000*\cos(q5+q2+q3-q4)+(-1/2000*\sin(-2*q6-2*q5+q4)+1/1000*\cos(q6+2*q5+q4)+1/1000*\sin(2*q5+q4)+1/1000*\sin(-2*q5+q4)+1/50*\cos(q5+q4)-1/100*\sin(q6+q5+q4)-1/100*\sin(-q6-q5+q4)-1/50*\cos(-q5+q4)-1/1000*\cos(-q6-2*q5+q4)-1/2000*\sin(2*q6+2*q5+q4)-3/1000*\sin(q4)+1/1000*\cos(-q6+q4)-1/1000*\cos(q6+q4))*qv4*qv5+(-1/2000*\sin(2*q5+2*q4)+1/4000*\sin(2*q6+2*q5+2*q4)+1/25*\cos(q5)+1/2000*\sin(-2*q5+2*q4)-1/50*\sin(q6+q5)+1/1000*\sin(2*q5)-1/2000*\sin(2*q6+2*q5)-1/2000*\cos(2*q5+2*q4+q6)+1/1000*\cos(q6+2*q5)-1/2000*\cos(-2*q5+2*q4-q6)-1/4000*\sin(-2*q6-2*q5+2*q4))*qv2*qv5+(1/2000*\cos(q6+q3+q2-q4)-3/2000*\sin(q2+q3+q4)-1/4000*\sin(2*q5-2*q4+q3+q2)-1/200*\sin(q6+q5+q2+q3+q4)+1/200*\sin(-q6-q5+q2+q3-q4)+1/4000*\sin(-2*q6-2*q5+q3+q2-q4)-1/200*\sin(-q6-q5+q2+q3+q4)-1/100*\cos(-q5+q2+q3+q4)+1/100*\cos(q5+q2+q3+q4)+1/100*\cos(-q5+q2+q3-q4)+1/4000*\sin(-2*q5-2*q4+q3+q2)+1/200*\sin(q6+q5+q2+q3-q4)+1/8000*\sin(-2*q6-2*q5+2*q4+q3+q2)+1/4000*\cos(-2*q5+2*q4+q3+q2-q6)-1/100*\cos(q5+q2+q3-q4)+1/2000*\sin(2*q5+q4+q3+q2)-1/2000*\sin(2*q5-q4+q3+q2)-1/2000*\cos(q6+2*q5-q4+q3+q2)+3/2000*\sin(q2+q3-q4)+1/8000*\sin(2*q6+2*q5-2*q4+q3+q2)-1/2000*\cos(-q6-2*q5+q3+q2+q4)+1/2000*\sin(-2*q5+q4+q3+q2)+1/2000*\cos(-q6-2*q5-q4+q3+q2)+1/4000*\cos(q6+2*q5+2*q4+q3+q2)-1/4000*\sin(-2*q6-2*q5+q3+q2+q4)-1/4000*\sin(2*q6+2*q5+q3+q2+q4)-1/2000*\sin(-2*q5-q4+q3+q2)+1/2000*\cos(-q6+q3+q2+q4)+1/4000*\sin(2*q5+2*q4+q3+q2)-1/4000*\cos(2*q5-2*q4+q6+q3+q2)-1/2000*\cos(q6+q4+q3+q2)-1/4000*\sin(-2*q5+2*q4+q3+q2)-1/8000*\sin(-2*q6-2*q5-2*q4+q3+q2)+1/4000*\sin(2*q6+2*q5+q3+q2-q4)-1/2000*\cos(-q6-q4+q3+q2)-1/8000*\sin(2*q6+2*q5+2*q4+q3+q2)+1/2000*\cos(q6+2*q5+q4+q3+q2)-1/4000*\cos(-q6-2*q5-2*q4+q3+q2))*qv1*qv5+(-1/1000*\sin(q4)+1/2000*\cos(-q6+q4)-1/2000*\cos(q6+q4)-1/100*\sin(q6+q5+q4)-1/100*\sin(-q6-q5+q4)-1/2000*\sin(-2*q6-2*q5+q4)+1/2000*\cos(q6+2*q5+q4)-1/2000*\cos(-q6-2*q5+q4)-1/2000*\sin(2*q6+2*q5+q4))*qv4*qv6+(-1/100*\sin(q6+q5+q4)+1/100*\sin(-q6-q5+q4)-1/1000*\cos(-q6+q4)-1/1000*\cos(q6+q4))*qv5*qv6+(-3/8000*\cos(2*q4+q3+q2)-1/400*\cos(q6+q5+q2+q3-q4)-1/8000*\sin(-q6+2*q4+q3+q2)-1/400*\cos(-q6-q5+q2+q3+q4)+1/400*\cos(q6+q5+q2+q3+q4)+3/8000*\cos(-2*q4+q3+q2)-1/8000*\sin(-2*q4+q3+q2+q6)+1/16000*\cos(2*q6+2*q5+2*q4+q3+q2)+1/8000*\cos(2*q5-2*q4+q3+q2)+1/4000*\sin(-q6-2*q5+q3+q2+q4)+1/400*\cos(-q6-q5+q2+q3-q4)+1/4000*\cos(-2*q5+q4+q3+q2)-1/4000*\sin(-q6-2*q5-q4+q3+q2)-1/200*\sin(q5+q2+q3-q4)+1/8000*\sin(q6+2*q5+2*q4+q3+q2)-1/8000*\sin(2*q5-2*q4+q6+q3+q2)-1/200*\sin(-q5+q2+q3-q4)-1/8000*\cos(-2*q5+2*q4+q3+q2)+1/16000*\cos(-2*q6-2*q5+2*q4+q3+q2)+1/200*\sin(q5+q2+q3+q4)+1/4000*\cos(2*q5-q4+q3+q2)+1/200*\sin(-q5+q2+q3+q4)-1/4000*\sin(q6+2*q5-q4+q3+q2)-1/8000*\cos(-2*q6-2*q5+q3+q2+q4)+1/8000*\cos(2*q6+2*q5+q3+q2+q4)-1/4000*\cos(-2*q5-q4+q3+q2)-1/8000*\cos(2*q5+2*q4+q3+q2)-1/8000*\sin(-2*q5+2*q4+q3+q2-q6)+1/8000*\sin(-q6-2*q4+q3+q2)+1/4000*\sin(q6+2*q5+q4+q3+q2)+1/8000*\sin(-q6-2*q5-2*q4+q3+q2)+1/8000*\cos(-2*q6-2*q5+q3+q2-q4)-1/4000*\cos(2*q5+q4+q3+q2)-1/16000*\cos(2*q6+2*q5-2*q4+q3+q2)+1/8000*\sin(q6+2*q4+q3+q2)+1/8000*\cos(-2*q5-2*q4+q3+q2)-1/16000*\cos(-2*q6-2*q5-2*q4+q3+q2)-1/8000*\cos(2*q6+2*q5+q3+q2-q4))*qa1+(1/4000*\cos(2*q5+2*q4)-1/8000*\cos(2*q6+2*q5+2*q4)+1/25*\sin(q5)+1/4000*\cos(-2*q5+2*q4)+1/50*\cos(q6+q5)+3/4000*\cos(2*q4)-3/2000*\sin(q6)+1/4000*\sin(2*q4-q6)-1/2000*\cos(2*q5)+1/4000*\cos(2*q6+2*q5)-1/4000*\sin(2*q5+2*q4+q6)+1/2000*\sin(q6+2*q5)+1/40000*\sin(-2*q5+2*q4-q6)+4809/4000-1/8000*\cos(-2*q6-2*q5+2*q4)-1/4000*\sin(q6+2*q4))*qa3+(-1/4000*\cos(-2*q6-2*q5+q4)+1/2000*\sin(q6+2*q5+q4)-1/2000*\cos(2*q5+q4)+1/2000*\cos(-2*q5+q4)+1/100*\sin(q5+q4)+1/200*\cos(q6+q5+q4)-1/200*\cos(-q6-q5+q4)+1/100*\sin(-q5+q4)+1/2000*\sin(-q6-2*q5+q4)+1/4000*\cos(2*q6+2*q5+q4))*qa4+(3/1000*\cos(q4)+1/100*\sin(q5+q4)+1/100
\end{aligned}$$

$$\begin{aligned}
& 0*\sin(-q_6+q_4)-1/1000*\sin(q_6+q_4)+1/200*\cos(q_6+q_5+q_4)+1/200*\cos(-q_6-q_5+q_4)-1/100*\sin(-q_5+q_4) \\
& 4))*q_a5+(1/1000*\cos(q_4)+1/2000*\sin(-q_6+q_4)-1/2000*\sin(q_6+q_4)+1/200*\cos(q_6+q_5+q_4)+1/200* \\
& \cos(-q_6-q_5+q_4))*q_a6+(1/4000*\cos(2*q_5+2*q_4)+1/200*\cos(-q_5-q_4+q_3)-1/200*\sin(-q_6-q_5+q_3)-6/5 \\
& *\sin(q_3)+4809/4000+1/200*\cos(q_5-q_4+q_3)-1/8000*\cos(2*q_6+2*q_5+2*q_4)+1/25*\sin(q_5)+1/200*c \\
& \cos(-q_5+q_4+q_3)+1/4000*\cos(-2*q_5+2*q_4)+1/50*\cos(q_6+q_5)+3/4000*\cos(2*q_4)-3/2000*\sin(q_6)+1/ \\
& 100*\cos(q_3+q_5)+1/4000*\sin(2*q_4-q_6)-1/400*\sin(q_6+q_5-q_4+q_3)+1/400*\sin(-q_6-q_5-q_4+q_3)-1/2000 \\
& *\cos(2*q_5)+1/4000*\cos(2*q_6+2*q_5)-1/4000*\sin(2*q_5+2*q_4+q_6)+1/200*\cos(q_5+q_4+q_3)-1/200*si \\
& n(q_6+q_5+q_3)+1/2000*\sin(q_6+2*q_5)+1/4000*\sin(-2*q_5+2*q_4-q_6)-1/400*\sin(q_6+q_5+q_4+q_3)-1/100 \\
& *\cos(q_3-q_5)-1/8000*\cos(-2*q_6-2*q_5+2*q_4)+1/400*\sin(-q_6-q_5+q_4+q_3)-1/4000*\sin(q_6+2*q_4))*q_a2 \\
& +(-1/4000*\sin(2*q_6+2*q_5+q_3+q_2)+1/2000*\sin(-2*q_5+q_3+q_2)+1/2000*\cos(q_6+q_3+q_2)+1/2000*si \\
& n(2*q_5+q_3+q_2)+1/2000*\cos(q_6+2*q_5+q_3+q_2)-1/2000*\cos(-q_6+q_3+q_2)-1/2000*\cos(-2*q_5+q_3+q_2 \\
& -q_6)-1/4000*\sin(-2*q_6-2*q_5+q_3+q_2)+3/2000*\sin(q_2+q_3)+1/4000*\sin(2*q_5-2*q_4+q_3+q_2)-1/200*s \\
& in(q_6+q_5+q_2+q_3+q_4)+1/200*\sin(-q_6-q_5+q_2+q_3-q_4)+1/4000*\sin(-2*q_6-2*q_5+q_3+q_2-q_4)+1/200*si \\
& n(-q_6-q_5+q_2+q_3+q_4)+3/4000*\sin(2*q_4+q_3+q_2)+1/100*\cos(-q_5+q_2+q_3+q_4)+1/100*\cos(q_5+q_2+q_3 \\
& +q_4)+1/100*\cos(-q_5+q_2+q_3-q_4)+1/4000*\sin(-2*q_5-2*q_4+q_3+q_2)-1/200*\sin(q_6+q_5+q_2+q_3-q_4)-1/ \\
& 8000*\sin(-2*q_6-2*q_5+2*q_4+q_3+q_2)-1/4000*\cos(-2*q_5+2*q_4+q_3+q_2-q_6)+1/100*\cos(q_5+q_2+q_3-q \\
& 4)+1/2000*\sin(2*q_5+q_4+q_3+q_2)+1/2000*\sin(2*q_5-q_4+q_3+q_2)+1/2000*\cos(q_6+2*q_5-q_4+q_3+q_2)- \\
& 1/4000*\cos(-q_6-2*q_4+q_3+q_2)-1/8000*\sin(2*q_6+2*q_5-2*q_4+q_3+q_2)+1/2000*\cos(-q_6-2*q_5+q_3+q_2 \\
& +q_4)+1/4000*\cos(q_6+2*q_4+q_3+q_2)-1/2000*\sin(-2*q_5+q_4+q_3+q_2)+1/2000*\cos(-q_6-2*q_5-q_4+q_3+ \\
& q_2)+1/4000*\cos(q_6+2*q_5+2*q_4+q_3+q_2)+1/4000*\sin(-2*q_6-2*q_5+q_3+q_2+q_4)-1/4000*\sin(2*q_6+2 \\
& *q_5+q_3+q_2+q_4)-1/2000*\sin(-2*q_5-q_4+q_3+q_2)-1/4000*\cos(-q_6+2*q_4+q_3+q_2)+1/4000*\sin(2*q_5+2 \\
& *q_4+q_3+q_2)+1/4000*\cos(2*q_5-2*q_4+q_6+q_3+q_2)+1/4000*\sin(-2*q_5+2*q_4+q_3+q_2)-1/8000*\sin(-2 \\
& *q_6-2*q_5-2*q_4+q_3+q_2)-1/4000*\sin(2*q_6+2*q_5+q_3+q_2-q_4)+3/4000*\sin(-2*q_4+q_3+q_2)+1/4000*c \\
& \cos(-2*q_4+q_3+q_2+q_6)-1/8000*\sin(2*q_6+2*q_5+2*q_4+q_3+q_2)+1/2000*\cos(q_6+2*q_5+q_4+q_3+q_2)-1/ \\
& 4000*\cos(-q_6-2*q_5-2*q_4+q_3+q_2))*q_v1*q_v4+(1/200*\sin(-q_5-q_4+q_3)+1/200*\cos(-q_6-q_5+q_3)+6/5* \\
& \cos(q_3)+1/200*\sin(q_5-q_4+q_3)+1/200*\sin(-q_5+q_4+q_3)+1/100*\sin(q_3+q_5)+1/400*\cos(q_6+q_5-q_4+q_3 \\
&)-1/400*\cos(-q_6-q_5-q_4+q_3)+1/200*\sin(q_5+q_4+q_3)+1/200*\cos(q_6+q_5+q_3)+1/400*\cos(q_6+q_5+q_4+ \\
& q_3)-1/100*\sin(q_3-q_5)-1/400*\cos(-q_6-q_5+q_4+q_3))*q_v2^2+(1/100*\cos(q_5+q_4)-1/200*\sin(q_6+q_5+q_4 \\
&)+1/200*\sin(-q_6-q_5+q_4)+1/100*\cos(-q_5+q_4))*q_v5^2+(-1/200*\sin(q_6+q_5+q_4)+1/200*\sin(-q_6-q_5+q \\
& 4)-1/2000*\cos(-q_6+q_4)-1/2000*\cos(q_6+q_4))*q_v6^2
\end{aligned}$$

$$\begin{aligned}
& (-1/4000*\cos(q_6+q_3+q_2-q_4)+1/2000*\sin(2*q_6+2*q_5+q_3+q_2)-1/2000*\cos(q_6+q_3+q_2)-1/2000*\sin(\\
& q_2+q_3+q_4)-1/2000*\cos(q_6+2*q_5+q_3+q_2)-1/2000*\cos(-q_6+q_3+q_2)-1/2000*\cos(-2*q_5+q_3+q_2-q_6)- \\
& 1/2000*\sin(-2*q_6-2*q_5+q_3+q_2)+1/4000*\sin(-2*q_6-2*q_5+q_3+q_2-q_4)-1/4000*\cos(q_6+2*q_5-q_4+q_3 \\
& +q_2)-1/2000*\sin(q_2+q_3-q_4)+1/4000*\cos(-q_6-2*q_5+q_3+q_2+q_4)+1/4000*\cos(-q_6-2*q_5-q_4+q_3+q_2) \\
& +1/4000*\sin(-2*q_6-2*q_5+q_3+q_2+q_4)+1/4000*\sin(2*q_6+2*q_5+q_3+q_2+q_4)+1/4000*\cos(-q_6+q_3+q_2 \\
& +q_4)-1/4000*\cos(q_6+q_4+q_3+q_2)+1/4000*\sin(2*q_6+2*q_5+q_3+q_2-q_4)+1/4000*\cos(-q_6-q_4+q_3+q_2)- \\
& 1/4000*\cos(q_6+2*q_5+q_4+q_3+q_2))*q_v1*q_v6-981/40000*\sin(q_6+q_5+q_2+q_3+q_4)-981/40000*\sin(-q \\
& 6-q_5+q_2+q_3-q_4)+(1/2000*\sin(2*q_5+2*q_4)-1/2000*\cos(2*q_4-q_6)-1/4000*\sin(2*q_6+2*q_5+2*q_4)+1 \\
& /2000*\cos(2*q_5+2*q_4+q_6)-1/2000*\cos(-2*q_5+2*q_4-q_6)-1/4000*\sin(-2*q_6-2*q_5+2*q_4)+1/2000*c \\
& \cos(q_6+2*q_4)+1/2000*\sin(-2*q_5+2*q_4)+3/2000*\sin(2*q_4))*q_v2*q_v3+(3/1000*\sin(q_4)-1/2000*\sin(\\
& -2*q_6-2*q_5+q_4)+1/1000*\cos(q_6+2*q_5+q_4)-1/1000*\cos(-q_6+q_4)+1/1000*\cos(q_6+q_4)+1/1000*\sin(\\
& 2*q_5+q_4)+1/1000*\sin(-2*q_5+q_4)-1/1000*\cos(-q_6-2*q_5+q_4)-1/2000*\sin(2*q_6+2*q_5+q_4))*q_v2*q_v \\
& 5+981/40000*\sin(-q_6-q_5+q_2+q_3+q_4)+(-1/2000*\sin(-2*q_6-2*q_5+q_4)+1/2000*\cos(q_6+2*q_5+q_4)-1/ \\
& 2000*\cos(-q_6-2*q_5+q_4)-1/2000*\sin(2*q_6+2*q_5+q_4)+1/1000*\sin(q_4)-1/2000*\cos(-q_6+q_4)+1/2000
\end{aligned}$$

$$\begin{aligned}
& * \cos(q_6+q_4)) * q_v^2 * q_v^6 + (3/1000 * \sin(q_4) - 1/2000 * \sin(-2 * q_6 - 2 * q_5 + q_4) + 1/1000 * \cos(q_6 + 2 * q_5 + q_4) - 1 \\
& / 1000 * \cos(-q_6 + q_4) + 1/1000 * \cos(q_6 + q_4) + 1/1000 * \sin(2 * q_5 + q_4) + 1/1000 * \sin(-2 * q_5 + q_4) - 1/1000 * \cos \\
& (-q_6 - 2 * q_5 + q_4) - 1/2000 * \sin(2 * q_6 + 2 * q_5 + q_4)) * q_v^3 * q_v^5 + 981/20000 * \cos(-q_5 + q_2 + q_3 + q_4) + 981/2000 \\
& 0 * \cos(q_5 + q_2 + q_3 + q_4) - 981/20000 * \cos(-q_5 + q_2 + q_3 - q_4) + 981/40000 * \sin(q_6 + q_5 + q_2 + q_3 - q_4) - 981/2000 \\
& 0 * \cos(q_5 + q_2 + q_3 - q_4) + (-1/2000 * \sin(-2 * q_6 - 2 * q_5 + q_4) + 1/2000 * \cos(q_6 + 2 * q_5 + q_4) - 1/2000 * \cos(-q_6 - 2 * \\
& q_5 + q_4) - 1/2000 * \sin(2 * q_6 + 2 * q_5 + q_4) + 1/1000 * \sin(q_4) - 1/2000 * \cos(-q_6 + q_4) + 1/2000 * \cos(q_6 + q_4)) * q_v \\
& 3 * q_v^6 + (-1/500 * \sin(2 * q_5) + 1/1000 * \sin(2 * q_6 + 2 * q_5) - 1/500 * \cos(q_6 + 2 * q_5)) * q_v^4 * q_v^5 + (-1/1000 * \cos(\\
& q_6) + 1/1000 * \sin(2 * q_6 + 2 * q_5) - 1/1000 * \cos(q_6 + 2 * q_5)) * q_v^4 * q_v^6 + (-1/800 * \cos(-q_6 - q_5 + q_4 + q_3) + 1/160 \\
& 00 * \sin(2 * q_6 + 2 * q_5 + 2 * q_3 + 2 * q_2 - q_4) + 1/16000 * \sin(-2 * q_5 + 2 * q_4 + 2 * q_3 + 2 * q_2) - 1/16000 * \cos(-2 * q_4 + 2 \\
& * q_3 + 2 * q_2 + q_6) - 1/400 * \sin(-q_5 - q_4 + q_3 + 2 * q_2) + 1/400 * \cos(2 * q_3 + 2 * q_2 + q_5 + q_4) - 1/8000 * \sin(2 * q_5 + 2 * q \\
& 4) + 1/32000 * \sin(2 * q_6 + 2 * q_5 - 2 * q_4 + 2 * q_3 + 2 * q_2) + 1/8000 * \cos(2 * q_4 - q_6) - 1/32000 * \sin(-2 * q_6 - 2 * q_5 + 2 \\
& * q_4 + 2 * q_3 + 2 * q_2) + 1/800 * \cos(q_6 + q_5 + q_4 + q_3 + 2 * q_2) - 1/16000 * \cos(-q_6 - 2 * q_5 + 2 * q_4 + 2 * q_3 + 2 * q_2) - 1/8 \\
& 000 * \cos(-q_6 - 2 * q_5 - q_4 + 2 * q_3 + 2 * q_2) + 1/16000 * \sin(2 * q_6 + 2 * q_5 + 2 * q_4) - 1/8000 * \cos(2 * q_5 + 2 * q_4 + q_6) - \\
& 1/8000 * \sin(2 * q_5 - q_4 + 2 * q_3 + 2 * q_2) + 1/16000 * \cos(-q_6 - 2 * q_5 - 2 * q_4 + 2 * q_3 + 2 * q_2) - 1/400 * \cos(2 * q_3 + 2 * q \\
& 2 + q_5 - q_4) + 1/400 * \sin(q_5 + q_4 + q_3 + 2 * q_2) + 1/16000 * \sin(2 * q_5 + 2 * q_4 + 2 * q_3 + 2 * q_2) + 1/800 * \sin(2 * q_3 + 2 * \\
& q_2 + q_6 + q_5 - q_4) - 1/800 * \sin(2 * q_3 + 2 * q_2 - q_6 - q_5 - q_4) + 1/400 * \cos(2 * q_3 + 2 * q_2 - q_5 + q_4) + 1/8000 * \cos(-2 * q_5 \\
& + 2 * q_4 - q_6) - 1/800 * \sin(2 * q_3 + 2 * q_2 + q_6 + q_5 + q_4) + 1/800 * \sin(2 * q_3 + 2 * q_2 - q_6 - q_5 + q_4) + 1/16000 * \sin(-2 * \\
& q_6 - 2 * q_5 + 2 * q_4) - 1/400 * \cos(2 * q_3 + 2 * q_2 - q_5 - q_4) - 1/800 * \cos(q_6 + q_5 - q_4 + q_3) + 1/800 * \cos(-q_6 - q_5 - q_4 + q_3 \\
&) + 1/800 * \cos(q_6 + q_5 + q_4 + q_3) - 1/8000 * \cos(q_6 + 2 * q_5 + 2 * q_3 + 2 * q_2 - q_4) - 1/16000 * \cos(-q_6 + 2 * q_4 + 2 * q_3 + \\
& 2 * q_2) + 1/8000 * \sin(2 * q_5 + q_4 + 2 * q_3 + 2 * q_2) - 1/16000 * \sin(2 * q_6 + 2 * q_5 + q_4 + 2 * q_3 + 2 * q_2) - 1/16000 * \cos(\\
& q_6 + 2 * q_5 - 2 * q_4 + 2 * q_3 + 2 * q_2) + 1/400 * \sin(-q_5 + q_4 + q_3 + 2 * q_2) + 1/16000 * \cos(-q_6 - 2 * q_4 + 2 * q_3 + 2 * q_2) - 1/ \\
& 8000 * \cos(q_6 + 2 * q_4) - 1/400 * \sin(-q_5 - q_4 + q_3) + 1/16000 * \sin(-2 * q_6 - 2 * q_5 + q_4 + 2 * q_3 + 2 * q_2) - 1/800 * \cos(- \\
& q_6 - q_5 + q_4 + q_3 + 2 * q_2) - 3/16000 * \sin(-2 * q_4 + 2 * q_3 + 2 * q_2) + 1/32000 * \sin(-2 * q_6 - 2 * q_5 - 2 * q_4 + 2 * q_3 + 2 * q_2 \\
&) - 1/400 * \sin(q_5 - q_4 + q_3 + 2 * q_2) - 1/8000 * \sin(-2 * q_5 + 2 * q_4) - 1/16000 * \sin(-2 * q_6 - 2 * q_5 + 2 * q_3 + 2 * q_2 - q_4) + \\
& 1/400 * \sin(q_5 + q_4 + q_3) - 1/32000 * \sin(2 * q_6 + 2 * q_5 + 2 * q_4 + 2 * q_3 + 2 * q_2) + 1/8000 * \cos(-q_6 - 2 * q_5 + q_4 + 2 * q \\
& 3 + 2 * q_2) - 1/8000 * \sin(-2 * q_5 + q_4 + 2 * q_3 + 2 * q_2) - 3/8000 * \sin(2 * q_4) - 1/800 * \cos(q_6 + q_5 - q_4 + q_3 + 2 * q_2) + 1/ \\
& 8000 * \cos(q_6 + 2 * q_5 + 2 * q_3 + 2 * q_2 + q_4) + 1/16000 * \cos(q_6 + 2 * q_4 + 2 * q_3 + 2 * q_2) + 3/16000 * \sin(2 * q_4 + 2 * q \\
& 3 + 2 * q_2) - 1/400 * \sin(q_5 - q_4 + q_3) + 1/400 * \sin(-q_5 + q_4 + q_3) - 1/16000 * \sin(2 * q_5 - 2 * q_4 + 2 * q_3 + 2 * q_2) - 1/160 \\
& 00 * \sin(-2 * q_5 - 2 * q_4 + 2 * q_3 + 2 * q_2) + 1/8000 * \sin(-2 * q_5 - q_4 + 2 * q_3 + 2 * q_2) + 1/800 * \cos(-q_6 - q_5 - q_4 + q_3 + 2 * \\
& q_2) + 1/16000 * \cos(2 * q_5 + 2 * q_4 + 2 * q_3 + 2 * q_2 + q_6)) * q_v^1^2 + (1/4000 * \sin(2 * q_6 + 2 * q_5 + q_3 + q_2) - 1/2000 * \sin(2 * q_5 + q_3 + q_2) - 1/2000 * \cos(q_6 + q_3 + q_2) - 1/2000 * \cos(q_6 + 2 * q_5 + q_3 + q_2) \\
& + 1/2000 * \cos(-q_6 + q_3 + q_2) + 1/2000 * \cos(-2 * q_5 + q_3 + q_2 - q_6) + 1/4000 * \sin(-2 * q_6 - 2 * q_5 + q_3 + q_2) - 3/2000 \\
& * \sin(q_2 + q_3) - 1/4000 * \sin(2 * q_5 - 2 * q_4 + q_3 + q_2) + 1/200 * \sin(q_6 + q_5 + q_2 + q_3 + q_4) - 1/200 * \sin(-q_6 - q_5 + q_2 + \\
& q_3 - q_4) - 1/4000 * \sin(-2 * q_6 - 2 * q_5 + q_3 + q_2 - q_4) - 1/200 * \sin(-q_6 - q_5 + q_2 + q_3 + q_4) - 3/4000 * \sin(2 * q_4 + q_3 + q_2 \\
&) - 1/100 * \cos(-q_5 + q_2 + q_3 + q_4) - 1/100 * \cos(q_5 + q_2 + q_3 + q_4) - 1/100 * \cos(-q_5 + q_2 + q_3 - q_4) - 1/4000 * \sin(-2 * \\
& q_5 - 2 * q_4 + q_3 + q_2) + 1/200 * \sin(q_6 + q_5 + q_2 + q_3 - q_4) + 1/8000 * \sin(-2 * q_6 - 2 * q_5 + 2 * q_4 + q_3 + q_2) + 1/4000 * \cos \\
& (-2 * q_5 + 2 * q_4 + q_3 + q_2 - q_6) - 1/100 * \cos(q_5 + q_2 + q_3 - q_4) - 1/2000 * \sin(2 * q_5 + q_4 + q_3 + q_2) - 1/2000 * \sin(2 * q \\
& 5 - q_4 + q_3 + q_2) - 1/2000 * \cos(q_6 + 2 * q_5 - q_4 + q_3 + q_2) + 1/4000 * \cos(-q_6 - 2 * q_4 + q_3 + q_2) + 1/8000 * \sin(2 * q_6 + \\
& 2 * q_5 - 2 * q_4 + q_3 + q_2) - 1/2000 * \cos(-q_6 - 2 * q_5 + q_3 + q_2 + q_4) - 1/4000 * \cos(q_6 + 2 * q_4 + q_3 + q_2) + 1/2000 * \sin(- \\
& 2 * q_5 + q_4 + q_3 + q_2) - 1/2000 * \cos(-q_6 - 2 * q_5 - q_4 + q_3 + q_2) - 1/4000 * \cos(q_6 + 2 * q_5 + 2 * q_4 + q_3 + q_2) - 1/4000 * \sin \\
& (-2 * q_6 - 2 * q_5 + q_3 + q_2 + q_4) + 1/4000 * \sin(2 * q_6 + 2 * q_5 + q_3 + q_2 + q_4) + 1/2000 * \sin(-2 * q_5 - q_4 + q_3 + q_2) + 1/4 \\
& 000 * \cos(-q_6 + 2 * q_4 + q_3 + q_2) - 1/4000 * \sin(2 * q_5 + 2 * q_4 + q_3 + q_2) - 1/4000 * \cos(2 * q_5 - 2 * q_4 + q_6 + q_3 + q_2) - 1/ \\
& 4000 * \sin(-2 * q_5 + 2 * q_4 + q_3 + q_2) + 1/8000 * \sin(-2 * q_6 - 2 * q_5 - 2 * q_4 + q_3 + q_2) + 1/4000 * \sin(2 * q_6 + 2 * q_5 + q_3 \\
& + q_2 - q_4) - 3/4000 * \sin(-2 * q_4 + q_3 + q_2) - 1/4000 * \cos(-2 * q_4 + q_3 + q_2 + q_6) + 1/8000 * \sin(2 * q_6 + 2 * q_5 + 2 * q_4 + \\
& q_3 + q_2) - 1/2000 * \cos(q_6 + 2 * q_5 + q_4 + q_3 + q_2) + 1/4000 * \cos(-q_6 - 2 * q_5 - 2 * q_4 + q_3 + q_2)) * q_v^1 * q_v^3 + (1/4000
\end{aligned}$$

$$\begin{aligned}
& * \sin(2*q_6+2*q_5+q_3+q_2)-1/2000*\sin(-2*q_5+q_3+q_2)-1/2000*\cos(q_6+q_3+q_2)-1/2000*\sin(2*q_5+q_3+ \\
& q_2)-1/2000*\cos(q_6+2*q_5+q_3+q_2)+1/2000*\cos(-q_6+q_3+q_2)+1/2000*\cos(-2*q_5+q_3+q_2-q_6)+1/4000 \\
& * \sin(-2*q_6-2*q_5+q_3+q_2)-3/2000*\sin(q_2+q_3)-1/4000*\sin(2*q_5-2*q_4+q_3+q_2)+1/200*\sin(q_6+q_5+q \\
& 2+q_3+q_4)-1/200*\sin(-q_6-q_5+q_2+q_3-q_4)-1/4000*\sin(-2*q_6-2*q_5+q_3+q_2-q_4)-1/200*\sin(-q_6-q_5+q_2 \\
& +q_3+q_4)-3/4000*\sin(2*q_4+q_3+q_2)-1/100*\cos(-q_5+q_2+q_3+q_4)-1/100*\cos(q_5+q_2+q_3+q_4)-1/100*c \\
& os(-q_5+q_2+q_3-q_4)-1/4000*\sin(-2*q_5-2*q_4+q_3+q_2)+1/200*\sin(q_6+q_5+q_2+q_3-q_4)+1/8000*\sin(-2*q \\
& 6-2*q_5+2*q_4+q_3+q_2)+1/4000*\cos(-2*q_5+2*q_4+q_3+q_2-q_6)-1/200*\cos(q_6+q_5+q_4+q_2)-1/100*\cos(\\
& q_5+q_2+q_3-q_4)+1/200*\cos(q_6+q_5+q_4-q_2)-1/2000*\sin(2*q_5+q_4+q_3+q_2)-1/2000*\sin(2*q_5-q_4+q_3+q \\
& 2)-1/2000*\cos(q_6+2*q_5-q_4+q_3+q_2)+1/100*\sin(-q_5+q_4-q_2)+1/4000*\cos(-q_6-2*q_4+q_3+q_2)+1/8000 \\
& * \sin(2*q_6+2*q_5-2*q_4+q_3+q_2)-1/200*\cos(-q_6-q_5+q_4-q_2)-1/2000*\cos(-q_6-2*q_5+q_3+q_2+q_4)-1/400 \\
& 0*\cos(q_6+2*q_4+q_3+q_2)+1/2000*\sin(-2*q_5+q_4+q_3+q_2)-1/2000*\cos(-q_6-2*q_5-q_4+q_3+q_2)+1/100*s \\
& in(q_5+q_4-q_2)-1/4000*\cos(q_6+2*q_5+2*q_4+q_3+q_2)-1/4000*\sin(-2*q_6-2*q_5+q_3+q_2+q_4)-1/100*\sin(\\
& q_5+q_4+q_2)+1/4000*\sin(2*q_6+2*q_5+q_3+q_2+q_4)+1/2000*\sin(-2*q_5-q_4+q_3+q_2)+1/4000*\cos(-q_6+2 \\
& *q_4+q_3+q_2)+1/200*\cos(-q_6-q_5+q_4+q_2)-1/4000*\sin(2*q_5+2*q_4+q_3+q_2)-1/4000*\cos(2*q_5-2*q_4+q \\
& 6+q_3+q_2)-1/4000*\sin(-2*q_5+2*q_4+q_3+q_2)+1/8000*\sin(-2*q_6-2*q_5-2*q_4+q_3+q_2)+1/4000*\sin(2* \\
& q_6+2*q_5+q_3+q_2-q_4)-3/4000*\sin(-2*q_4+q_3+q_2)-1/100*\sin(-q_5+q_4+q_2)-1/4000*\cos(-2*q_4+q_3+q_2 \\
& +q_6)+1/8000*\sin(2*q_6+2*q_5+2*q_4+q_3+q_2)-1/2000*\cos(q_6+2*q_5+q_4+q_3+q_2)+1/4000*\cos(-q_6-2* \\
& q_5-2*q_4+q_3+q_2))*q_v1*q_v2+(1/200*\cos(q_5+q_4+q_2)-1/400*\cos(q_6+q_5+q_2+q_3-q_4)+1/400*\cos(-q_6- \\
& q_5+q_2+q_3+q_4)-1/400*\cos(q_6+q_5+q_2+q_3+q_4)+1/400*\sin(-q_6-q_5+q_4+q_2)-1/4000*\cos(2*q_6+2*q_5+ \\
& q_3+q_2)+1/2000*\cos(-2*q_5+q_3+q_2)+1/200*\cos(-q_5+q_4+q_2)+1/400*\sin(-q_6-q_5+q_4-q_2)-1/4000*\sin(\\
& -q_6-2*q_5+q_3+q_2+q_4)+1/400*\cos(-q_6-q_5+q_2+q_3-q_4)-1/4000*\cos(-2*q_5+q_4+q_3+q_2)+3/2000*\cos(q \\
& 2+q_3)-1/4000*\sin(-q_6-2*q_5-q_4+q_3+q_2)-1/200*\sin(q_5+q_2+q_3-q_4)-1/200*\sin(-q_5+q_2+q_3-q_4)-1/200 \\
& * \sin(q_5+q_2+q_3+q_4)+1/4000*\cos(2*q_5-q_4+q_3+q_2)+1/2000*\cos(2*q_5+q_3+q_2)-1/200*\sin(-q_5+q_2+q \\
& 3+q_4)-1/4000*\sin(q_6+2*q_5-q_4+q_3+q_2)+1/8000*\cos(-2*q_6-2*q_5+q_3+q_2+q_4)-1/2000*\sin(q_6+q_3+q \\
& 2)-1/8000*\cos(2*q_6+2*q_5+q_3+q_2+q_4)-1/4000*\cos(-2*q_5-q_4+q_3+q_2)+1/2000*\sin(-q_6+q_3+q_2)-1/2 \\
& 000*\sin(q_6+2*q_5+q_3+q_2)-1/400*\sin(q_6+q_5+q_4+q_2)+1/200*\cos(-q_5+q_4-q_2)-1/4000*\sin(q_6+2*q_5 \\
& +q_4+q_3+q_2)+1/8000*\cos(-2*q_6-2*q_5+q_3+q_2-q_4)+1/4000*\cos(2*q_5+q_4+q_3+q_2)-1/400*\sin(q_6+q_5 \\
& +q_4-q_2)+1/2000*\sin(-2*q_5+q_3+q_2-q_6)+1/200*\cos(q_5+q_4-q_2)-1/4000*\cos(-2*q_6-2*q_5+q_3+q_2)-1/8 \\
& 000*\cos(2*q_6+2*q_5+q_3+q_2-q_4))*q_a1+(-1/4000*\cos(-2*q_6-2*q_5+q_4)-1/200*\cos(-q_5-q_4+q_3)+1/20 \\
& 00*\sin(q_6+2*q_5+q_4)-1/200*\cos(q_5-q_4+q_3)+1/200*\cos(-q_5+q_4+q_3)-1/2000*\cos(2*q_5+q_4)+1/400* \\
& \sin(q_6+q_5-q_4+q_3)+1/2000*\cos(-2*q_5+q_4)-1/400*\sin(-q_6-q_5-q_4+q_3)+1/100*\sin(q_5+q_4)+1/200*\cos \\
& (q_5+q_4+q_3)+1/200*\cos(q_6+q_5+q_4)-1/200*\cos(-q_6-q_5+q_4)+1/100*\sin(-q_5+q_4)+1/2000*\sin(-q_6-2* \\
& q_5+q_4)-1/400*\sin(q_6+q_5+q_4+q_3)+1/400*\sin(-q_6-q_5+q_4+q_3)+1/4000*\cos(2*q_6+2*q_5+q_4))*q_a2+ \\
& (-1/4000*\cos(-2*q_6-2*q_5+q_4)+1/2000*\sin(q_6+2*q_5+q_4)-1/2000*\cos(2*q_5+q_4)+1/2000*\cos(-2*q_5 \\
& +q_4)+1/100*\sin(q_5+q_4)+1/200*\cos(q_6+q_5+q_4)-1/200*\cos(-q_6-q_5+q_4)+1/100*\sin(-q_5+q_4)+1/2000 \\
& * \sin(-q_6-2*q_5+q_4)+1/4000*\cos(2*q_6+2*q_5+q_4))*q_a3+(-1/1000*\sin(q_6)+1/1000*\cos(2*q_5)-1/200 \\
& 0*\cos(2*q_6+2*q_5)+3/2000-1/1000*\sin(q_6+2*q_5))*q_a4+(-1/2000*\cos(q_6+q_3+q_2-q_4)+1/2000*\sin(\\
& 2*q_6+2*q_5+q_3+q_2)+1/1000*\sin(-2*q_5+q_3+q_2)-1/1000*\sin(2*q_5+q_3+q_2)-3/2000*\sin(q_2+q_3+q_4)- \\
& 1/1000*\cos(q_6+2*q_5+q_3+q_2)-1/1000*\cos(-2*q_5+q_3+q_2-q_6)-1/2000*\sin(-2*q_6-2*q_5+q_3+q_2)+1/40 \\
& 00*\sin(-2*q_6-2*q_5+q_3+q_2-q_4)-1/2000*\sin(2*q_5+q_4+q_3+q_2)-1/2000*\sin(2*q_5-q_4+q_3+q_2)-1/2000 \\
& * \cos(q_6+2*q_5-q_4+q_3+q_2)-3/2000*\sin(q_2+q_3-q_4)+1/2000*\cos(-q_6-2*q_5+q_3+q_2+q_4)-1/2000*\sin(- \\
& 2*q_5+q_4+q_3+q_2)+1/2000*\cos(-q_6-2*q_5-q_4+q_3+q_2)+1/4000*\sin(-2*q_6-2*q_5+q_3+q_2+q_4)+1/4000* \\
& \sin(2*q_6+2*q_5+q_3+q_2+q_4)-1/2000*\sin(-2*q_5-q_4+q_3+q_2)+1/2000*\cos(-q_6+q_3+q_2+q_4)-1/2000*co \\
& s(q_6+q_4+q_3+q_2)+1/4000*\sin(2*q_6+2*q_5+q_3+q_2-q_4)+1/2000*\cos(-q_6-q_4+q_3+q_2)-1/2000*\cos(q_6+ \\
& 2*q_5+q_4+q_3+q_2))*q_v1*q_v5+(1/4000*\sin(2*q_5+2*q_4)-1/4000*\cos(2*q_4-q_6)-1/8000*\sin(2*q_6+2*
\end{aligned}$$

$$q_5+2q_4)+1/4000*\cos(2q_5+2q_4+q_6)-1/4000*\cos(-2q_5+2q_4-q_6)-1/8000*\sin(-2q_6-2q_5+2q_4)+1/4000*\cos(q_6+2q_4)+1/4000*\sin(-2q_5+2q_4)+3/4000*\sin(2q_4))*qv^3^2+(1/4000*\sin(2q_5+2q_4)-1/200*\sin(-q_5-q_4+q_3)-1/200*\sin(q_5-q_4+q_3)-1/8000*\sin(2q_6+2q_5+2q_4)+1/200*\sin(-q_5+q_4+q_3)+1/4000*\sin(-2q_5+2q_4)+3/4000*\sin(2q_4)-1/4000*\cos(2q_4-q_6)-1/400*\cos(q_6+q_5-q_4+q_3)+1/400*\cos(-q_6-q_5-q_4+q_3)+1/4000*\cos(2q_5+2q_4+q_6)+1/200*\sin(q_5+q_4+q_3)-1/4000*\cos(-2q_5+2q_4-q_6)+1/400*\cos(q_6+q_5+q_4+q_3)-1/8000*\sin(-2q_6-2q_5+2q_4)-1/400*\cos(-q_6-q_5+q_4+q_3)+1/4000*\cos(q_6+2q_4))*qv^2^2$$

$$-1/500*\cos(q_6)*qv^5*qv^6+(1/2000*\sin(2q_5+2q_4)-1/25*\cos(q_5)-1/4000*\sin(2q_6+2q_5+2q_4)+1/2000*\cos(2q_5+2q_4+q_6)-1/1000*\sin(2q_5)+1/50*\sin(q_6+q_5)+1/2000*\sin(2q_6+2q_5)+1/2000*\cos(-2q_5+2q_4-q_6)+1/4000*\sin(-2q_6-2q_5+2q_4)-1/1000*\cos(q_6+2q_5)-1/2000*\sin(-2q_5+2q_4))*qv^2*qv^3+(-1/1000*\cos(-q_6+q_4)-1/1000*\cos(q_6+q_4))*qv^2*qv^6+(-3/1000*\sin(q_4)+1/2000*\sin(-2q_6-2q_5+q_4)-1/1000*\cos(q_6+2q_5+q_4)+1/1000*\cos(-q_6+q_4)-1/1000*\cos(q_6+q_4)-1/1000*\sin(2q_5+q_4)-1/1000*\sin(-2q_5+q_4)+1/1000*\cos(-q_6-2q_5+q_4)+1/2000*\sin(2q_6+2q_5+q_4))*qv^2*qv^4-981/40000*\sin(q_6+q_5+q_2+q_3+q_4)+(-3/1000*\sin(q_4)+1/2000*\sin(-2q_6-2q_5+q_4)-1/1000*\cos(q_6+2q_5+q_4)+1/1000*\cos(-q_6+q_4)-1/1000*\cos(q_6+q_4)-1/1000*\sin(2q_5+q_4)-1/1000*\sin(-2q_5+q_4)+1/1000*\cos(-q_6-2q_5+q_4)+1/2000*\sin(2q_6+2q_5+q_4))*qv^3*qv^4+(-1/1000*\cos(-q_6+q_4)-1/1000*\cos(q_6+q_4))*qv^3*qv^6+(1/1000*\sin(2q_5)-1/2000*\sin(2q_6+2q_5)+1/1000*\cos(q_6+2q_5))*qv^4^2+(1/4000*\sin(2q_5+2q_4)-1/50*\cos(q_5)-1/8000*\sin(2q_6+2q_5+2q_4)+1/4000*\cos(2q_5+2q_4+q_6)-1/2000*\sin(2q_5)+1/100*\sin(q_6+q_5)+1/4000*\sin(2q_6+2q_5)+1/4000*\cos(-2q_5+2q_4-q_6)+1/8000*\sin(-2q_6-2q_5+2q_4)-1/2000*\cos(q_6+2q_5)-1/4000*\sin(-2q_5+2q_4))*qv^3^2+981/10000*\cos(q_2+q_3-q_5)+981/10000*\cos(q_2+q_3+q_5)-981/40000*\sin(-q_6-q_5+q_2+q_3-q_4)+(-1/2000*\cos(q_6+q_3+q_2-q_4)+3/2000*\sin(q_2+q_3+q_4)+1/4000*\sin(2q_5-2q_4+q_3+q_2)+1/200*\sin(q_6+q_5+q_2+q_3+q_4)-1/200*\sin(-q_6-q_5+q_2+q_3-q_4)-1/4000*\sin(-2q_6-2q_5+q_3+q_2-q_4)+1/200*\sin(-q_6-q_5+q_2+q_3+q_4)+1/100*\cos(-q_5+q_2+q_3+q_4)-1/100*\cos(q_5+q_2+q_3+q_4)-1/100*\cos(-q_5+q_2+q_3-q_4)-1/4000*\sin(-2q_5-2q_4+q_3+q_2)-1/200*\sin(q_6+q_5+q_2+q_3-q_4)-1/8000*\sin(-2q_6-2q_5+2q_4+q_3+q_2)-1/4000*\cos(-2q_5+2q_4+q_3+q_2-q_6)+1/100*\cos(q_5+q_2+q_3-q_4)-1/2000*\sin(2q_5+q_4+q_3+q_2)+1/2000*\sin(2q_5-q_4+q_3+q_2)+1/2000*\cos(q_6+2q_5-q_4+q_3+q_2)-3/2000*\sin(q_2+q_3-q_4)-1/8000*\sin(2q_6+2q_5-2q_4+q_3+q_2)+1/2000*\cos(-q_6-2q_5+q_3+q_2+q_4)-1/2000*\sin(-2q_5+q_4+q_3+q_2)-1/2000*\cos(-q_6-2q_5-q_4+q_3+q_2)-1/4000*\cos(q_6+2q_5+2q_4+q_3+q_2)+1/4000*\sin(-2q_6-2q_5+q_3+q_2+q_4)+1/4000*\sin(2q_6+2q_5+q_3+q_2+q_4)+1/2000*\sin(-2q_5-q_4+q_3+q_2)-1/2000*\cos(-q_6+q_3+q_2+q_4)-1/4000*\sin(2q_5+2q_4+q_3+q_2)+1/4000*\cos(2q_5-2q_4+q_6+q_3+q_2)+1/2000*\cos(q_6+q_4+q_3+q_2)+1/4000*\sin(-2q_5+2q_4+q_3+q_2)+1/8000*\sin(-2q_6-2q_5-2q_4+q_3+q_2)-1/4000*\sin(2q_6+2q_5+q_3+q_2-q_4)+1/2000*\cos(-q_6-q_4+q_3+q_2)+1/8000*\sin(2q_6+2q_5+2q_4+q_3+q_2)-1/2000*\cos(q_6+2q_5+q_4+q_3+q_2)+1/4000*\cos(-q_6-2q_5-2q_4+q_3+q_2))*qv^1*qv^3-981/40000*\sin(-q_6-q_5+q_2+q_3+q_4)-981/20000*\cos(-q_5+q_2+q_3+q_4)+981/20000*\cos(q_5+q_2+q_3+q_4)-981/20000*\cos(-q_5+q_2+q_3-q_4)-981/40000*\sin(q_6+q_5+q_2+q_3-q_4)-981/20000*\sin(q_6+q_2+q_3+q_5)+981/20000*\sin(-q_6+q_2+q_3-q_5)+981/20000*\cos(q_5+q_2+q_3-q_4)+(1/800*\cos(-q_6-q_5+q_4+q_3)-1/8000*\sin(2q_6+2q_5+2q_3+2q_2-q_4)-1/16000*\sin(-2q_5+2q_4+2q_3+2q_2)-3/8000*\sin(-2q_5+2q_3+2q_2)-1/400*\cos(-q_6-q_5+q_3+2q_2)-1/400*\sin(-q_5-q_4+q_3+2q_2)+1/400*\cos(2q_3+2q_2+q_5+q_4)-1/8000*\sin(2q_5+2q_4)-1/32000*\sin(2q_6+2q_5-2q_4+2q_3+2q_2)+1/32000*\sin(-2q_6-2q_5+2q_4+2q_3+2q_2)+1/800*\cos(q_6+q_5+q_4+q_3+2q_2)+1/16000*\cos(-q_6-2q_5+2q_4+2q_3+2q_2)+1/200*\cos(2q_3+2q_2+q_5)-1/4000*\cos(-q_6-2q_5-q_4+2q_3+2q_2)-1/100*\cos(q_5)+1/16000*\sin(2q_6+2q_5+2q_4)-1/8000*\cos(2q_5+2q_4+q_6)+1/4000*\sin(2q_5-q_4+2q_3+2q_2)+1/200*\sin(q_5+q_3+2q_2)+1/16000*\cos(-q_6-2q_5-2q_4+2q_3+2q_2)+1/2000*\sin(q_3-q_5)+1/400*\cos(2q_3+2q_2+q_5-q_4)+1/4000*\sin(2q_5)+1/400*\sin(q_5+q_4+q_3+2q_2)+3/8$$

$$\begin{aligned}
& 000*\cos(q6+2*q5+2*q3+2*q2)+1/200*\sin(q6+q5)+1/200*\cos(2*q3+2*q2-q5)+1/16000*\sin(2*q5 \\
& +2*q4+2*q3+2*q2)-1/800*\sin(2*q3+2*q2+q6+q5-q4)-1/800*\sin(2*q3+2*q2-q6-q5-q4)+1/400*co \\
& s(q6+q5+q3)+3/8000*\sin(2*q5+2*q3+2*q2)-1/8000*\sin(2*q6+2*q5)-1/400*\cos(2*q3+2*q2-q5+q \\
& 4)-1/8000*\cos(-2*q5+2*q4-q6)-1/800*\sin(2*q3+2*q2+q6+q5+q4)-1/800*\sin(2*q3+2*q2-q6-q5+q \\
& 4)-1/16000*\sin(-2*q6-2*q5+2*q4)-1/400*\cos(2*q3+2*q2-q5-q4)+1/800*\cos(q6+q5-q4+q3)+1/80 \\
& 0*\cos(-q6-q5-q4+q3)+1/400*\sin(2*q3+2*q2-q6-q5)+1/800*\cos(q6+q5+q4+q3)+1/4000*\cos(q6+2 \\
& *q5+2*q3+2*q2-q4)-1/400*\sin(2*q3+2*q2+q6+q5)+1/4000*\sin(2*q5+q4+2*q3+2*q2)-1/8000*si \\
& n(2*q6+2*q5+q4+2*q3+2*q2)+1/200*\sin(q3+q5)+1/16000*\cos(q6+2*q5-2*q4+2*q3+2*q2)-1/40 \\
& 0*\sin(-q5+q4+q3+2*q2)+1/4000*\cos(q6+2*q5)+3/8000*\cos(-q6-2*q5+2*q3+2*q2)-1/400*\sin(-q5 \\
& -q4+q3)-1/8000*\sin(-2*q6-2*q5+q4+2*q3+2*q2)+1/800*\cos(-q6-q5+q4+q3+2*q2)+1/400*\cos(q6 \\
& +q5+q3+2*q2)-3/16000*\sin(2*q6+2*q5+2*q3+2*q2)+1/32000*\sin(-2*q6-2*q5-2*q4+2*q3+2*q2) \\
& +1/400*\sin(q5-q4+q3+2*q2)+1/200*\sin(-q5+q3+2*q2)+1/8000*\sin(-2*q5+2*q4)-1/8000*\sin(-2*q \\
& 6-2*q5+2*q3+2*q2-q4)-1/400*\cos(-q6-q5+q3)+1/400*\sin(q5+q4+q3)+3/16000*\sin(-2*q6-2*q5+2 \\
& *q3+2*q2)-1/32000*\sin(2*q6+2*q5+2*q4+2*q3+2*q2)-1/4000*\cos(-q6-2*q5+q4+2*q3+2*q2)+1/ \\
& 4000*\sin(-2*q5+q4+2*q3+2*q2)+1/800*\cos(q6+q5-q4+q3+2*q2)+1/4000*\cos(q6+2*q5+2*q3+2* \\
& q2+q4)+1/400*\sin(q5-q4+q3)-1/400*\sin(-q5+q4+q3)+1/16000*\sin(2*q5-2*q4+2*q3+2*q2)-1/160 \\
& 00*\sin(-2*q5-2*q4+2*q3+2*q2)+1/4000*\sin(-2*q5-q4+2*q3+2*q2)+1/800*\cos(-q6-q5-q4+q3+2* \\
& q2)+1/16000*\cos(2*q5+2*q4+2*q3+2*q2+q6))*qv1^2+(-1/2000*\cos(q6+q3+q2-q4)+3/2000*\sin(\\
& q2+q3+q4)+1/4000*\sin(2*q5-2*q4+q3+q2)+1/200*\sin(q6+q5+q2+q3+q4)-1/200*\sin(-q6-q5+q2+q \\
& 3-q4)-1/4000*\sin(-2*q6-2*q5+q3+q2-q4)+1/200*\sin(-q6-q5+q2+q3+q4)+1/100*\cos(-q5+q2+q3+q \\
& 4)-1/100*\cos(q5+q2+q3+q4)-1/100*\cos(-q5+q2+q3-q4)-1/4000*\sin(-2*q5-2*q4+q3+q2)-1/200*si \\
& n(q6+q5+q2+q3-q4)-1/8000*\sin(-2*q6-2*q5+2*q4+q3+q2)-1/4000*\cos(-2*q5+2*q4+q3+q2-q6)-1 \\
& /200*\cos(q6+q5+q4+q2)+1/100*\cos(q5+q2+q3-q4)+1/200*\cos(q6+q5+q4-q2)-1/2000*\sin(2*q5+q \\
& 4+q3+q2)+1/2000*\sin(2*q5-q4+q3+q2)+1/2000*\cos(q6+2*q5-q4+q3+q2)-3/2000*\sin(q2+q3-q4)- \\
& 1/100*\sin(-q5+q4-q2)-1/8000*\sin(2*q6+2*q5-2*q4+q3+q2)+1/200*\cos(-q6-q5+q4-q2)+1/2000*c \\
& os(-q6-2*q5+q3+q2+q4)-1/2000*\sin(-2*q5+q4+q3+q2)-1/2000*\cos(-q6-2*q5-q4+q3+q2)+1/100*s \\
& in(q5+q4-q2)-1/4000*\cos(q6+2*q5+2*q4+q3+q2)+1/4000*\sin(-2*q6-2*q5+q3+q2+q4)-1/100*\sin(\\
& q5+q4+q2)+1/4000*\sin(2*q6+2*q5+q3+q2+q4)+1/2000*\sin(-2*q5-q4+q3+q2)-1/200*\cos(-q6-q5+ \\
& q4+q2)-1/2000*\cos(-q6+q3+q2+q4)-1/4000*\sin(2*q5+2*q4+q3+q2)+1/4000*\cos(2*q5-2*q4+q6+ \\
& q3+q2)+1/2000*\cos(q6+q4+q3+q2)+1/4000*\sin(-2*q5+2*q4+q3+q2)+1/8000*\sin(-2*q6-2*q5-2* \\
& q4+q3+q2)-1/4000*\sin(2*q6+2*q5+q3+q2-q4)+1/100*\sin(-q5+q4+q2)+1/2000*\cos(-q6-q4+q3+q2 \\
&)+1/8000*\sin(2*q6+2*q5+2*q4+q3+q2)-1/2000*\cos(q6+2*q5+q4+q3+q2)+1/4000*\cos(-q6-2*q5- \\
& 2*q4+q3+q2))*qv1*qv2+(1/200*\cos(q5+q4+q2)+1/400*\cos(q6+q5+q2+q3-q4)-1/400*\cos(-q6-q5 \\
& +q2+q3+q4)-1/400*\cos(q6+q5+q2+q3+q4)-1/400*\sin(-q6-q5+q4+q2)-1/200*\cos(-q5+q4+q2)-1/40 \\
& 0*\sin(-q6-q5+q4-q2)+1/400*\cos(-q6-q5+q2+q3-q4)+1/200*\sin(q5+q2+q3-q4)-1/2000*\sin(-q6+q3 \\
& +q2+q4)+1/2000*\sin(q6+q4+q3+q2)-1/200*\sin(-q5+q2+q3-q4)+3/2000*\cos(q2+q3-q4)-3/2000*co \\
& s(q2+q3+q4)-1/200*\sin(q5+q2+q3+q4)+1/200*\sin(-q5+q2+q3+q4)+1/2000*\sin(-q6-q4+q3+q2)-1/ \\
& 400*\sin(q6+q5+q4+q2)-1/200*\cos(-q5+q4-q2)-1/400*\sin(q6+q5+q4-q2)+1/200*\cos(q5+q4-q2)-1/ \\
& 2000*\sin(q6+q3+q2-q4))*qa1+(-1/200*\cos(-q5-q4+q3)+1/200*\sin(-q6-q5+q3)+1/200*\cos(q5-q4+ \\
& q3)+3/1000*\cos(q4)-1/200*\cos(-q5+q4+q3)+1/100*\cos(q3+q5)-1/400*\sin(q6+q5-q4+q3)-1/400*si \\
& n(-q6-q5-q4+q3)+1/100*\sin(q5+q4)+1/1000*\sin(-q6+q4)+1/200*\cos(q5+q4+q3)-1/1000*\sin(q6+q \\
& 4)+1/200*\cos(q6+q5+q4)-1/200*\sin(q6+q5+q3)+1/200*\cos(-q6-q5+q4)-1/100*\sin(-q5+q4)-1/400* \\
& sin(q6+q5+q4+q3)+1/100*\cos(q3-q5)-1/400*\sin(-q6-q5+q4+q3))*qa2+(3/1000*\cos(q4)+1/100*\sin \\
& (q5+q4)+1/1000*\sin(-q6+q4)-1/1000*\sin(q6+q4)+1/200*\cos(q6+q5+q4)+1/200*\cos(-q6-q5+q4)-1/ \\
& 100*\sin(-q5+q4))*qa3+(-1/500*\sin(q6)+3/1000)*qa5+(1/1000-1/1000*\sin(q6))*qa6+(1/4000*\sin(
\end{aligned}$$

$$\begin{aligned}
& 2*q5+2*q4)-1/200*\sin(-q5-q4+q3)-1/200*\cos(-q6-q5+q3)+1/200*\sin(q5-q4+q3)-1/8000*\sin(2*q6 \\
& +2*q5+2*q4)-1/50*\cos(q5)-1/200*\sin(-q5+q4+q3)-1/4000*\sin(-2*q5+2*q4)+1/100*\sin(q6+q5)+1/ \\
& 100*\sin(q3+q5)+1/400*\cos(q6+q5-q4+q3)+1/400*\cos(-q6-q5-q4+q3)-1/2000*\sin(2*q5)+1/4000*s \\
& \sin(2*q6+2*q5)+1/4000*\cos(2*q5+2*q4+q6)+1/200*\sin(q5+q4+q3)+1/200*\cos(q6+q5+q3)-1/2000 \\
& *\cos(q6+2*q5)+1/4000*\cos(-2*q5+2*q4-q6)+1/400*\cos(q6+q5+q4+q3)+1/100*\sin(q3-q5)+1/800 \\
& 0*\sin(-2*q6-2*q5+2*q4)+1/400*\cos(-q6-q5+q4+q3))*qv^2^2+(1/2000*\cos(q6+q3+q2-q4)-1/2000* \\
& \sin(2*q6+2*q5+q3+q2)-1/1000*\sin(-2*q5+q3+q2)+1/1000*\sin(2*q5+q3+q2)+3/2000*\sin(q2+q3+ \\
& q4)+1/1000*\cos(q6+2*q5+q3+q2)+1/1000*\cos(-2*q5+q3+q2-q6)+1/2000*\sin(-2*q6-2*q5+q3+q2 \\
&)-1/4000*\sin(-2*q6-2*q5+q3+q2-q4)+1/2000*\sin(2*q5+q4+q3+q2)+1/2000*\sin(2*q5-q4+q3+q2) \\
& +1/2000*\cos(q6+2*q5-q4+q3+q2)+3/2000*\sin(q2+q3-q4)-1/2000*\cos(-q6-2*q5+q3+q2+q4)+1/20 \\
& 00*\sin(-2*q5+q4+q3+q2)-1/2000*\cos(-q6-2*q5-q4+q3+q2)-1/4000*\sin(-2*q6-2*q5+q3+q2+q4)-1 \\
& /4000*\sin(2*q6+2*q5+q3+q2+q4)+1/2000*\sin(-2*q5-q4+q3+q2)-1/2000*\cos(-q6+q3+q2+q4)+1/2 \\
& 000*\cos(q6+q4+q3+q2)-1/4000*\sin(2*q6+2*q5+q3+q2-q4)-1/2000*\cos(-q6-q4+q3+q2)+1/2000*c \\
& \cos(q6+2*q5+q4+q3+q2))*qv1*qv4+(1/2000*\cos(-q6+q3+q2+q4)+1/2000*\cos(q6+q4+q3+q2)-1/2 \\
& 000*\cos(-q6-q4+q3+q2)-1/2000*\cos(q6+q3+q2-q4))*qv1*qv6-1/1000*\cos(q6)*qv6^2
\end{aligned}$$

$$\begin{aligned}
& (-1/4000*\cos(q6+q3+q2-q4)+1/2000*\sin(q2+q3+q4)+1/200*\sin(q6+q5+q2+q3+q4)-1/200*\sin(-q6- \\
& q5+q2+q3-q4)-1/4000*\sin(-2*q6-2*q5+q3+q2-q4)+1/200*\sin(-q6-q5+q2+q3+q4)-1/200*\sin(q6+q \\
& 5+q2+q3-q4)-1/8000*\sin(-2*q6-2*q5+2*q4+q3+q2)-1/8000*\cos(-2*q5+2*q4+q3+q2-q6)+1/4000* \\
& \cos(q6+2*q5-q4+q3+q2)-1/2000*\sin(q2+q3-q4)+1/8000*\cos(-q6-2*q4+q3+q2)-1/8000*\sin(2*q6+ \\
& 2*q5-2*q4+q3+q2)+1/4000*\cos(-q6-2*q5+q3+q2+q4)-1/8000*\cos(q6+2*q4+q3+q2)-1/4000*\cos(- \\
& q6-2*q5-q4+q3+q2)-1/8000*\cos(q6+2*q5+2*q4+q3+q2)+1/4000*\sin(-2*q6-2*q5+q3+q2+q4)+1/4 \\
& 000*\sin(2*q6+2*q5+q3+q2+q4)-1/8000*\cos(-q6+2*q4+q3+q2)-1/4000*\cos(-q6+q3+q2+q4)+1/80 \\
& 00*\cos(2*q5-2*q4+q6+q3+q2)+1/4000*\cos(q6+q4+q3+q2)+1/8000*\sin(-2*q6-2*q5-2*q4+q3+q2) \\
& -1/4000*\sin(2*q6+2*q5+q3+q2-q4)+1/4000*\cos(-q6-q4+q3+q2)+1/8000*\cos(-2*q4+q3+q2+q6)+ \\
& 1/8000*\sin(2*q6+2*q5+2*q4+q3+q2)-1/4000*\cos(q6+2*q5+q4+q3+q2)+1/8000*\cos(-q6-2*q5-2* \\
& q4+q3+q2))*qv1*qv3+(1/4000*\cos(q6+q3+q2-q4)-1/2000*\sin(2*q6+2*q5+q3+q2)+1/2000*\cos(q \\
& 6+q3+q2)+1/2000*\sin(q2+q3+q4)+1/2000*\cos(q6+2*q5+q3+q2)+1/2000*\cos(-q6+q3+q2)+1/2000 \\
& *\cos(-2*q5+q3+q2-q6)+1/2000*\sin(-2*q6-2*q5+q3+q2)-1/4000*\sin(-2*q6-2*q5+q3+q2-q4)+1/40 \\
& 00*\cos(q6+2*q5-q4+q3+q2)+1/2000*\sin(q2+q3-q4)-1/4000*\cos(-q6-2*q5+q3+q2+q4)-1/4000*co \\
& s(-q6-2*q5-q4+q3+q2)-1/4000*\sin(-2*q6-2*q5+q3+q2+q4)-1/4000*\sin(2*q6+2*q5+q3+q2+q4)-1/ \\
& 4000*\cos(-q6+q3+q2+q4)+1/4000*\cos(q6+q4+q3+q2)-1/4000*\sin(2*q6+2*q5+q3+q2-q4)-1/4000 \\
& *\cos(-q6-q4+q3+q2)+1/4000*\cos(q6+2*q5+q4+q3+q2))*qv1*qv4-981/40000*\sin(q6+q5+q2+q3+ \\
& q4)+(1/800*\cos(-q6-q5+q4+q3)-1/8000*\sin(2*q6+2*q5+2*q3+2*q2-q4)-1/400*\cos(-q6-q5+q3+2* \\
& q2)+1/32000*\cos(-2*q4+2*q3+2*q2+q6)-1/32000*\sin(2*q6+2*q5-2*q4+2*q3+2*q2)-1/16000*co \\
& s(2*q4-q6)+1/32000*\sin(-2*q6-2*q5+2*q4+2*q3+2*q2)+1/800*\cos(q6+q5+q4+q3+2*q2)+1/3200 \\
& 0*\cos(-q6-2*q5+2*q4+2*q3+2*q2)-1/8000*\cos(-q6-2*q5-q4+2*q3+2*q2)+1/16000*\sin(2*q6+2* \\
& q5+2*q4)-1/16000*\cos(2*q5+2*q4+q6)+1/1600*\cos(q6)+1/32000*\cos(-q6-2*q5-2*q4+2*q3+2*q \\
& 2)+3/16000*\cos(q6+2*q5+2*q3+2*q2)+1/200*\sin(q6+q5)-1/800*\sin(2*q3+2*q2+q6+q5-q4)-1/80 \\
& 0*\sin(2*q3+2*q2-q6-q5-q4)+1/400*\cos(q6+q5+q3)-1/8000*\sin(2*q6+2*q5)-1/16000*\cos(-2*q5+ \\
& 2*q4-q6)-1/800*\sin(2*q3+2*q2+q6+q5+q4)-1/800*\sin(2*q3+2*q2-q6-q5+q4)-1/16000*\cos(2*q3+ \\
& 2*q2+q6)-1/16000*\sin(-2*q6-2*q5+2*q4)+1/800*\cos(q6+q5-q4+q3)+1/800*\cos(-q6-q5-q4+q3)+1 \\
& /400*\sin(2*q3+2*q2-q6-q5)+1/800*\cos(q6+q5+q4+q3)+1/8000*\cos(q6+2*q5+2*q3+2*q2-q4)+1/ \\
& 32000*\cos(-q6+2*q4+2*q3+2*q2)-1/400*\sin(2*q3+2*q2+q6+q5)-1/8000*\sin(2*q6+2*q5+q4+2*q \\
& 3+2*q2)+1/32000*\cos(q6+2*q5-2*q4+2*q3+2*q2)+1/32000*\cos(-q6-2*q4+2*q3+2*q2)+1/8000*
\end{aligned}$$

$$\begin{aligned}
& \cos(q_6+2*q_5)-1/16000*\cos(q_6+2*q_4)+3/16000*\cos(-q_6-2*q_5+2*q_3+2*q_2)-1/8000*\sin(-2*q_6-2*q_5+q_4+2*q_3+2*q_2)+1/800*\cos(-q_6-q_5+q_4+q_3+2*q_2)+1/400*\cos(q_6+q_5+q_3+2*q_2)-3/16000*\sin(2*q_6+2*q_5+2*q_3+2*q_2)+1/32000*\sin(-2*q_6-2*q_5-2*q_4+2*q_3+2*q_2)-1/8000*\sin(-2*q_6-2*q_5+2*q_3+2*q_2-q_4)-1/400*\cos(-q_6-q_5+q_3)+3/16000*\sin(-2*q_6-2*q_5+2*q_3+2*q_2)-1/32000*\sin(2*q_6+2*q_5+2*q_4+2*q_3+2*q_2)-1/8000*\cos(-q_6-2*q_5+q_4+2*q_3+2*q_2)+1/800*\cos(q_6+q_5-q_4+q_3+2*q_2)+1/8000*\cos(q_6+2*q_5+2*q_3+2*q_2+q_4)+1/32000*\cos(q_6+2*q_4+2*q_3+2*q_2)-1/16000*\cos(-q_6+2*q_3+2*q_2)+1/800*\cos(-q_6-q_5-q_4+q_3+2*q_2)+1/32000*\cos(2*q_5+2*q_4+2*q_3+2*q_2+q_6))*qv1^2-981/400000*\sin(-q_6-q_5+q_2+q_3-q_4)+(-1/2000*\cos(-q_6+q_3+q_2+q_4)-1/2000*\cos(q_6+q_4+q_3+q_2)+1/2000*\cos(-q_6-q_4+q_3+q_2)+1/2000*\cos(q_6+q_3+q_2-q_4))*qv1*qv5-981/400000*\sin(-q_6-q_5+q_2+q_3+q_4)+(-1/400000*\sin(2*q_6+2*q_5+2*q_4)+1/50*\sin(q_6+q_5)+3/2000*\cos(q_6)+1/4000*\cos(2*q_4-q_6)+1/2000*\sin(2*q_6+2*q_5)+1/4000*\cos(2*q_5+2*q_4+q_6)-1/2000*\cos(q_6+2*q_5)+1/4000*\cos(-2*q_5+2*q_4-q_6)+1/40000*\sin(-2*q_6-2*q_5+2*q_4)+1/4000*\cos(q_6+2*q_4))*qv2*qv3-981/400000*\sin(q_6+q_5+q_2+q_3-q_4)-981/200000*\sin(q_6+q_2+q_3+q_5)+981/200000*\sin(-q_6+q_2+q_3-q_5)+(-1/4000*\cos(q_6+q_3+q_2-q_4)+1/2000*\sin(q_2+q_3+q_4)+1/2000*\sin(q_6+q_5+q_2+q_3+q_4)-1/2000*\sin(-q_6-q_5+q_2+q_3-q_4)-1/4000*\sin(-2*q_6-2*q_5+q_3+q_2-q_4)+1/2000*\sin(-q_6-q_5+q_2+q_3+q_4)-1/2000*\sin(q_6+q_5+q_2+q_3-q_4)-1/8000*\sin(-2*q_6-2*q_5+2*q_4+q_3+q_2)-1/8000*\cos(-2*q_5+2*q_4+q_3+q_2-q_6)-1/2000*\cos(q_6+q_5+q_4+q_2)+1/2000*\cos(q_6+q_5+q_4-q_2)+1/4000*\cos(q_6+2*q_5-q_4+q_3+q_2)-1/2000*\sin(q_2+q_3-q_4)+1/8000*\cos(-q_6-2*q_4+q_3+q_2)-1/800000*\sin(2*q_6+2*q_5-2*q_4+q_3+q_2)+1/2000*\cos(-q_6-q_5+q_4-q_2)+1/4000*\cos(-q_6-2*q_5+q_3+q_2+q_4)-1/800000*\cos(q_6+2*q_4+q_3+q_2)-1/4000*\cos(-q_6-2*q_5-q_4+q_3+q_2)-1/800000*\cos(q_6+2*q_5+2*q_4+q_3+q_2)+1/4000*\sin(-2*q_6-2*q_5+q_3+q_2+q_4)+1/4000*\sin(2*q_6+2*q_5+q_3+q_2+q_4)-1/800000*\cos(-q_6+2*q_4+q_3+q_2)-1/2000*\cos(-q_6-q_5+q_4+q_2)-1/4000*\cos(-q_6+q_3+q_2+q_4)+1/800000*\cos(2*q_5-2*q_4+q_6+q_3+q_2)+1/4000*\cos(q_6+q_4+q_3+q_2)+1/800000*\sin(-2*q_6-2*q_5-2*q_4+q_3+q_2)-1/4000*\sin(2*q_6+2*q_5+q_3+q_2+q_4)+1/4000*\cos(-q_6-q_4+q_3+q_2)+1/800000*\cos(-2*q_4+q_3+q_2+q_6)+1/800000*\sin(2*q_6+2*q_5+2*q_4+q_3+q_2)-1/4000*\cos(q_6+2*q_5+q_4+q_3+q_2)+1/800000*\cos(-q_6-2*q_5-2*q_4+q_3+q_2))*qv1*qv2+(-1/200000*\cos(-q_6-q_5+q_3)-1/800000*\sin(2*q_6+2*q_5+2*q_4)+1/100000*\sin(q_6+q_5)+3/400000*\cos(q_6)+1/800000*\cos(2*q_4-q_6)+1/400000*\cos(q_6+q_5-q_4+q_3)+1/400000*\cos(-q_6-q_5-q_4+q_3)+1/400000*\sin(2*q_6+2*q_5)+1/800000*\cos(2*q_5+2*q_4+q_6)+1/200000*\cos(q_6+q_5+q_3)-1/400000*\cos(q_6+2*q_5)+1/800000*\cos(-2*q_5+2*q_4-q_6)+1/400000*\cos(q_6+q_5+q_4+q_3)+1/800000*\sin(-2*q_6-2*q_5+2*q_4)+1/400000*\cos(-q_6-q_5+q_4+q_3)+1/800000*\cos(q_6+2*q_4))*qv2^2+(-1/1000000*\sin(q_4)+1/2000000*\cos(-q_6+q_4)-1/2000000*\cos(q_6+q_4)+1/2000000*\sin(-2*q_6-2*q_5+q_4)-1/2000000*\cos(q_6+2*q_5+q_4)+1/2000000*\cos(-q_6-2*q_5+q_4)+1/2000000*\sin(2*q_6+2*q_5+q_4))*qv2*qv4+(1/1000000*\cos(-q_6+q_4)+1/1000000*\cos(q_6+q_4))*qv2*qv5+(-1/1000000*\sin(q_4)+1/2000000*\cos(-q_6+q_4)-1/2000000*\cos(q_6+q_4)+1/2000000*\sin(-2*q_6-2*q_5+q_4)-1/2000000*\cos(q_6+2*q_5+q_4)+1/2000000*\cos(-q_6-2*q_5+q_4)+1/2000000*\sin(2*q_6+2*q_5+q_4))*qv3*qv4+(1/1000000*\cos(-q_6+q_4)+1/1000000*\cos(q_6+q_4))*qv3*qv5+1/1000000*qa6+(1/400000*\cos(q_6+q_5+q_2+q_3-q_4)-1/400000*\cos(-q_6-q_5+q_2+q_3+q_4)-1/400000*\cos(q_6+q_5+q_2+q_3+q_4)-1/400000*\sin(-q_6-q_5+q_4+q_2)-1/400000*\sin(-q_6-q_5+q_4-q_2)+1/400000*\cos(-q_6-q_5+q_2+q_3-q_4)-1/4000000*\sin(-q_6+q_3+q_2+q_4)+1/4000000*\sin(q_6+q_4+q_3+q_2)+1/2000000*\cos(q_2+q_3-q_4)-1/2000000*\cos(q_2+q_3+q_4)+1/4000000*\sin(-q_6-q_4+q_3+q_2)-1/4000000*\sin(q_6+q_5+q_4+q_2)-1/4000000*\sin(q_6+q_5+q_4-q_2)-1/4000000*\sin(q_6+q_3+q_2-q_4))*qa1+(1/2000000*\sin(-q_6-q_5+q_3)+1/1000000*\cos(q_4)-1/4000000*\sin(q_6+q_5-q_4+q_3)-1/4000000*\sin(-q_6-q_5-q_4+q_3)+1/2000000*\sin(-q_6+q_4)-1/2000000*\sin(q_6+q_4)+1/2000000*\cos(q_6+q_5+q_4)-1/2000000*\sin(q_6+q_5+q_3)+1/2000000*\cos(-q_6-q_5+q_4)-1/4000000*\sin(q_6+q_5+q_4+q_3)-1/4000000*\sin(-q_6-q_5+q_4+q_3))*qa2+(1/1000000000*\cos(q_4)+1/2000000000*\sin(-q_6+q_4)-1/2000000000*\sin(q_6+q_4)+1/2000000000*\cos(q_6+q_5+q_4)+1/2000000000*\cos(-q_6-q_5+q_4))*qa3+(1/1000000000-1/1000000000*\sin(q_6))*qa5+(1/2000000000*\cos(q_6)-1/2000000000*\sin(2*q_6+2*q_5)+1/2000000000*\cos(q_6+2*q_5))*qv4^2+(-1/8000000000*\sin(2*q_6+2*q_5+2*q_4)+1/10000000000*\sin(q_6+q_5)+3/40000000000*\cos(q_6)+1/80000000000*\cos(2*q_4-q_6)+1/400000000000*\sin(2*q_6+2*q_5)+1/800000000000*\cos(2*q_5+2*q_4+q_6)-1/400000000000*\cos(q_6+2*q_5)+1/800000000000*\cos(-2*q_5+2*q_4-q_6)+1/800000000000*\sin(-2*q_6-2*q_5+2*q_4)+1/800000000000*\cos(q_6+2*q_4))*qv3^2+1/1000000000000*\cos(q_6)*qv5^2
\end{aligned}$$